The Role of the Tropopause in Stratospheric-Tropospheric Exchange Processes

By

E.R. Reiter, M.E. Glasser, and J.D. Mahlman

Department of Atmospheric Science
Colorado State University
Fort Collins, Colorado

COO13409

**Colorado
State**
University

**Department of
Atmospheric Science**

Paper No. 107

THE ROLE OF THE TROPOPAUSE IN
STRATOSPHERIC-TROPOSPHERIC
EXCHANGE PROCESSES

by

E. R. Reiter, M. E. Glasser, and J. D. Mahlman

Department of Atmospheric Science
Colorado State University
Fort Collins, Colorado

January 1967

ABSTRACT

In a previous study Reiter and Mahlman (1965a) have estimated the amount of stratospheric air intruding into the stable layer of the jet stream front in a case of cyclogenesis not accompanied by surface radioactive fallout. In the present report the same case is examined on a more general basis. Outflow from, as well as inflow into, the stratosphere is estimated over the entire thickness of the "tropopause gap".

I. INTRODUCTION

Mass transport from the stratosphere into the troposphere has been studied primarily because of its relation to the problem of radioactive debris transport. Reed and Sanders (1953) and Reed (1955) first demonstrated that stratospheric air can enter the troposphere in association with intense baroclinic zones in the vicinity of the "jet stream front". Detailed analyses by many other authors have verified the existence of these air motions in the vicinity of the jet stream (Endlich and McLean, 1957; Reed and Danielsen, 1959; Danielsen, 1959a, b, 1964a, b; Murgatroyd, 1959; Staley, 1960, 1962; Danielsen, Bergman, and Paulson, 1962; Briggs and Roach, 1963; Reiter, 1961, 1963a, b, 1964; Reiter and Nania, 1964; Mahlman, 1964a, b, 1965; Reiter and Mahlman, 1964, 1965a; Reiter and Whitney, 1965).

A descent of stratospheric air to the rear of high-level cyclones has been hypothesized by Miyake et al. (1960, 1962). This could account for the correlation of surface radioactivity increases with cyclonic activity at the 500 mb level.

In their "waterspout model" of the upper tropospheric frontal zone, Reed and Danielsen (1959) concluded that intrusions of stratospheric air into the troposphere were associated with a "folding" of the tropopause. Flight measurements have shown that high values of radioactivity are associated with stratospheric air in this upper level frontal zone (Staley, 1962; Danielsen, Bergman, and Paulson, 1962; Danielsen, 1964b). In particular Staley (1960, 1962) demonstrated by the use of trajectories that air in dry stable layers with high beta activities could be traced back to the stratosphere.

Staley (1960) suggests as a possible mechanism for producing the observed seasonal variations in radioactive fallout, the tendency of the tropopause to re-form at higher levels in spring. Such a process will incorporate contaminated stratospheric air into the troposphere. During the fall season, the reverse mechanism has to be expected with the widespread lowering of tropopause levels.

Turbulent mixing can be listed among the diverse mechanisms that have been advanced to account for mass transport between the stratosphere and the troposphere and the related radioactive fallout patterns. Mixing downward through the tropopause has been assumed by Stewart et al. (1955, 1957), Libby (1956), and Martell and Drevinsky (1960).

The correlation between high-level cyclones and surface radioactive fallout suggested by Storebø (1959), Miyake et al. (1960, 1962), and Staley (1962) was corroborated by Mahlman (1964a, b, 1965). Danielsen (1964a) and Mahlman (1964a, b, 1965) further suggested that surface fallout increases occur in association with strong cyclogenesis in the upper troposphere. The reality of this cyclogenetic mechanism was put on a firm basis by the case studies of Danielsen (1964b) and Reiter and Mahlman (1964, 1965a, b). The physical process, revealed by trajectory analyses, shows descent on the cyclonic side of the jet axis from the stratosphere into the troposphere in the vicinity of the jet stream front under quasi-conservation of potential vorticity. A detailed statistical study of the upper level cyclonic activity associated with these transport situations has been carried out by Mahlman (1964c, 1965, 1966). A "cyclone index" was developed which proved to be a statistically reliable indication of the relative intensity of cyclonic activity in the upper troposphere. Rapid decreases of the cyclone index proved to be associated with the short-period fluctuations of fallout that are superimposed on the main seasonal variation. One could distinguish between instances of index decrease with or without subsequent fallout. It was also noted that the intensity of cyclogenetic activity had a bearing on the amount of mass involved in the intrusion of stratospheric air into the troposphere.

All case studies previously mentioned traced a well-defined body of stratospheric air on its descent through the troposphere. The three-dimensional extent of such intrusions was established by quasi-conservative air mass properties, such as potential vorticity and moisture

content, and corroborated by in-flight or ground-based radioactive debris sampling. No attention has been paid to the further development of the vertical exchange pattern in the jet stream region, once such an intrusion was identified.

In reviewing the role of the jet stream and of the "tropopause gap" (i. e., the region in which Reed and Danielsen (1959) assume the "folding" process to be active) in stratospheric-tropospheric mass exchange processes, the following unsolved questions remain:

(1) Are intrusions of stratospheric air into the troposphere "discrete" and well-defined processes, and are the estimates of mass involved in this transport representative for such events, or is there a "continuous seepage" of stratospheric air through the tropopause gap which would render previous quantitative estimates of such mass transfer too low?

(2) Are there preferred layers within the vertical extent of the tropopause gap in which intrusions of stratospheric air into the troposphere take place?

(3) Is there a return flow of tropospheric air into the stratosphere in the jet stream region?

(4) Is the jet stream flow as efficient in importing tropospheric air into the stratosphere as it appears to be in carrying stratospheric air towards the ground?

The present study contains a preliminary effort to answer these questions. In view of the vast amount of analytical work involved, only one typical jet stream case can be presented in detail. The results, therefore, should not be considered final. An extension of the present investigation over wider regions, longer periods of time, and different upper flow patterns will be necessary before a complete assessment of the role of jet streams and of the tropopause gap in vertical transport processes of both, positive and negative signs, will be possible.

For the present study the period 18 to 21 April 1963 was chosen. In a previous investigation of the same period, Reiter and Mahlman (1965a) traced an intrusion of stratospheric air which did not reach the ground. Consequently, no surface radioactive fallout increase was observed. According to Mahlman (1965), the cyclogenetic activity over North America, on the dates indicated above, was of only average intensity. The "cyclone index" change was below the threshold value postulated for cyclogenesis associated with radioactive fallout. The potential temperatures characteristic of the intrusion were higher than those found in cases in which stratospheric air had descended to the ground. Furthermore, the mass of intruding stratospheric air, estimated to be 0.25×10^{12} metric tons, was less by a factor of approximately 2 in this case, as compared with cases of cyclogenesis which produced dry fallout at the ground. Isentropic trajectory analyses by Reiter and Mahlman (1965a) indicated, furthermore, the prevalence of cyclonic trajectory curvature within the stable layer containing the intruding stratospheric air, in contrast with strong anticyclonic curvature observed with cases producing surface fallout.

From the foregoing it appears that the present study deals with a jet stream of only average intensity and of average cyclogenetic activity. This investigation, therefore, will serve well in estimating the efficiency of transport processes characteristic of a majority of synoptic situations. Nevertheless, the extension of the analyses and computations to extreme cases would be highly desirable.

As it became apparent that any quantitative estimate of vertical mass transfer processes hinges on the definition of the "tropopause", the implications of the latter are reviewed in detail.

II. THE CONCEPT OF THE TROPOPAUSE

The operationally-used definition of the tropopause, as it is identified on individual temperature soundings, is based on the difference in lapse rate of stratospheric and tropospheric air. It is marked at the lower boundary of a layer in which the vertical temperature gradient is $< 0.2^{\circ}C/100$ m. The layer has to be at least 2 km thick. Since in the vicinity of the tropopause gap the jet stream front may show similar degrees of stability and a similar thickness, this tropopause definition becomes rather vague in the region where most of the intrusions of stratospheric air into the troposphere seem to occur.

Furthermore, observers coding the radiosonde measurements are given considerable leeway in reporting "significant points" along the sounding. Above the 500 mb surface, such points have to be reported only if a straight connection between temperature values on standard isobaric surfaces would lead to an error of more than $2^{\circ}C$ as compared with the actually measured temperatures (Endlich, 1954). This rule provides for a distinct tendency of the tropopause to be reported on either a standard isobaric surface, or on a convenient centibar level in-between standard surfaces.

Fig. 1 shows a frequency distribution of tropopause reports over the Northern Hemisphere during January 1956 (Defant, 1958). It may easily be seen that the convenient, but inaccurate, coding of tropopause levels may lead to errors in the estimate of stratospheric-tropospheric mass transfer. Assuming the average distance between radiosonde stations in the contiguous United States to be 350 km, the representative area of one upper-air observation is of the order of 1.2×10^5 km^2. The mass contained in a 10 mb layer spreading over this area is 1.2×10^{16} grams, or 1.2×10^{10} metric tons. A 50 mb layer of the same horizontal extent contains 6×10^{10} metric tons. According to Reiter and Mahlman (1965), the intrusion of stratospheric air in the present case contained

0.25×10^{12} metric tons. Thus, a 10 mb error in the coded tropopause level on one sounding could introduce a 4.8% error in the estimate of a mass transfer process of average intensity. A 50 mb error in tropopause location would lead to a 24% error in the mass computation.

In estimating large-scale transfer processes, such errors would have to be considered serious if they occurred systematically over a large region. One may assume, however, that all stations in this region will not misplace the reported tropopause in the same direction. Considering the statistical tropopause behavior over a large area, one, therefore, may be justified in assuming that positive and negative errors will cancel.

When tracking individual air parcels in the vicinity of the tropopause, the arbitrariness of tropopause definition becomes much more aggravating, especially near regions of jet-stream velocities, or where shallow stable layers extend from the stratosphere into the troposphere. This was recognized by Danielsen (1959b) who proposed as an additional criterion for the correct placement of the tropopause the condition that isentropic surfaces reach a relative maximum of height along the intersection line with the tropopause. Detailed analyses of vertical cross sections through the atmosphere and of isentropic charts are necessary to determine the location of the tropopause following this revised concept. This will eliminate to a certain degree the errors introduced by the $2^{\circ}C$ tolerance allowed in coding significant points in radiosonde measurements.

As has been realized from earlier investigations (Palmén, 1933; Bjerknes and Palmén, 1937; McClain and Danielsen, 1955; Danielsen, 1959; Reed and Danielsen, 1959), the tropopause is not a "substantial" or "physical" surface which contains the same air parcels all the time. It has been demonstrated in the radioactive fallout studies mentioned earlier that the tropopause is permeable to vertical transport processes of considerable magnitude.

On the other hand, we have to realize that over large areas the tropopause tends to follow an isentropic surface. Thus, over regions with little or no baroclinicity the tropopause will have advective characteristics for adiabatic motions.

The difficulty in estimating the magnitude of mass transfer across the tropopause level stems from the more or less arbitrary decision that will have to be made on how far to let the advective properties of the tropopause be governed by conservative properties of the air masses involved in the vertical mass transfer. As such a conservative property, one may conveniently chose the potential vorticity

$$P = - Q_\theta \, \partial\theta/\partial p \qquad (1)$$

where Q_θ is the absolute vorticity measured on an isentropic surface, and $\partial\theta/\partial p$ is the vertical stability, expressed in terms of potential temperature gradient in a pressure-coordinate system. Mainly because of the difference in air mass stability, air of stratospheric origin has much higher values of potential vorticity than tropospheric air. Air masses transported across an arbitrary tropopause level will retain reasonably well their values of potential vorticity and, with the condition

$$Q_\theta \, \partial\theta/\partial p = \text{const} , \qquad (2)$$

it is observed that their stability changes only slowly. Thus, a layer of stratospheric air whose bottom rested along the "tropopause" before it underwent downward displacement, still will appear as a stable layer with the same potential vorticity and the same potential temperatures. In view of the advective properties of the tropopause mentioned before, one will have to decide whether to retain the tropopause--at a new potential temperature surface--at its original height, or to lower the tropopause together with the descending stable layer. Similar

considerations will have to be made when tropospheric air of low stability and low potential vorticity rises through an arbitrary tropopause level.

Using Danielsen's concept of a tropopause, it usually is not too difficult to determine a meaningful "tropopause level" in individual cross sections. However, in trying to circumvent the dilemma posed by the advective properties of the tropopause described above, Danielsen's criterion proved to be insufficient when dealing with mass transfer estimates. In addition, one has to postulate that mass transfer processes across the tropopause be irreversible; that is, stratospheric air once intruded into the troposphere should remain there and not return to the stratosphere before losing its quasi-conservative properties. The same condition is imposed upon tropospheric air flowing into the stratosphere.

It is obvious that quantitative estimates of mass transfer across the tropopause, when considering all the requirements stated above, involve laborious analyses and calculations. The case described in this report represents a feasibility study of such estimates.

III. SYNOPTIC SITUATION, 18 TO 21 APRIL 1963

Fig. 2 shows the 500 mb contour analyses at 00 GMT for the period 16 to 21 April 1963. The shaded areas indicate wind speeds in excess of 50 knots. According to the study by Reiter and Mahlman (1965), the main intrusion of stratospheric air into the tropospheric jet stream front occurred between 18 April 12 GMT and 19 April 00 GMT. This intrusion was associated with a cyclone which moved with a short-wave trough across the midwestern United States.

The migration of this short-wave trough may be seen from Fig. 3 which shows 12-hour height changes of the 500 mb surface. During the period ending on 18 April 00 GMT, the short-wave disturbance travels through the long-wave trough position over California and Nevada. Height changes during this period remained relatively small. A sharp increase in the amplitude of height changes is experienced during the subsequent 12 hours as the disturbance moves across the Rocky Mountains. Equally strong decreases of the 500 mb heights are recorded during the following half-day periods. If we take the 500 mb height changes as an indicator of cyclogenetic activity in the middle troposphere, the 12-hour period ending on 18 April 12 GMT marks the first event of the case under investigation.

The development of the surface cyclone may be seen from Fig. 4 which contains frontal positions and minimum surface pressure values at 06 and 18 GMT for the period 17 to 20 April. The frontal wave deepens into a cyclone between 06 and 18 GMT on 18 April.

The 24-hour surface pressure changes given in Fig. 5 are strongest for the period ending 19 April 12 GMT; although the period ending on 19 April 00 GMT also experienced appreciable pressure falls. The pressure fall ending on 19 April 12 GMT is mostly due to movement of the surface cyclone while the period ending on 19 April 00 GMT results from an appreciable deepening effect. As a result, this is not inconsistent with the earlier conclusion that the cyclogenetically most active period was between 00 and 12 GMT on 18 April.

The jet stream configuration during the period of stratospheric air intrusion may be seen from Fig. 6. The surface cyclone, as is to be expected, is associated with a strong jet stream aloft. This jet stream is split into three distinct branches which may be identified at consecutive observation times. It would be fallacious to say that the southernmost of these branches corresponds to the subtropical jet stream, the northernmost to the polar front jet. As is evident from the cross sections shown in Figs. 7 and 8, the southern branch of the jet stream system overlies a strong frontal zone which extends throughout the troposphere. Thus, the southern jet branch would qualify as a polar front jet in spite of the fact that the core is located above the 250 mb level. Reiter and Whitney (1965) have commented on the ambiguity of currently used jet stream nomenclature.

Values of potential vorticity have been entered numerically in the cross sectional analyses of Fig. 7. The sharp contrast in potential vorticity between stratospheric and tropospheric air aids in the identification of the air mass sources after the intrusion processes have started. Relative humidities, shown in Fig. 7, give a rough indication of areas in which sinking or rising air motions are underway. It will have to be considered, however, that humidity measurements become rather unreliable in the upper troposphere. The deep moist layer preceding the cold front on 18 and 19 April (Fig. 7, Sections LND-BRJ) is associated with convective motions and precipitation. A pre-frontal squall line was reported in this area later on the same day (Reiter et al., 1965). The dry air in the vicinity of the jet-stream front, on the other hand, indicates strong sinking motions, especially between Denver and Dodge City on 18 April 12 GMT. As will be shown later, the main intrusion of stratospheric air into the troposphere occurs in this region.

IV. FLOW PROCESSES NEAR TROPOPAUSE LEVEL

The difficulties in tropopause analysis have been enumerated in Chapter II. If all criteria for tropopause identification listed before are properly taken into account, one arrives at the analyses shown in Fig. 9. Potential temperatures of the tropopause level are shown in °K. Small dots represent stations over which the coded tropopause, as reported by the Weather Bureau observers, agrees with the re-defined tropopause, especially after the criterion of "irreversibility" of intrusion processes has been applied. Numerical values at stations indicate the differences in °C that have to be applied to the analysis in order to arrive at the "coded" tropopause levels. A value of +86, for instance, would indicate that the tropopause level reported in the teletype radio-sonde message lies at a potential temperature of 86°C higher than the re-defined value shown by the analysis.

It is of interest to note that in the case at hand the tropopause level--if not given accurately--is over-estimated. This may be due to the strict application of the stability criterion given in Chapter II in identifying the tropopause. Semi-stable regions, which are frequently found adjacent to the coded tropopause levels, are considered by observers to belong to the troposphere. If area and time continuity is taken into account, as has been done in the analyses of Fig. 9, these layers often have to be considered as belonging to the stratosphere. This is evident from Fig. 10 in which soundings are plotted over each station: Plain arrows indicate the "Weather Bureau tropopause"; arrows with dots indicate the re-defined tropopause level. Horizontal marks along the sounding curves indicate potential temperatures at 10°C intervals. The 330°K level is marked by the station circle.

Considerable difficulty would be encountered if one attempted to analyze the "pattern" of difference values plotted in Fig. 9. This demonstrates that the tropopause levels coded under present regulations

are of questionable value. If there were an easily identifiable pattern
in these difference values, one might at least assume that a level of
prominent lapse rate discontinuity within the stratosphere occupied
a considerable area, thus warranting special attention. This, how-
ever, does not seem to be the case, at least not with any time con-
tinuity. The large "discrepancy values" over the southern United
States on 18 April 12 GMT are due to a rather conspicuous "tropical
tropopause" which caught the observers' attention and overshadowed
the lapse rate discontinuity associated with the polar tropopause.

In comparing Fig. 9 with Fig. 2, we find lowest tropopause
"levels" over the cold dome. (The location of the latter may be
identified, for instance, by the closed -30°C isotherm on the 500 mb
chart of 19 April 00 GMT.) This is in agreement with earlier findings
by Hsieh (1949, 1950). The cold dome, as well as the "trough" in
tropopause potential temperatures (which may crudely be interpreted
as tropopause height), lags considerably behind the 500 mb trough
and the surface cyclone, especially during the period of rapid cyclo-
genesis (prior to 19 April 00 GMT). As the storm reaches its mature
stage, the axis connecting the surface low, the 500 mb trough, and the
lowest tropopause height becomes more nearly vertical, as has been
pointed out by Fleagle (1947).

This leads to the following qualitative conclusions which later
will be substantiated by quantitative estimates: During a period of
strong cyclogenesis (as the "tropopause trough" lags considerably
behind the surface cyclone), the advective properties of the tropo-
pause, described in Chapter II, are less dominant than is normally
the case. It is during such periods that stratospheric air moves
across its boundaries, shown by the potential isotherms in Fig. 9,
thus causing intrusions of stratospheric air into the troposphere.
For an individual air parcel, the condition $d\theta/dt = 0$ is closely
satisfied during an intrusion event. The same parcel may, however,

cross the potential isotherms in Fig. 9 since they only indicate boundaries of the tropopause which has to be considered a "non-physical", or "non-substantial" surface.

As the cyclone grows towards its mature stage, the "tropo-pause trough" travels at faster than normal rate, eventually catching up with the location of the mid-tropospheric trough and the surface cyclone. Again, during this growth period the advective properties of the tropopause are overshadowed by mass flow across its boundaries. We might expect incorporation of tropospheric air into the stratosphere along the leading edge of the fast-traveling "tropopause trough", and outflow from the stratosphere along the rear side of the trough.

With the cyclone having reached its mature stage, it travels in phase with the tropopause depression. Transport processes across the tropopause are expected to cease, or at least to reach very small magnitudes.

These conclusions are corroborated by Figs. 11 to 15. They show the boundaries of the "re-defined" tropopause as a heavy solid line, and the borders of intruded stratospheric or tropospheric air as dashed-dotted lines. Portions of soundings near the isentropic levels under consideration have been entered in these diagrams. The intersections of the respective isentropic surfaces with the soundings are indicated by the locations of the station circles. The intersections of other potential temperature surfaces investigated are given for reference by small horizontal marks along the soundings. Thin solid lines are isobars on the respective isentropic surface.

On the 300°K isentropic surface a relatively small amount of air with stratospheric qualities is already found at tropospheric levels on 18 April 12 GMT (Fig. 11). Twelve hours later some of this strato-spheric air reaches the lowest levels of the troposphere. This rapid sinking may have occurred in association with strong chinook winds to the lee of the Rocky Mountains (Reiter et al., 1965; Beran, 1966).

By 19 April 12 GMT all stratospheric air originally at 300^OK is now well within the troposphere (see also Fig. 9). The lowest portions of the "tropopause trough" thus contribute only towards outflow of stratospheric air and not towards inflow of tropospheric air, during the case of cyclogenesis presently under investigation.

Similar conditions hold on the 305^OK isentropic surface (Fig. 12). Stratospheric air originally found at this potential temperature level is entirely incorporated into the troposphere by 19 April 12 GMT.

On the 310^OK isentropic surface (Fig. 13), the intrusion process is already well established along the leading edge of the tropopause depression by 18 April 12 GMT, when--according to Fig. 3-- mid-tropospheric cyclogenesis is well on its way. Within the next 12 hours, when the "tropopause trough" over the cold dome lags far behind the surface cyclone, the amount of stratospheric air mass intruded along the leading edge of the tropopause depression undergoes only little change, as may be seen from Fig. 13. As the tropopause trough moves over the surface cyclone (19 April 12 GMT), an additional amount of stratospheric air is incorporated into the troposphere to the rear of the advancing trough. This is in agreement with the hypothesis stated earlier.

According to Fig. 13, the 310^OK isentropic surface is characterized by outflow of stratospheric air only during the period under investigation. The 320^OK surface (Fig. 14) reveals less pronounced intrusions of strato- spheric or tropospheric air across the tropopause. As may be seen from the cross sections of Figs. 7 and 8, this isentropic surface lies <u>above</u> the stable layer of the jet stream front, and <u>below</u> the core of maximum winds in the jet stream. Small amounts of tropospheric air seem to be identifiable within the stratosphere ahead of the position of the surface cyclone, but these intrusion estimates are within the accuracy limits of the analysis.

The 330°K isentropic surface may be considered characteristic of the jet stream core (see Figs. 7 and 8). On this surface again areas occupied by tropospheric or stratospheric air on the "wrong" side of the tropopause intersection line are relatively small on 19 April (Fig. 15). The layers in, and immediately underneath, the jet stream core most of the time, seem to contain "undecided" air, which flows along the tropopause gap without transgressing far into the stratosphere or troposphere. "Continuous seepage" of air through the tropopause gap, mentioned as a possible transport mechanism in the Introduction (Chapter I), thus may be present but is difficult to identify from Figs. 14 and 15.

The intrusion of tropospheric air on 18 April 12 GMT, shown in Fig. 16 over the Great Lakes region, does not occupy a large area. However, the strong jet stream winds blowing across the quasi-stationary tropopause at this level (compare Fig. 6 with Fig. 9) would indicate a significant import of tropospheric air masses into the stratosphere during the period of strongest cyclogenesis. The fact that this intrusion occurs close to the northern border of the dense radiosonde network of the United States makes it difficult to trace the advance of this tropospheric air by trajectory computations.

Potential temperature levels higher than 330°K have not been analyzed in this preliminary study. As may be seen from Figs. 7 and 8, the 340°K surface characterizes mostly stratospheric levels above the jet stream core.

V. TRAJECTORY AND MASS FLOW COMPUTATIONS

Fig. 16 shows 12-hour trajectories on the 310°K isentropic surface. Values of divergence, computed from

$$\nabla \cdot \vec{V}_\theta = - \frac{\dfrac{d}{dt} \dfrac{\partial p}{\partial \theta}}{\dfrac{\partial p}{\partial \theta}} \quad , \tag{3}$$

are entered numerically at trajectory midpoints (units $10^{-4} \sec^{-1}$). Here, $\vec{V}_\theta$ is a two-dimensional wind vector on the θ surface, ∇ the two-dimensional del-operator, and $\dfrac{d}{dt}$ the substantial time derivative. Positive values of $\nabla \cdot \vec{V}_\theta$ signify divergence, negative values convergence. Tropopause positions at the beginning and end of the trajectory periods are marked by heavy solid and dashed lines, respectively.

Stratospheric air at this isentropic level is undergoing divergence in the period from 18 April 12 GMT to 19 April 00 GMT. The subsequent 12-hour period shows divergence only along the southern border of the "tropopause trough" in the entrance region of the northern jet-stream branch (see Fig. 6).

Convergence is mainly found in the "entrance region" of the jet maxima. This is in agreement with the "classical" pattern of divergence near a jet stream and its relation to the vorticity advection pattern.

The trajectories on the 320°K isentropic surface are shown in Fig. 17. The distribution of divergence and convergence is consistent with the one computed for the 310°K surface.

On the 330°K isentropic surface divergence seems to be mainly confined to the region near the tropopause gap (Fig. 18). Significantly large values are associated with the middle jet branch near, and ahead of, the jet maximum. Convergence, again, seems to prevail to the rear of the wind maximum. The present small sample of analyses is not yet conclusive as to different behavior in divergence patterns with

mass transport from or into the stratosphere. This is in part due to the accuracy limitations in estimating divergence. There are, however, indications that intrusions of stratospheric air into the troposphere favor a convergent flow pattern, whereas import of tropospheric air into the stratosphere occurs with divergence.

The uncertainties in divergence estimates may be seen from the following example. In Fig. 19 the expansion of area A into area B during a 12-hour period has been indicated. The mean divergence computed from this area expansion has been estimated to be

$$\nabla \cdot \vec{V}_\theta \; = \; - \; \frac{1}{A} \; \frac{dA}{dt} \; = \; - \, 0.22 \times 10^{-4} \, \text{sec}^{-1}$$

Divergence, computed from changes in area-weighted stabilities observed in areas A and B is

$$\nabla \cdot \vec{V}_\theta \; = \; \frac{\dfrac{d}{dt} \; \overline{\dfrac{\partial p}{\partial \theta}}}{\overline{\dfrac{\partial p}{\partial \theta}}} \; = \; - \, 0.17 \times 10^{-4} \, \text{sec}^{-1}$$

where the "bar" indicates an area-averaging process. Finally, if one averages the five trajectory values plotted in Fig. 19 and computes divergence by use of Eq. (3), one obtains

$$\nabla \cdot \vec{V}_\theta \; = \; - \, 0.10 \times 10^{-4} \, \text{sec}^{-1} \; .$$

In order to study the mass export and import processes from and into the stratosphere, one has to consider the behavior of the intersection line between the tropopause and the isentropic surface under consideration. If $\vec{V}_T$ is the wind vector measured on the isentropic surface at this intersection line, and $\vec{C}_T$ is the displacement vector of this line, then $(\vec{V}_T - \vec{C}_T)_\theta$ signifies the motion of air relative to the moving tropopause. It is difficult to estimate $\vec{C}_T$ unless some assumptions are made. It appears reasonable, as a first approximation, to postulate that the

tropopause moves in the direction of the wind vector; thus, the vectors $\vec{V}_T$ and $\vec{C}_T$ are assumed to be parallel. Exceptions to this assumption may occur in regions where the tropopause undergoes rapid dissipation or re-formation.

The expression

$$(\vec{V}_T - \vec{C}_T)_\theta \cdot \sin \alpha \qquad (4)$$

gives the component of flow into (positive sign) or out of (negative sign) the stratosphere. α is the angle between the relative wind vector and the line element $\vec{ds}$ of the intersection line between isentropic surface and tropopause.

The air mass contained in a column of air of unit cross section and of height Δz is given by

$$\overline{\rho}\Delta z = -\frac{\Delta p}{g} \qquad (5)$$

where $\overline{\rho}$ designates the mean density in the layer, and g is the acceleration of gravity. The mass inflow and outflow into and from the stratosphere may therefore be computed from

$$M = -\frac{\Delta p}{g} (\vec{V}_T - \vec{C}_T)_\theta \cdot \sin \alpha \qquad (6)$$

Fig. 20 shows the tropopause intersections with the $310^\circ K$ isentropic surface at three successive map times beginning with 18 April 1963, 12 GMT. Wind directions are indicated by arrows, and wind speeds in mps are given numerically. Trajectories of tropopause displacement have been constructed under the assumption that the vector $\vec{C}_T$ is parallel to the vector $\vec{V}_T$. They are reproduced in Fig. 21.

Fig. 22 indicates numerical values of inflow and outflow in $^\circ$lat/12 hours for 19 April 00 GMT computed from expression (4). Tropopause displacement speeds $\vec{C}_T$ have been obtained by linear interpolation of trajectory lengths shown in Fig. 21 between the two 12-hour intervals beginning at 18 April 12 GMT.

The areas under the curves shown in Fig. 22 yield the mass inflow and outflow into and from the stratosphere, by applying Eq. (6). If we take Δp to be a layer of 1-mb thickness, one unit area of $(^{O}\text{lat}) \times (^{O}\text{lat}/12 \text{ hrs})$ in this diagram represents

$$1.05 \times 10^{7} \text{ metric tons/hr} \cdot \text{mb} \tag{7}$$

The amounts of inflow and outflow per hour and per 1-mb layer are indicated numerically in Fig. 22.

The main extrusion of stratospheric air on the 310°K isentropic surface, according to Fig. 22, amounts to 0.22×10^{9} metric tons/mb·hr, or to 0.29×10^{9} metric tons/mb·hr if one includes the small outflow region near the tip of the "tropopause trough". In Fig. 13 the region has been outlined in which the 310°K isentropic surface is contained within a stable layer in the troposphere. The thickness of this layer has been measured on 19 April 00 GMT as follows:

Amarillo	(363)	62 mb
Oklahoma City	(353)	58 mb
Omaha	(553)	40 mb
Topeka	(456)	120 mb
Dodge City	(451)	80 mb

An average value of approximately 70 mb may be taken for the thickness of the stable layer in this region. If one assumes the outflow rates given above to hold over the entire mean thickness of this layer, one arrives at a total outflow from the stratosphere in this region and in this layer of 0.22×10^{11} metric tons/hr.

According to previous estimates (Reiter and Mahlman, 1965a), the intrusion of stratospheric air into this stable layer amounted to 0.25×10^{12} metric tons. This would mean that the flow conditions found on 19 April 00 GMT would have to prevail for slightly less than 12 hours to account for the whole intrusion process.

The "tropopause trajectories" shown in Fig. 21 and the segments marked as inflow and outflow along the tropopause intersection line agree well with the isentropic trajectories presented in Fig. 16. Northwest of the tip of the "tropopause trough" the tropopause intersection line moves faster than advective processes would indicate, giving rise to apparent mass flow conditions with signs opposite to the ones indicated by the wind vectors in this region. This has been shown in Fig. 22 by shaded areas.

The net effect of flow in the region (outflow minus inflow) under the influence of cyclogenesis produces outflow from the stratosphere at the rate of 0.084×10^9 metric tons/mb·hr, or 0.07×10^{12} metric tons in a 70 mb layer during 12 hours. From this approximate estimate it would appear that inflow and outflow conditions near the 310°K isentropic level are nearly in balance. This estimate does not include air contained in the small cut-off regions, shown in Fig. 13, in which the tropopause re-establishes itself at higher potential temperature levels.

On the 320°K isentropic surface transport processes across the tropopause are considerably stronger developed than on 310°K (Figs. 20 to 22). This is brought about by the strong wind velocities prevailing in the "tropopause gap" near the jet core. Even small angles α in Eq. (4) would--under these circumstances--permit relatively large mass flow into, and out of, the stratosphere.

There is some uncertainty in the mass-flow computations at this level. As may be seen from Fig. 20, the tropopause intersection line with the 320°K isentropic surface shows several "waves" on 18 April 12 GMT which do not preserve time continuity. Consequently, no trajectories of tropopause displacement could be constructed for this region. Thus, the shaded area in Fig. 20 possibly indicates outflow of stratospheric air by virtue of a re-formation of the tropopause. No estimates of the mass of air involved in this re-formation process have been made, however, because the reliability of the analysis has to be questioned in this case.

From the cross section LND to BRJ on 19 April 00 GMT (Fig. 7),
one may see that the 320°K isentropic level is located somewhat below
the jet core, but <u>above</u> the stable layer of the "jet-stream" front. In
this region the tropopause is poorly defined even when using all criteria
enumerated in Chapter II of this report. For this reason the rather large
outflow of stratospheric air on the 320°K surface shown in Fig. 22
should be considered questionable. As may be seen from Fig. 14,
the areas occupied by stratospheric or tropospheric air on the "wrong"
side of the tropopause intersection line (heavy dashed lines) are rather
small, again indicating that flow processes across the tropopause are
difficult to define.

From the evidence presented here it appears that the vicinity of
the 320°K isentropic surface may very well witness some "seepage" pro-
cesses of air across the tropopause. Such processes have been mentioned
in Chapter I as a possible exchange mechanism between stratosphere and
troposphere. Although, for lack of adequate wind data in the jet stream
region, the numerical values given in Fig. 22 may be subject to doubt,
the possibility exists that the magnitude of "seepage" through the ill-
defined tropopause at jet stream level may be nearly as large as that
of the well-defined intrusions of stratospheric air in the stable "jet-
stream front" near 310°K.

The flow across the tropopause on the 330°K isentropic surface
is shown in Figs. 20 to 22. As may be seen from the cross sections in
Figs. 7 and 8, this isentropic level lies close to the jet core. The
"waves" in the portions of the tropopause intersection lines shown in
Fig. 20 that run nearly parallel to the jet axis, seem to be caused by
the same difficulties in defining the boundary of the stratosphere within
the "tropopause gap". Disregarding the smaller ones of these "waves"
in the construction of tropopause trajectories, one arrives at the tropo-
pause motion at 330°K shown in Fig. 21.

Fig. 22 at 330^OK still shows considerable outflow of stratospheric air (0.24 x 10^9 tons per hour per mb) close to the same geographic location as was found on the 310^OK and 320^OK isentropic surfaces. On the 330^OK isentropic surface, however, this outflow is associated with a relatively small and rapidly moving protuberance in the tropopause intersection line. The significance of this small area of stratospheric air extrusion, therefore, may appear questionable.

Of considerably greater importance is the fact that on this isentropic surface--in contrast to the ones previously described-- the tropopause intersection lines at each of the observation times analyzed bend sharply towards the east, crossing the jet axis near the location of the northernmost jet maximum. At the same time this portion of the intersection line moves only slowly northward. This gives an indication of a narrow region of return flow of tropospheric air into the stratosphere. In view of the wind speeds, however, even such a narrow region could allow a significant amount of mass transport into the stratosphere. The magnitude of this flow (0.47 x 10^9 tons per hour per mb) is twice the one of the outflow into the stable layer characterized by the 310^OK isentropic surface and considered earlier by Reiter and Mahlman (1965a).

This flow of tropospheric air into the stratosphere, found in the jet maximum at the 330^OK isentropic surface, does not appear at the lower isentropic levels shown in Figs. 20 to 22. Thus, we may conclude that this isentropic level probably characterizes the main return flow processes into the stratosphere. As is evident from the cross sections in Figs 7 and 8, flow characteristics similar to the ones described in Fig. 22 will hold in a layer of considerable depth, estimated to be approximately 70 mb. The total mass inflow into the stratosphere, therefore, will be of the order of 0.03 x 10^{12} metric tons/hour.

It should be pointed out that because of high wind speeds trajectories starting on 19 April 00 GMT in the region of estimated return flow from the troposphere to the stratosphere lead over the data-sparse regions of Canada and the Atlantic Ocean. It, therefore, could not be ascertained whether or not this apparent intrusion of tropospheric air into the stratosphere meets the criterion of "irreversibility" of the flow process which had been postulated in Chapter II.

Comparing the three parts of Fig. 22 with each other, the calculation suggests that the total outflow from the stratosphere, produced by the jet maximum under consideration, exceeds the total inflow almost by a factor of 2. (The net outflow along the tropopause periphery under consideration is of the order of 0.9 x 10^9 metric tons per hour per mb, assuming that the three isentropic levels 310°, 320°, and 330°K are characteristic of flow conditions in equally thick layers. If 70 mb could be considered a representative thickness of each of these three layers, the net outflow from the stratosphere would amount to approximately 0.06 x 10^{12} tons/hr, which is more than twice as large as the total intrusion of stratospheric air into the jet stream front estimated by Reiter and Mahlman (1965a). This estimate contains the uncertainties associated with the ill-defined tropopause at the 320° and 330°K isentropic levels. Additional case studies will be needed to check the significance of these numerical estimates.

Air masses exchanged between stratosphere and troposphere at jet stream level and as traced on the 320° and 330°K isentropic surface will have to conserve their potential vorticity, except for effects of friction, turbulent mixing, and gradients in diabatic heating (Staley, 1960). Trajectories constructed on these isentropic surfaces (Fig. 17) fulfill this requirement within a factor of approximately 2. Turbulence spectra derived from aircraft measurements in the vicinity

of jet streams indicate considerable velocity fluctuations over the whole wavelength region from several meters to several hundred kilometers (Pinus et al., 1966). Over this whole broad wavelength region there appears to be a correlation between spectral density and intensity of clear-air turbulence (CAT) experienced by aircraft. Flight measurements under severe CAT conditions near the jet stream reveal nearly one order of magnitude higher spectral densities at atmospheric perturbation wavelengths of approximately 100 km than flights under light CAT or smooth flying conditions.

The prevalence of CAT near the "tropopause gap" at the level of the jet core has been found from a number of statistical investigations of pilot reports (for references, see Reiter, 1961, 1963a). From this evidence one should expect a relatively large eddy exchange of quasi-conservative air mass properties, such as potential vorticity and radio-active debris concentration levels, through the "tropopause gap" above the stable "jet stream front". From the flight measurements mentioned above, it appears that this exchange is not confined to eddy sizes characteristic of small-scale turbulence and diffusion, but extends to eddies of meso-scale and even large (synoptic)-scale dimensions. This exchange again would contribute towards a "seepage" of stratospheric air into the troposphere and vice versa.

To check the rather crude estimates of such mass flow as given in Fig. 22 for the 320° and 330°K isentropic surfaces, one will have to take recourse to measurements more refined than those available from the standard radiosonde network. Constant-density balloons and/or artificial tracer material released at strategic points within the "tropopause gap" would help to obtain more reliable estimates of exchange processes in this region.

VI. CONCLUSIONS AND OUTLOOK

The present study was designed to gain a preliminary estimate on the transport processes between stratosphere and troposphere in the jet stream region under conditions of moderate cyclogenesis. Previous studies have mainly been concerned with tracing outflow of stratospheric air through the stable layer of the jet stream front. The analyses presented in the previous chapters take a more general approach, considering the whole depth of the "tropopause gap" and dealing with inflow as well as outflow processes into and from the stratosphere.

The limitations--both in quality and quantity--of wind data in the jet stream region were felt throughout this study. Hence, some of the numerical estimates presented in the preceding chapter have to be considered as being rather crude and subject to revision. Since no drastic improvement in the present radiosonde capabilities that might alleviate these shortcomings in upper-wind data may be foreseen for the immediate future, different measurement techniques are advocated to check the characteristics of mass flow across the tropopause.

With reference to the possible exchange processes, and to the questions posed in the introduction to this paper, the following pre-liminary conclusions may be reached from the foregoing analyses:

(1) The intrusions of stratospheric air into the troposphere through the stable layer of the "jet stream front" as investigated by Reed, Staley, Danielsen, Reiter and others, although well-defined and occurring in discrete events, do not seem to constitute the entire mass flow across the tropopause.

(2) The "Staley-process" of mass exchange by re-formation of the tropopause at levels higher or lower than those originally pre-sent, should be considered of importance. The disappearance of isolated areas of stratospheric air at the 300°, 305°, and $310^{\circ}K$ isen-tropic levels (Figs. 11, 12, and 13) may corroborate this hypothesis.

(3) Turbulent mixing, as proposed by Stewart, Libby, Martell, Drevinsky, and others, may be of importance in the "tropopause gap" above the stable layer of the jet stream front. Present data do not allow adequate estimates of the magnitude of these exchange processes. The 320°K isentropic surface which characterizes these exchange processes in the present case study seems to allow "seepage" of air through the ill-defined tropopause. The magnitude of this "seepage" produced by meso- and macroscale eddies detectable from the radiosonde data is difficult to estimate. However, it may well be of the same magnitude as the intrusions of stratospheric air traced through the stably stratified jet stream front. Whether or not this type of mass exchange is associated only with well-developed jet streams could not be determined from the present analyses. From the anology with turbulence data (Pinus et al., 1966) one would expect that a correlation exists between jet stream intensity and magnitude of turbulent mass exchange in the wavelength regime of large eddies.

(4) No "preferred layers" of intrusions of stratospheric air into the troposphere could be detected within the "tropopause gap". Such intrusions could be detected on all three isentropic surfaces investigated, 310°, 320°, and 330°K. Previous investigations showed, however, that stratospheric air at the latter two isentropic levels will not reach the ground without intensive turbulent mixing (Reiter and Mahlman, 1964, 1965a). Thus, for well-defined radioactive fallout cases under "dry" conditions, i. e., in the absence of precipitation, intrusions at the 310°K isentropic level will be of main interest.

(5) Return flow of tropospheric air into the stratosphere could be identified in significant magnitude at and above the level of the jet core (i. e., at and above the 330°K isentropic surface). Outflow and inflow from and into the stratosphere, therefore, seem to be associated with the same jet stream system.

(6) The present study--although not in a conclusive way--seems to indicate that the amount of outflow from the stratosphere accomplished by the jet stream system under consideration exceeds the inflow through the same system almost by a factor of 2. It cannot be stated yet with certainty whether or not the magnitude of net flow has to be considered characteristic, and whether or not it will require a replenishing flow from other regions.

Additional case studies will be required to check these conclusions and especially the validity of the numerical estimates in the foregoing chapter. The release of constant-density balloons or of chemical tracer material into the "tropopause gap" near the 320°K surface on the cyclonic side of the jet stream would help to establish the prevailing flow pattern and advective conditions across the tropopause to a much higher degree of certainty than can be done with present radiosonde data. The release of balloons between the isentropic surfaces 330° and 340°K in the jet stream core would aid the estimate of return flow of tropospheric air into the stratosphere.

ACKNOWLEDGEMENTS

REFERENCES

Beran, D. W., 1966: Large amplitude lee waves and chinook winds. Atmospheric Science Paper No. 75, Colorado State University, 93 pp.

Bjerknes, J., and E. Palmén, 1937: Investigation of selected European cyclones by means of serial ascents. Geofysiske Publikasjoner, 12, 62 pp.

Briggs, J., and W. T. Roach, 1963: Aircraft observation near jet streams. Quarterly Journal of the Royal Meteorological Society, 89, 225-247.

Danielsen, E. F., 1959a: A determination of the mass transported from stratosphere to troposphere over North America during a thirty-six hour interval (abstract). Mitteilungen des Deutschen Wetter-dienstes, 20, 10-11.

_____, 1959b: The laminar structure of the atmosphere and its relation to the concept of a tropopause. Archiv für Meteorologie, Geophysik und Bioklimatologie, A 11, 293-332.

_____, 1964a: Radioactivity transport from stratosphere to tropo-sphere. Mineral Industries, 33, 1-7.

_____, 1964b: Project Springfield Report. Defense Atomic Support Agency, 97 pp.

_____, K. H. Bergman, and C. A. Paulson, 1962: Radioisotopes, potential temperature and potential vorticity--a study of strato-spheric-tropospheric exchange processes. Department of Meteorology and Climatology, University of Washington, 54 pp.

Defant, F., 1958: Die allgemeine atmosphärische Zirkulation in neuerer Betrachtungsweise. Geophysica, 6, 189-217.

Endlich, R. M., 1954: A note on pressure at the tropopause. Bulletin of the American Meteorological Society, 35, 131-132.

_____, and G. S. McLean, 1957: The structure of the jet stream core. Journal of Meteorology, 14, 543-552.

Fleagle, R. G., 1947: The fields of temperature, pressure and three-dimensional motion in selected weather situations. Journal of Meteorology, 4, 165-185.

Hsieh, Y. P., 1949: An investigation of a selected cold vortex over North America. Journal of Meteorology, 6, 401-410.

_____, 1950: On the formation of shear lines in the upper atmosphere. Journal of Meteorology, 7, 382-387.

Libby, W. F., 1956: Radioactive strontium fallout. Proceedings of the National Academy of Sciences, 42, 365-390.

Mahlman, J. D., 1964a: Relation of stratospheric-tropospheric mass exchange mechansims to surface radioactivity peaks. M. S. Thesis, Colorado State University, 54 pp.

_____, 1964b: Relation of stratospheric-tropospheric mass exchange mechanisms to surface radioactivity peaks. Atmospheric Science Paper No. 58, Colorado State University, 1-19.

_____, 1964c: On the feasibility of relating seasonal fallout oscillations to hemispheric index patterns. Atmospheric Science Paper No. 58, Colorado State University, 55-58.

_____, 1965: Relation of tropopause-level index changes to radioactive fallout fluctuations. Atmospheric Science Paper No. 70, Colorado State University, 84-109.

_____, 1966: Atmospheric general circulation and transport of radioactive debris. Atmospheric Science Paper No. 103, Colorado State University, 184 pp.

Martell, E. A., and P. J. Drevinsky, 1960: Atmospheric transport of artificial radioactivity. Science, 132, 1523-1531.

McClain, E. P., and E. F. Danielsen, 1955: Zonal distribution of baroclinity for three Pacific storms. Journal of Meteorology, 12, 314-323.

Miyake, Y., K. Saruhashi, T. Katswagi, and T. Kanazawa, 1960: Radioactive fallout in Japan and its bearing on meteorological conditions. Papers in Meteorology and Geophysics, Tokyo, 9, 172-176.

_____, K. Saruhashi, Y. Katsuragi, and T. Kanazawa, 1962: Seasonal variation of radioactive fallout. Journal of Geophysical Research, 67, 189-193.

Murgatroyd, R. J., 1959: Jet stream flight of 6th March 1959. Unpublished report.

Palmén, E., 1933: Aerologische Untersuchungen der atmosphärischen Störungen. Mitt. meteor. Inst. Univ. Helsingf. No. 25.

Pinus, N. Z., E. R. Reiter, G. N. Shur, and N. K. Vinnichenko, 1966: Power spectra of turbulence in the free atmosphere (to be published in Tellus).

Reed, R. J., 1955: A study of a characteristic type of upper-level frontogenesis. Journal of Meteorology, 12, 226-237.

_____, and E. F. Danielsen, 1959: Fronts in the vicinity of the tropopause. Archiv für Meteorologie, Geophysik und Bioklimatologie, A 11, 1-17.

_____, and F. Sanders, 1953: An investigation of the development of a mid-tropospheric frontal zone and its associated vorticity field. Journal of Meteorology, 10, 338-349.

Reiter, E. R., 1961: Meteorologie der Strahlstrome (Jet Streams). Vienna, Springer, 473 pp.

_____, 1963a: Jet Stream Meteorology. University of Chicago Press, 513 pp.

_____, 1963b: A case study of radioactive fallout. Journal of Applied Meteorology, 2, 691-705.

_____, 1964: Comments on paper by S. Penn and E. A. Martell, "An analysis of the radioactive fallout over North America in late September 1961". Journal of Geophysical Research, 69, 786-788.

_____, D. W. Beran, J. D. Mahlman, and G. Wooldridge, 1965: Effect of large mountain ranges on atmospheric flow patterns as seen from Tiros satellites. Atmospheric Science Paper No. 69, Colorado State University, 111 pp.

_____, and J. D. Mahlman, 1964: Heavy radioactive fallout over the southern United States, November 1962. Atmospheric Science Paper No. 58, Colorado State University, 21-49.

_____, and J. D. Mahlman, 1965a: A case study of mass transport from stratosphere to troposphere, not associated with surface fallout. Atmospheric Science Paper No. 70, Colorado State University, 54-83.

Reiter, E. R. , 1965b: Heavy radioactive fallout over the southern United States, November 1962. Journal of Geophysical Research, 70, 4501-4520.

_____, and A. Nania, 1964: Jet stream structure and clear-air turbulence (CAT). Journal of Applied Meteorology, 3, 247-260.

_____, and L. F. Whitney, 1965: Subtropical or polar front jet stream? Atmospheric Science Paper No. 66, Colorado State University, 11 pp.

Staley, D. O. , 1960: Evaluation of potential vorticity changes near the tropopause and the related vertical motion, vertical advection of vorticity, and the transfer of radioactive debris from the strato- sphere to the troposphere. Journal of Meteorology, 17, 591-620.

_____, 1962: On the mechanism of mass and radioactivity transport from stratosphere to troposphere. Journal of the Atmospheric Sciences, 19, 450-457.

Stewart, N. G. , R. N. Crooks, and E. M. Fisher, 1955: Atomic Energy Research Establishment, Publication No. AERE HP/R 1701, Harwell.

_____, R. G. D. Osmond, R. N. Crooks, E. M. Fisher, and M. J. Owens, 1957: The world-wide deposition of long-lived fission products from nuclear explosions. Atomic Energy Research Establishment, Publication No. AERE HP/R 2790, Harwell.

Storebø, P. B. , 1959: Orographical and climatological influences on deposition of nuclear-bomb debris. Journal of Meteorology, 16, 600-108.
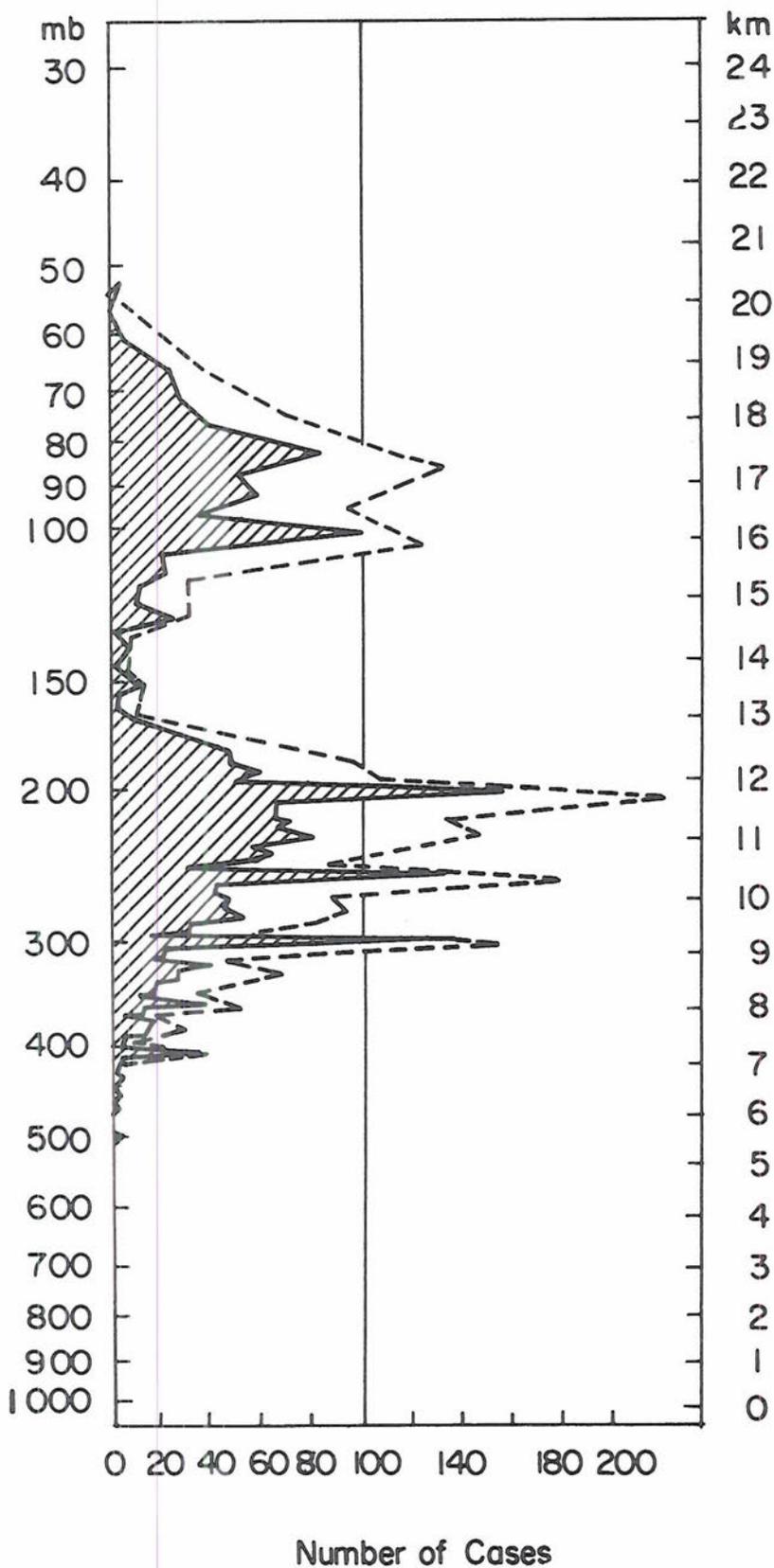
FIG. 1. Frequency distribution of tropopause pressures (mb), January 1956, for 2500 radio-sonde ascents over the Northern Hemisphere. Shaded: frequency distributions for 5-mb intervals; dashed: frequency distribution for 10-mb intervals (after Defant, 1958).
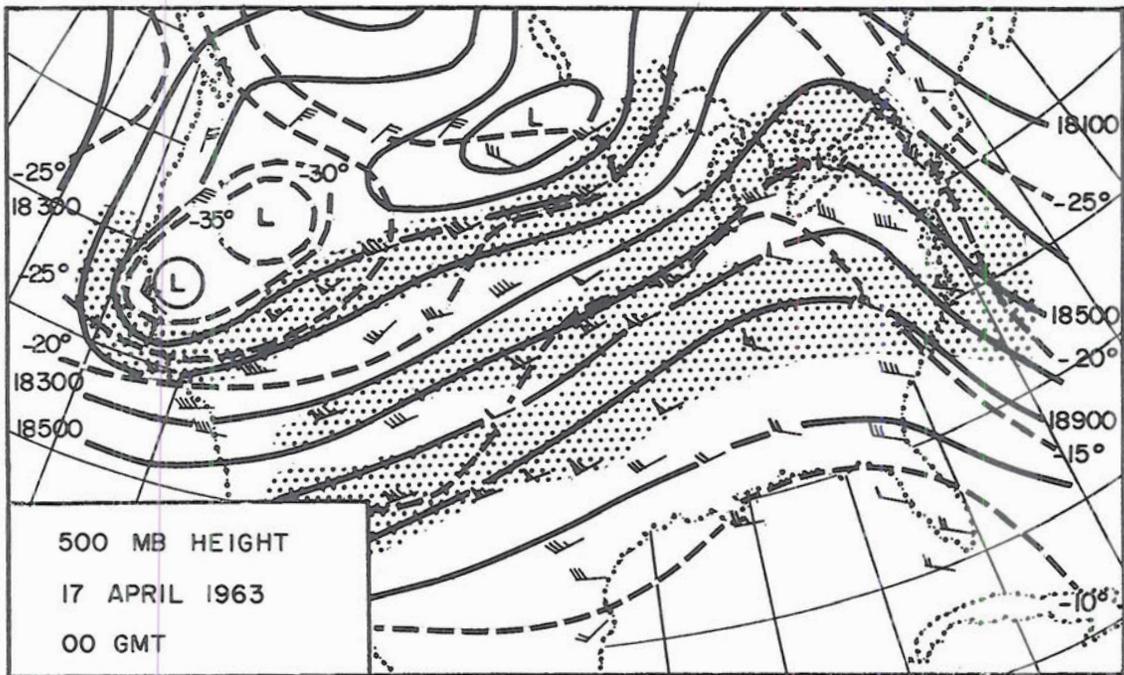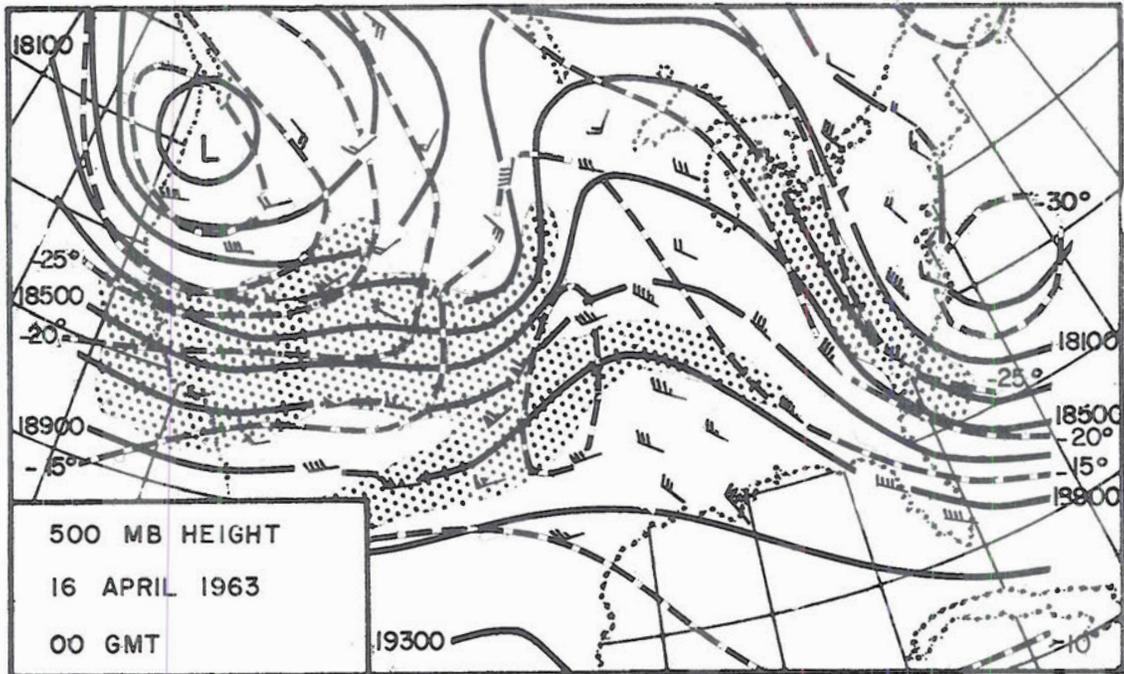
FIG. 2. 500-mb contour heights (ft, full lines), and isotherms (°C, dashed lines), for observation times as indicated. Areas with wind speeds > 50 knots are shaded (after U. S. Weather Bureau Daily Weather Map Series).

500 MB HEIGHT
18 APRIL 1963
00 GMT

500 MB HEIGHT
19 APRIL 1963
00 GMT
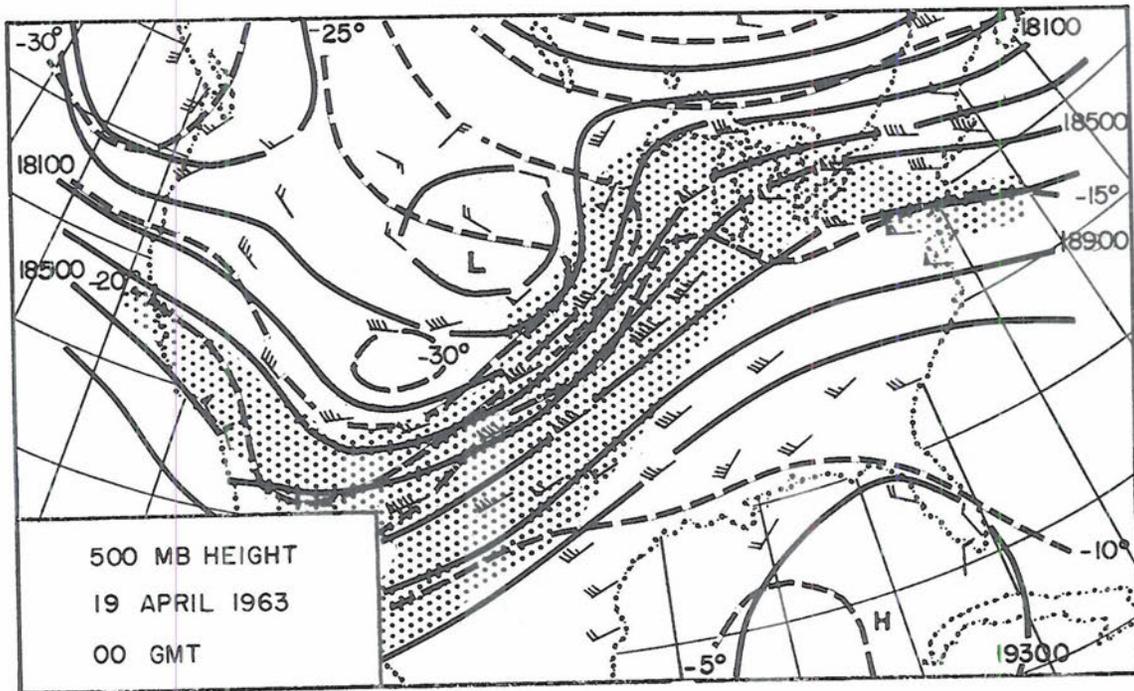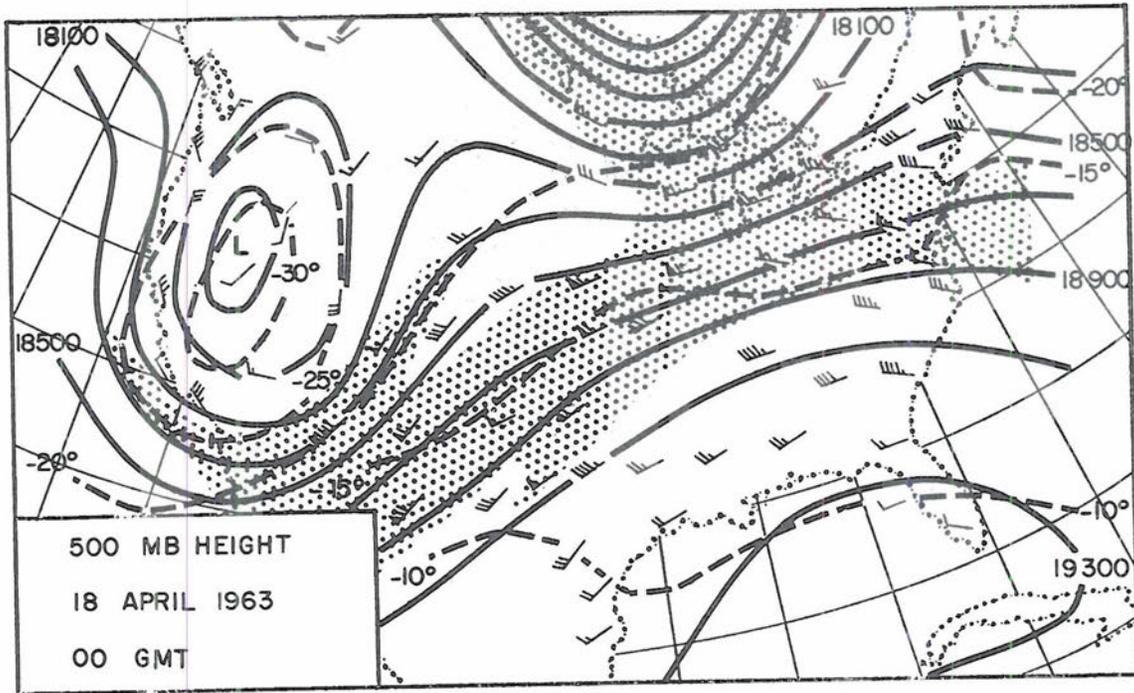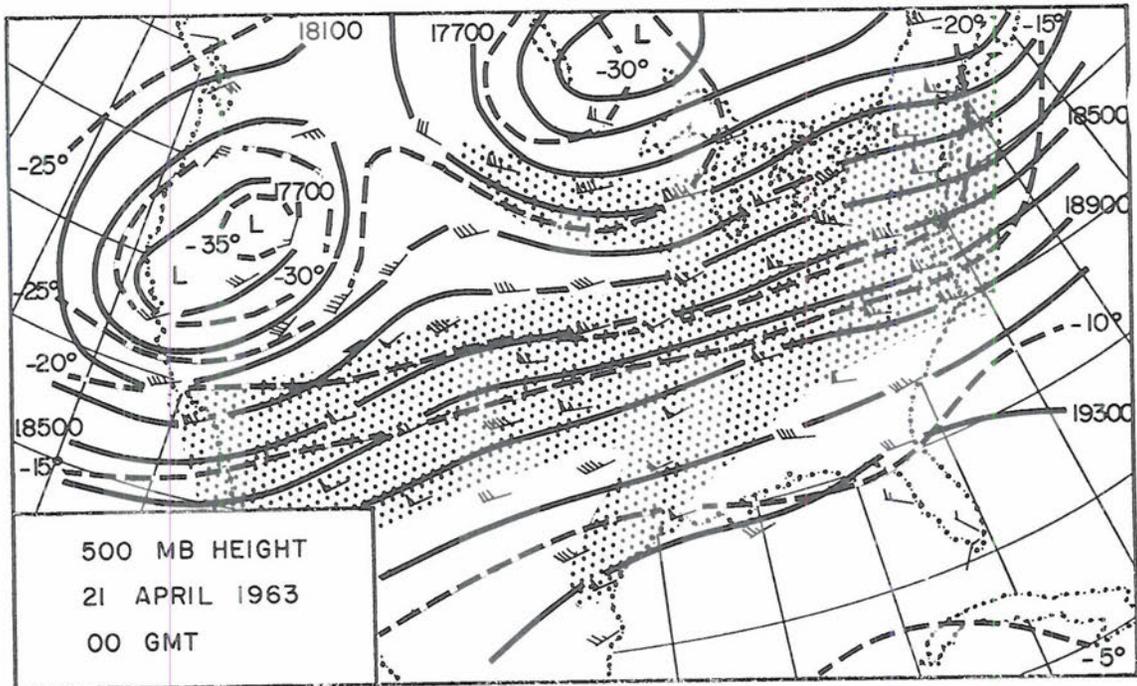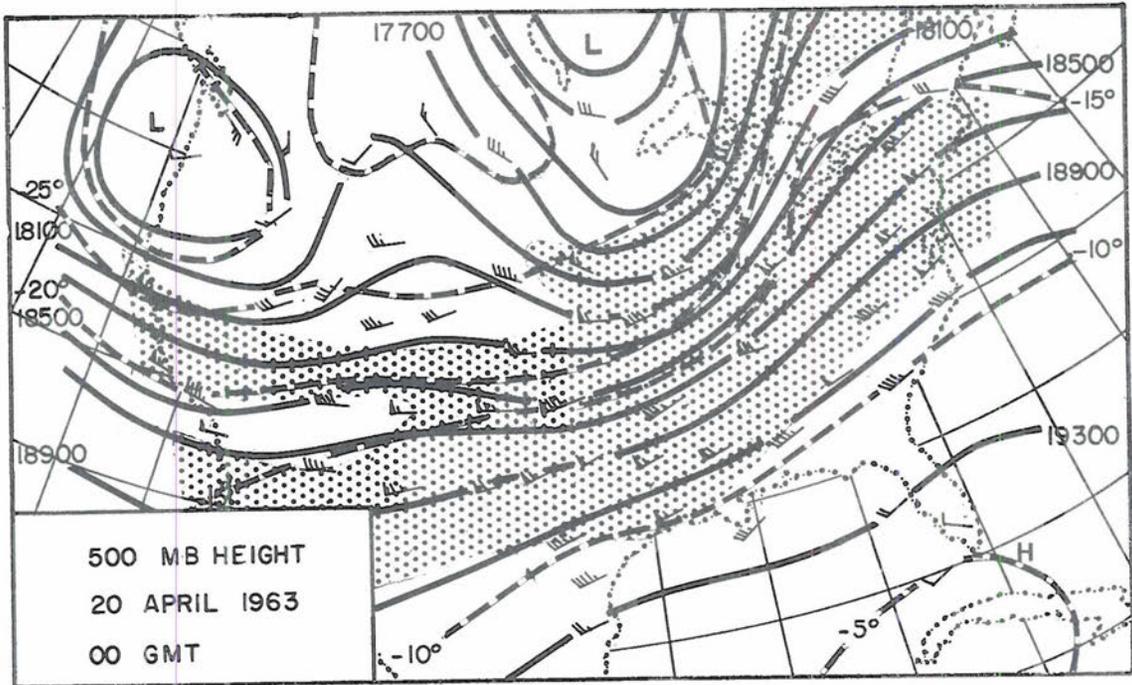
FIG. 2. Continued.

FIG. 2. Continued.
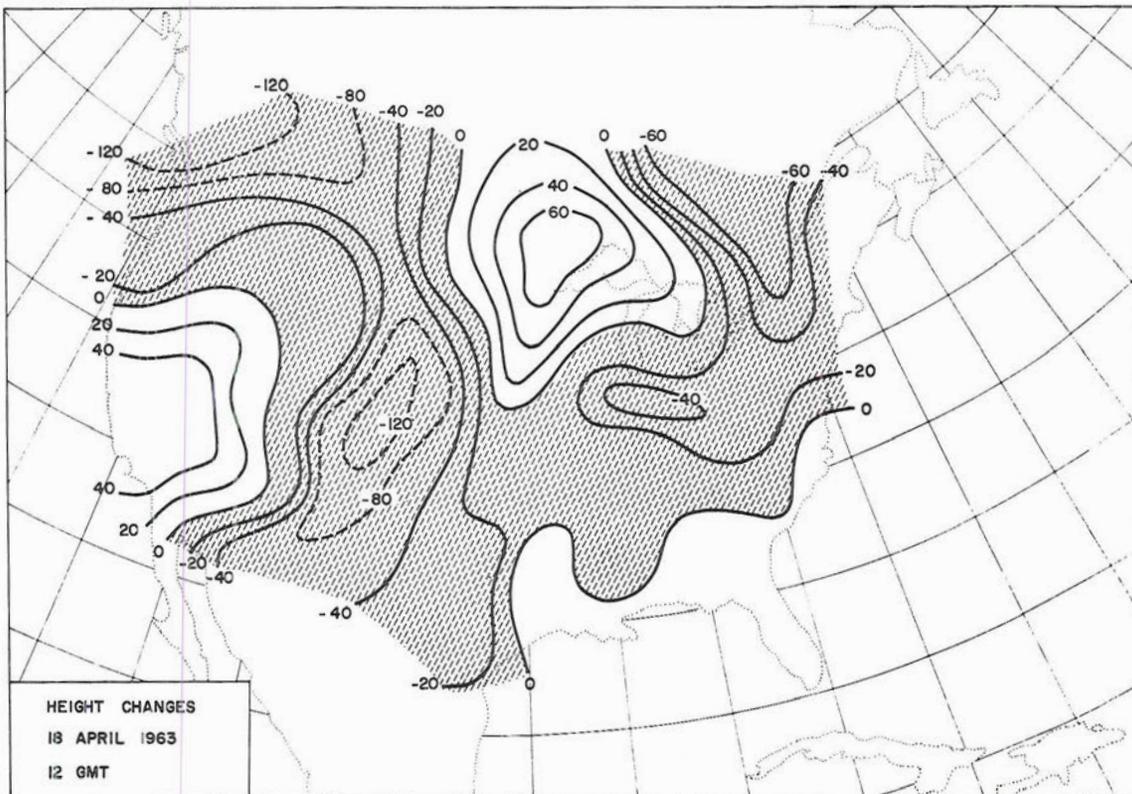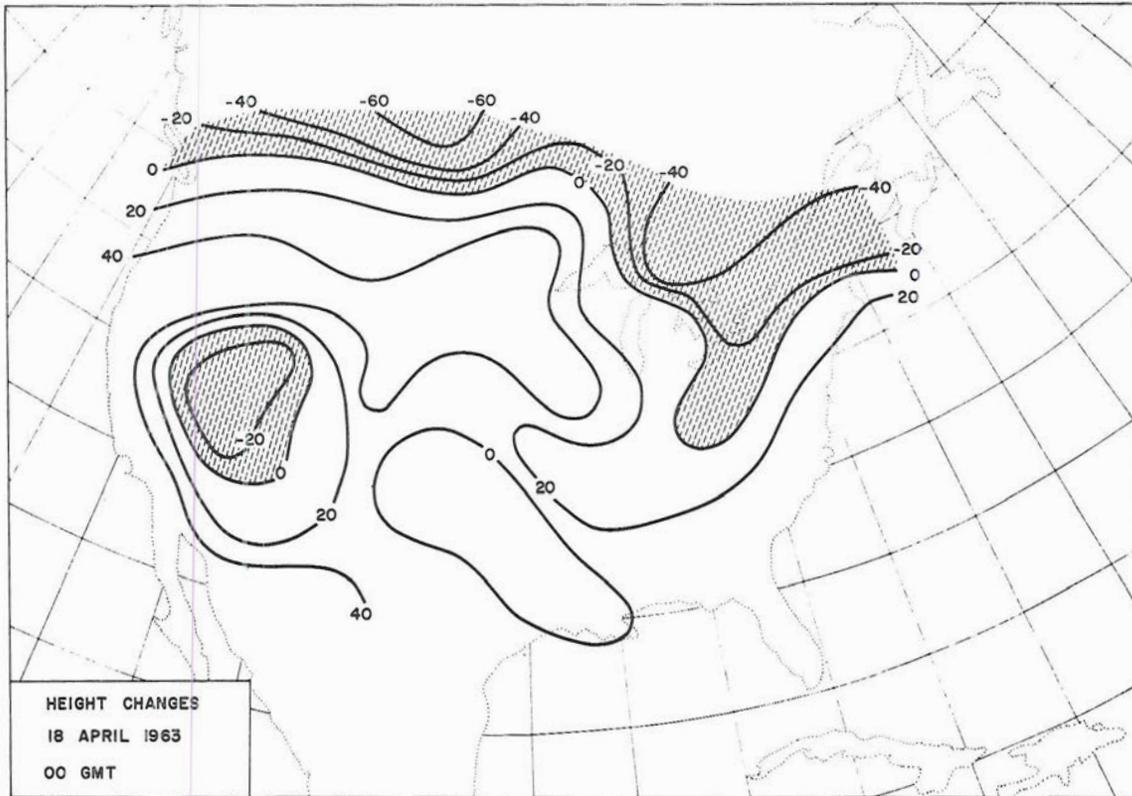
FIG. 3. Twelve-hour height changes (m) of the 500-mb level for periods ending at observation times indicated on map. Areas of height falls are shaded.

HEIGHT CHANGES
19 APRIL 1963
00 GMT

HEIGHT CHANGES
19 APRIL 1963
12 GMT

FIG. 3. Continued.

FIG. 4. Surface frontal positions and isobars of lowest pressure (mb) associated with developing cyclone, 17 April 1963, 06 GMT, to 20 April 06 GMT.
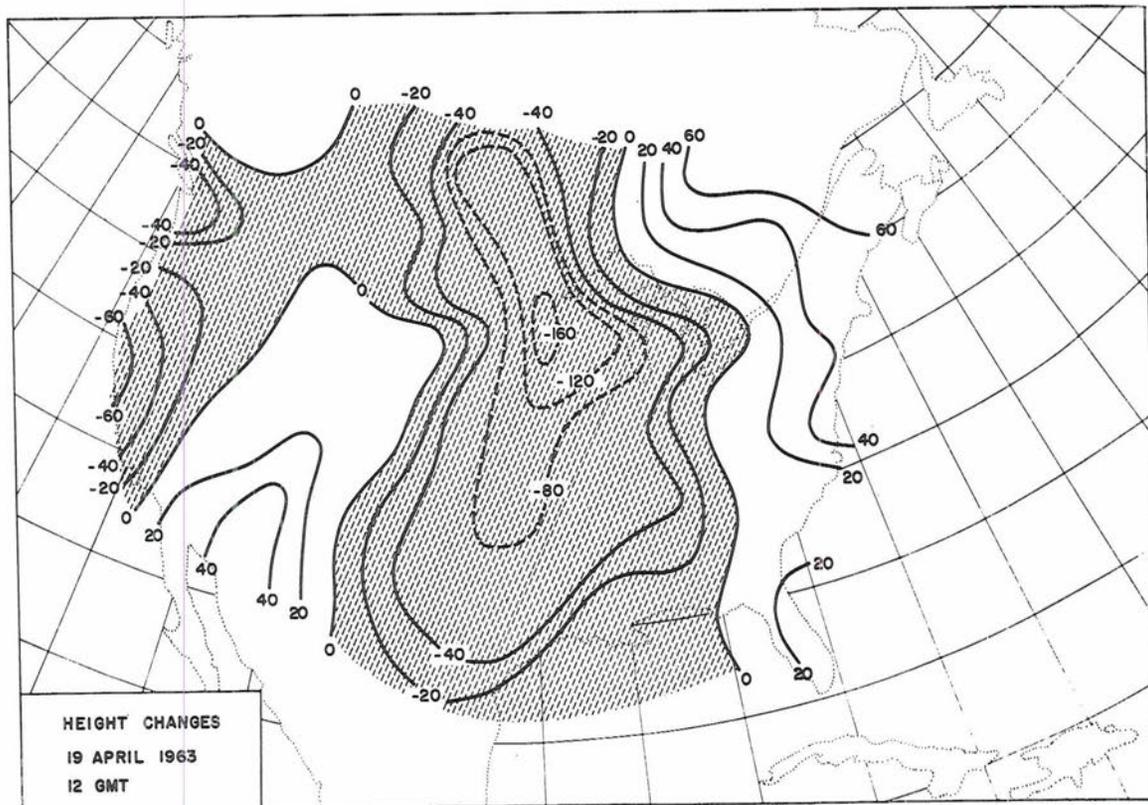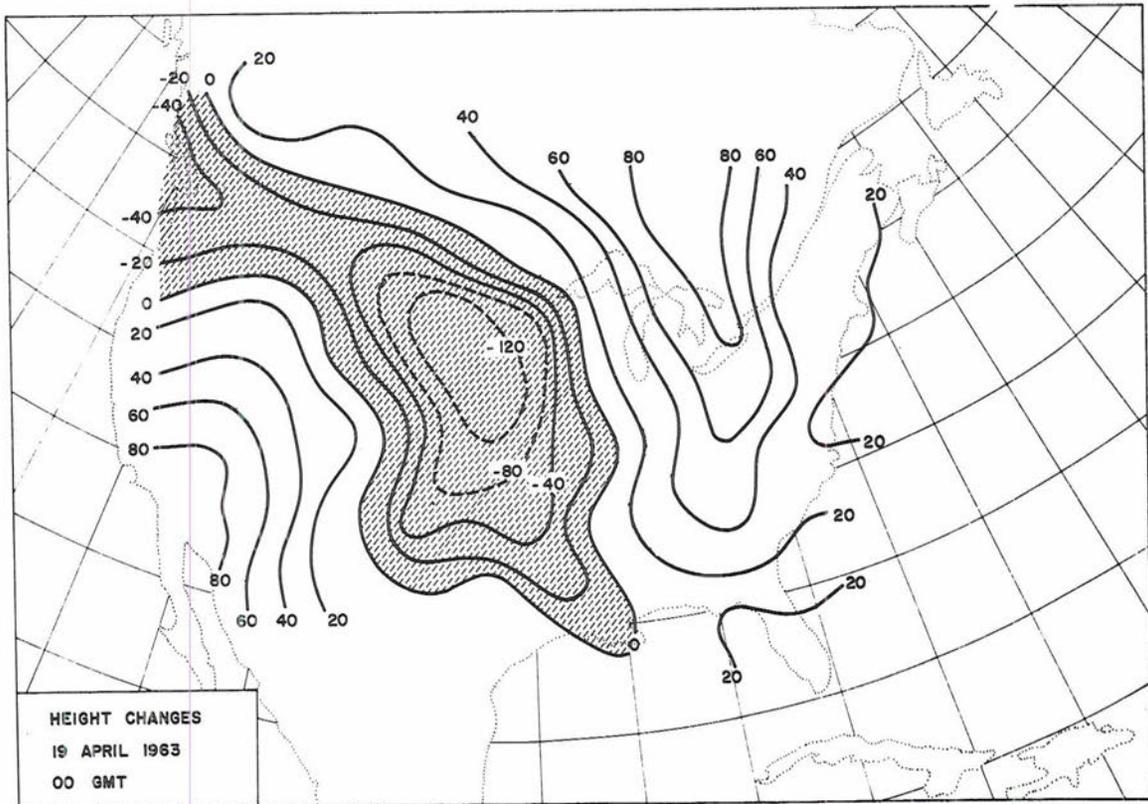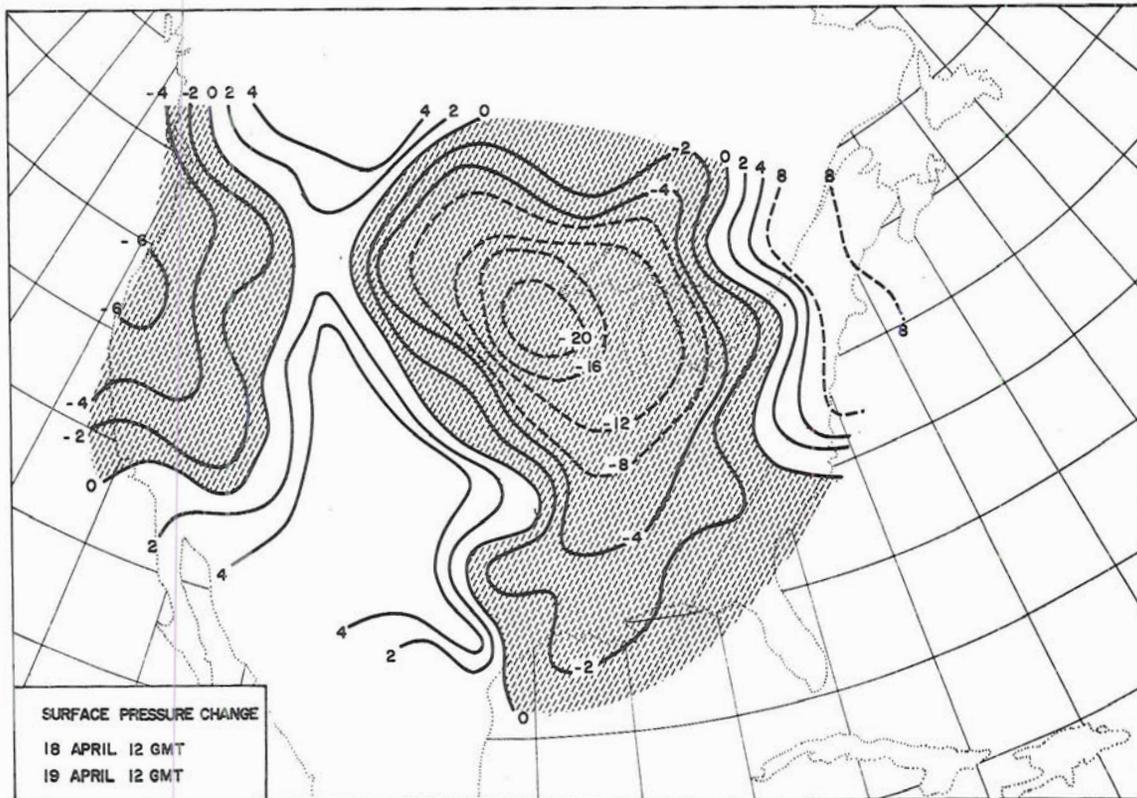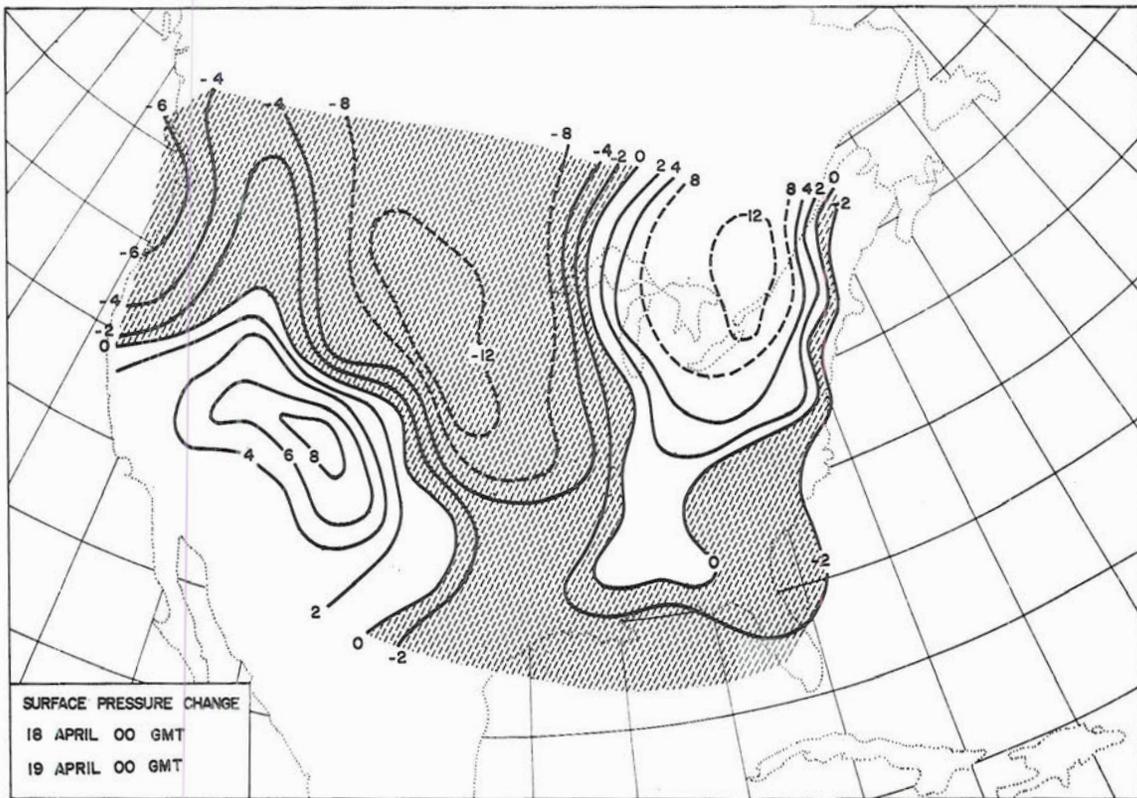
FIG. 5. Twenty-four hour surface pressure changes (mb) for periods as indicated. Regions with pressure falls are shaded.
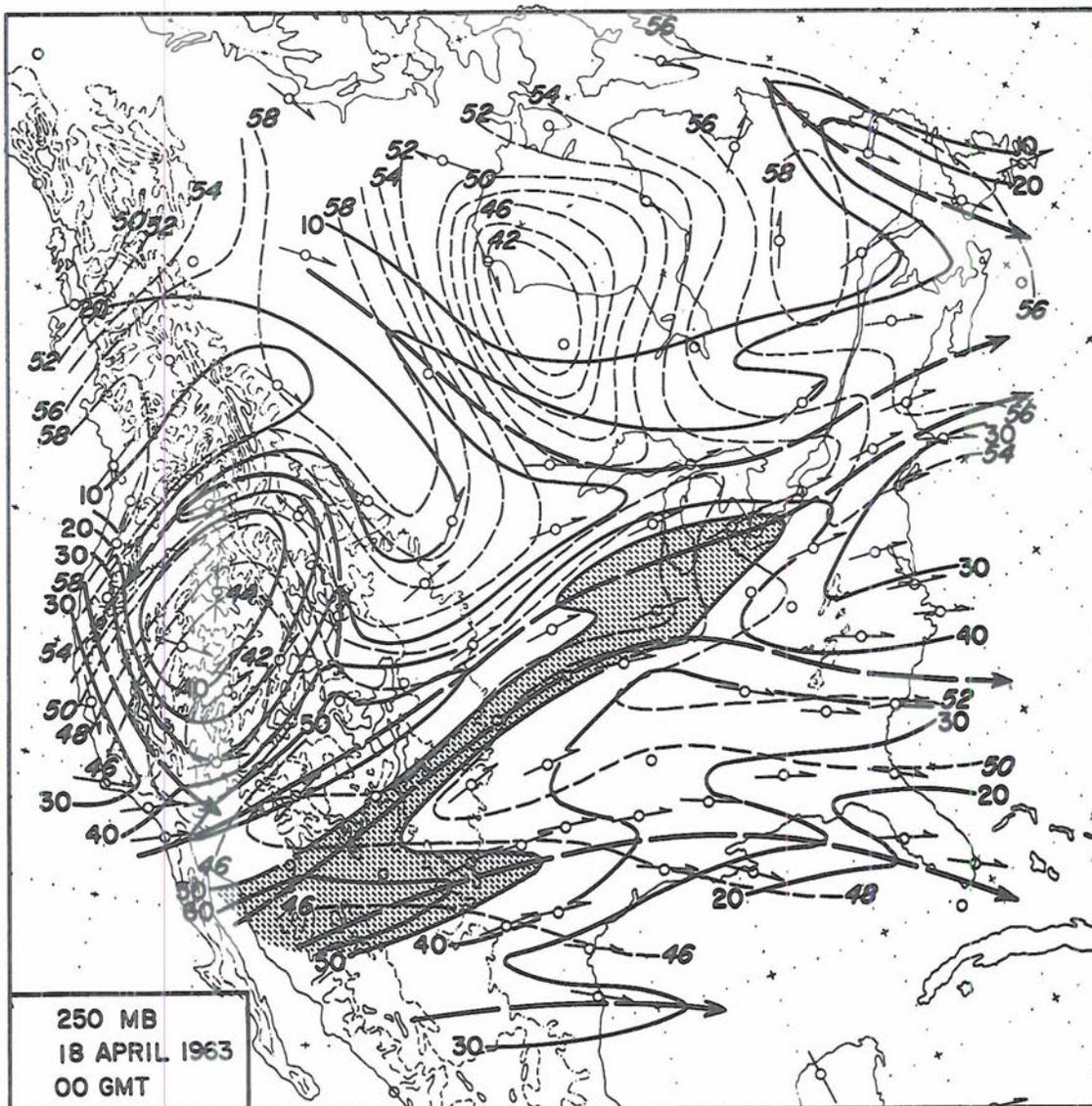
FIG. 6. 250-mb isotachs (solid lines, mps, vertical numbers, areas > 50 mps are shaded) and isotherms (thin dashed lines, $^{\circ}$C, slanting numbers, minus signs omitted) for dates and observation times as indicated. Jet axes are marked by heavy dashed lines with arrows (after Reiter et al., 1965).

250 MB
18 APRIL 1963
12 GMT

FIG. 6. Continued.

250 MB
19 APRIL 1963
00 GMT
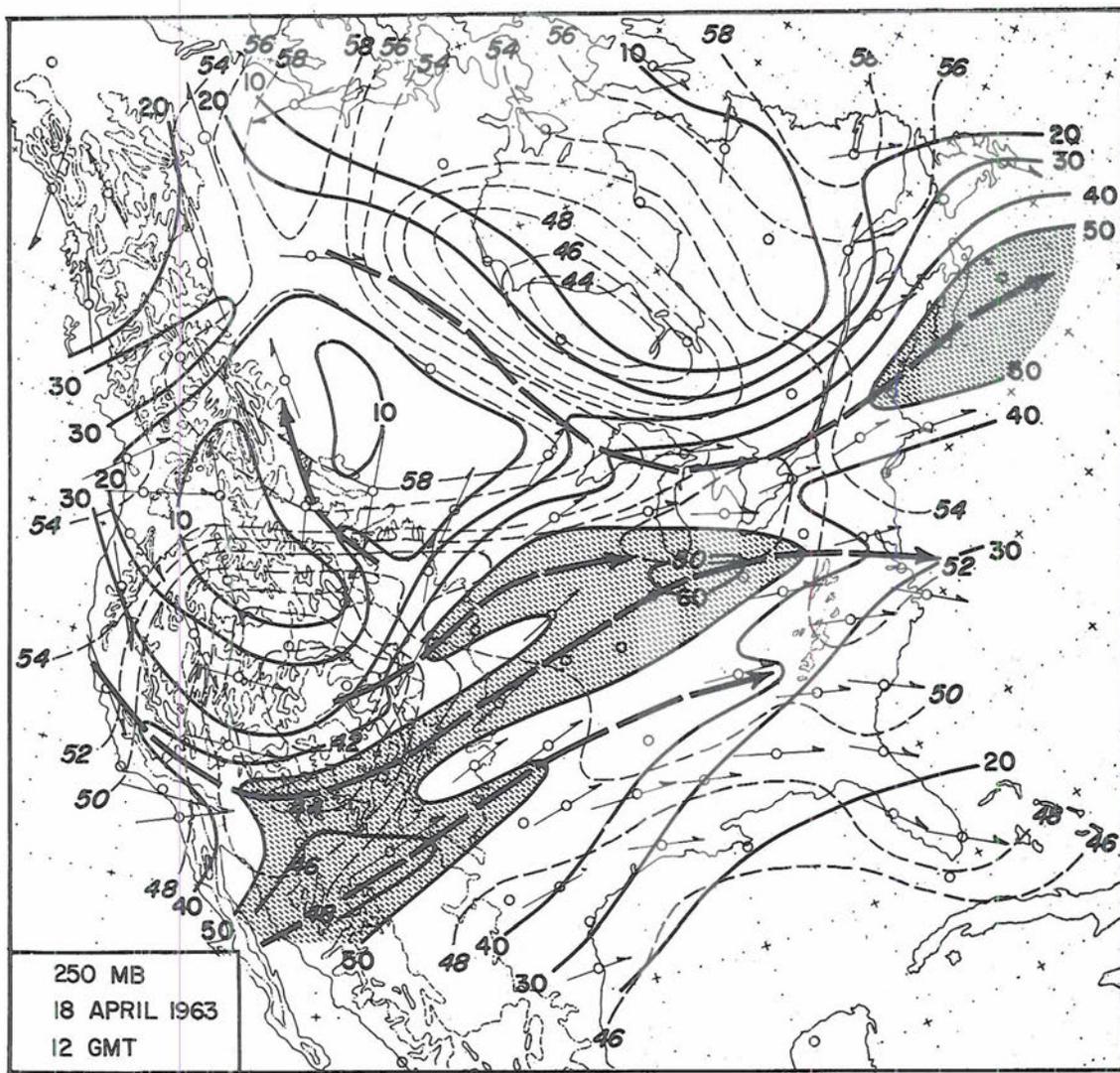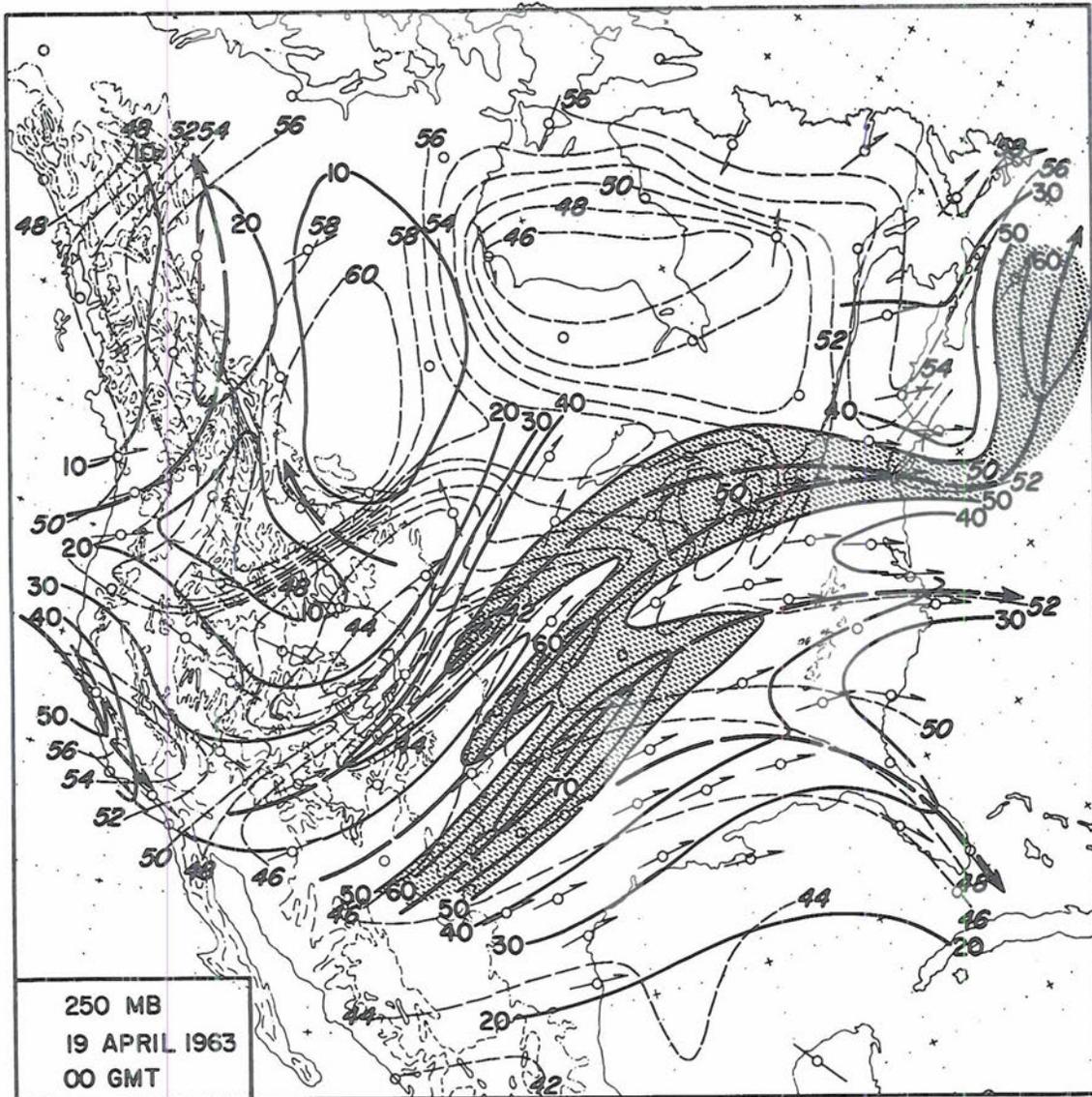
FIG. 6. Continued.

FIG. 7. Cross sections through the atmosphere for observation times and stations as indicated. Potential temperatures: $^\circ$K, solid and long dashed lines; relative humidities: per cent, short-dashed lines. "A" indicates "motorboating". Regions with "motorboating" reports are shaded. Stable layers and tropopause are marked by heavy dashed and solid lines. Potential vorticity values (10^{-9} cm sec deg g^{-1}) are entered numerically on the 310°, 320°, and 330°K isentropic surfaces.

Station Abbreviations:

ABI	Abilene, Texas	GJT	Grand Junction, Colorado
ALB	Albany, New York	INW	Winslow, Arizona
AMA	Amarillo, Texas	LND	Lander, Wyoming
BRJ	Burrwood, Louisiana	OKC	Oklahoma City, Oklahoma
CAR	Caribou, Maine	PWM	Portland, Maine
DCA	Washington, D. C.	SHV	Shreveport, Louisiana
DDC	Dodge City, Kansas	SLC	Salt Lake City, Utah
DEN	Denver, Colorado	TUS	Tucson, Arizona
DRT	Del Rio, Texas	ZV	Sept-Îles, Quebec
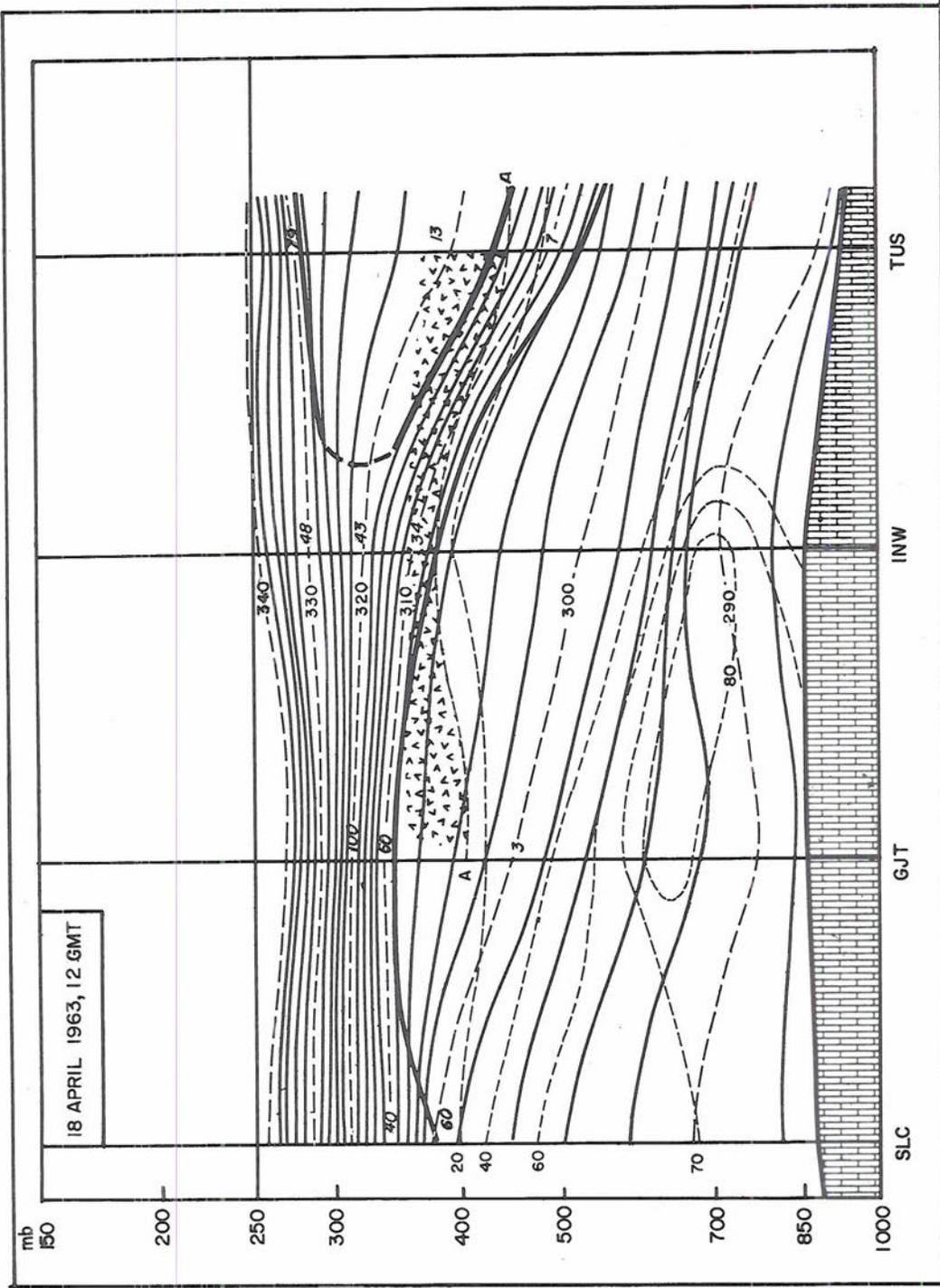
FIG. 7. Continued.
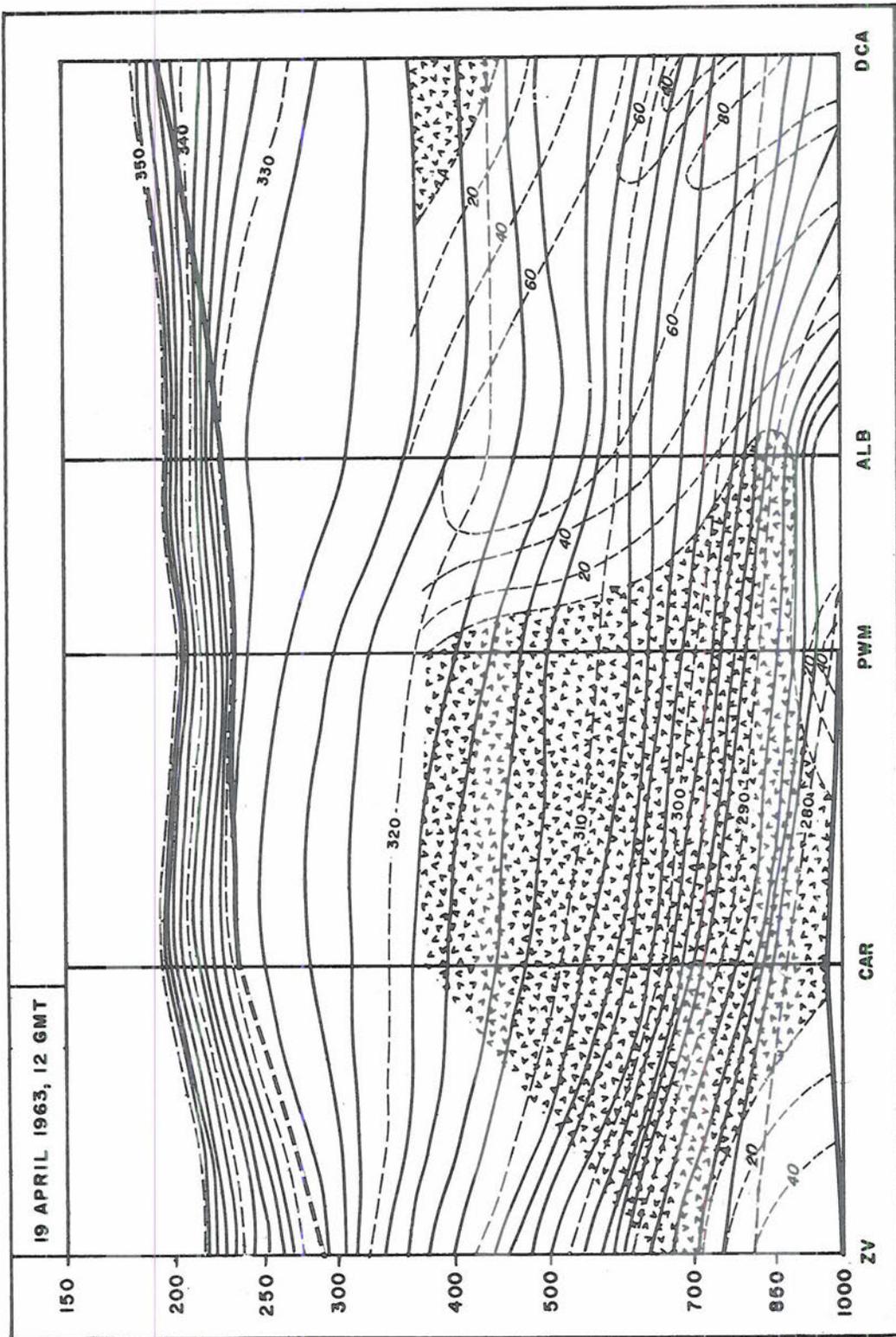
FIG. 7. Continued.
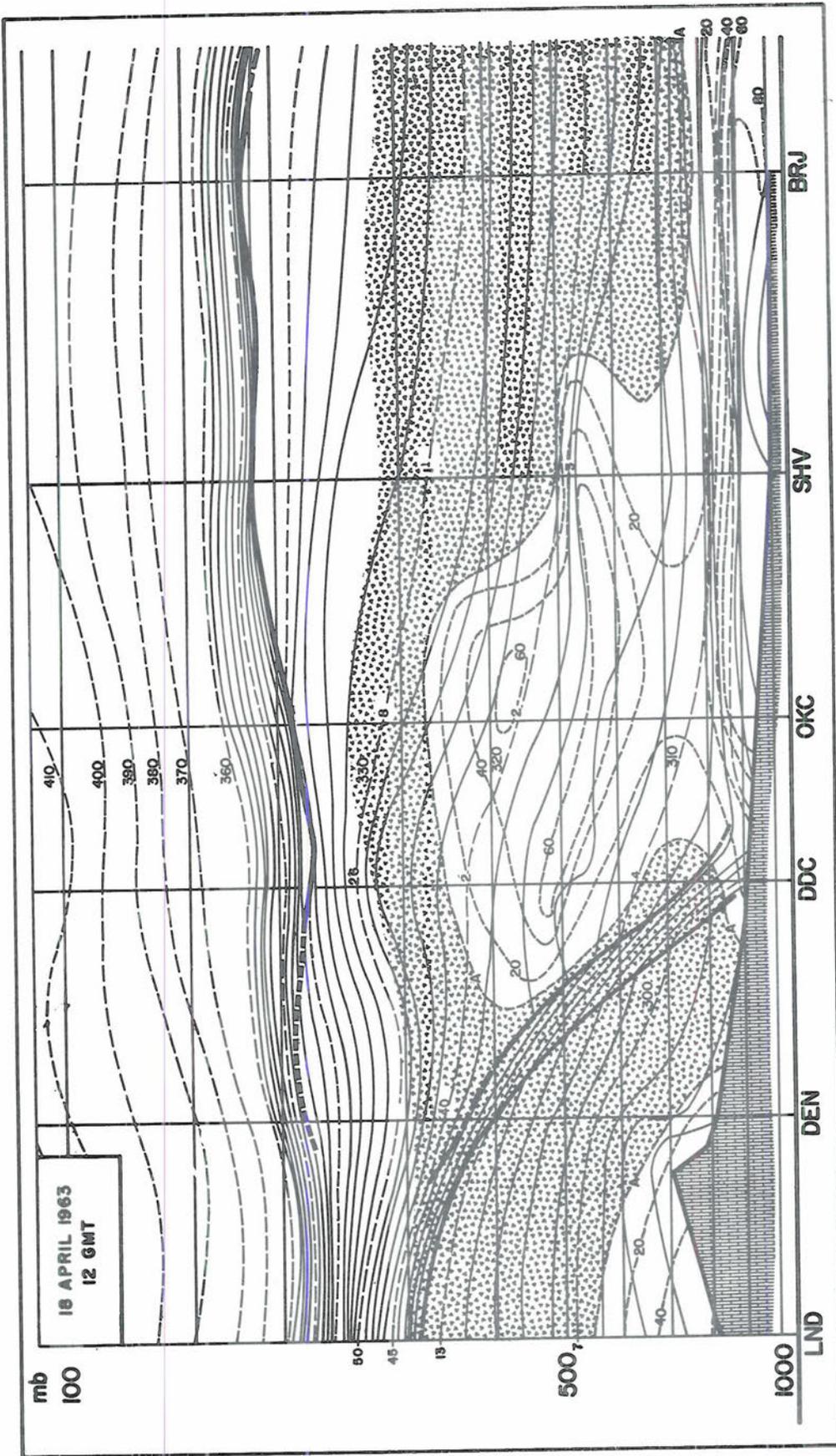
FIG. 7. Continued.
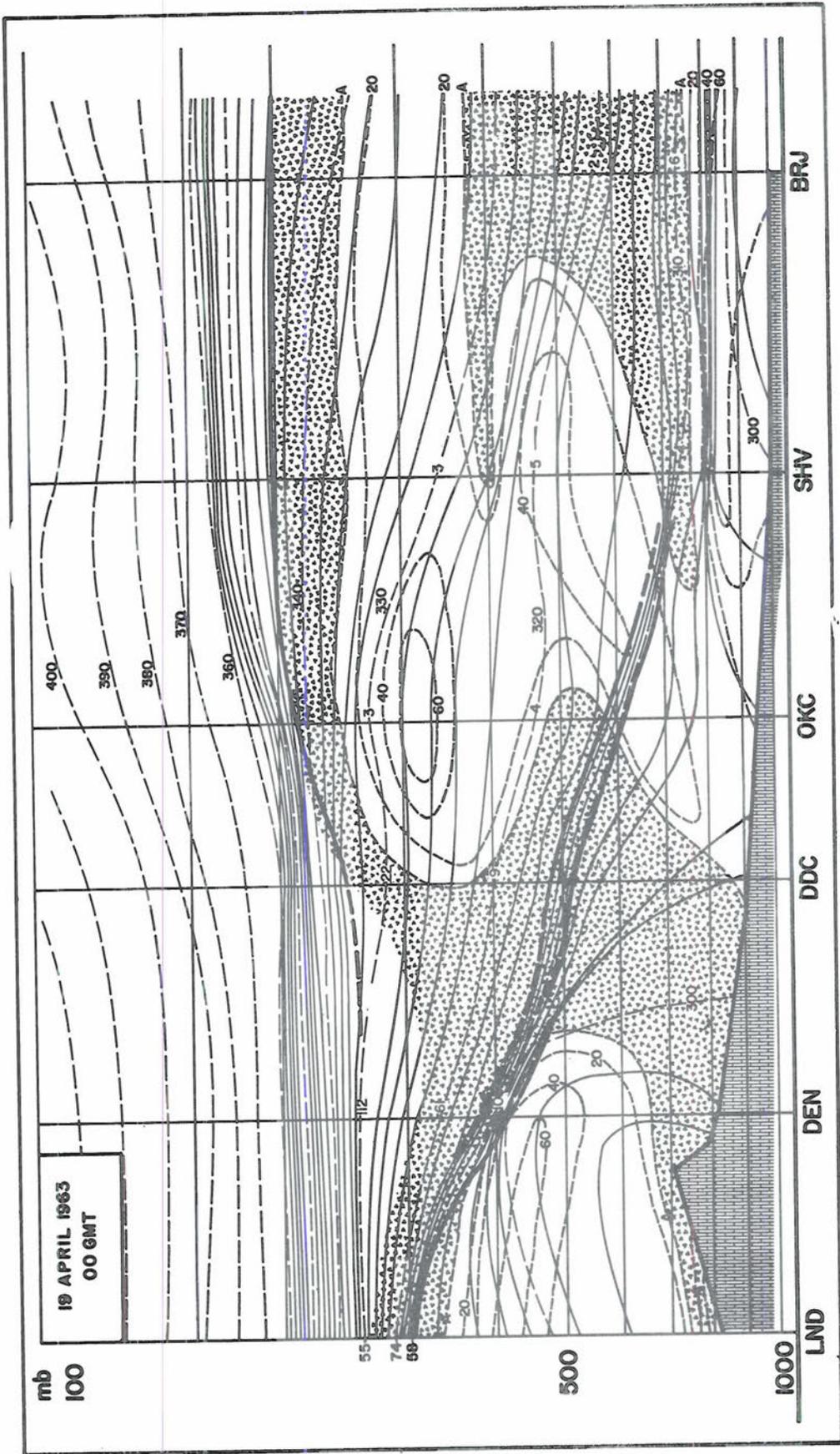
FIG. 7. Continued.
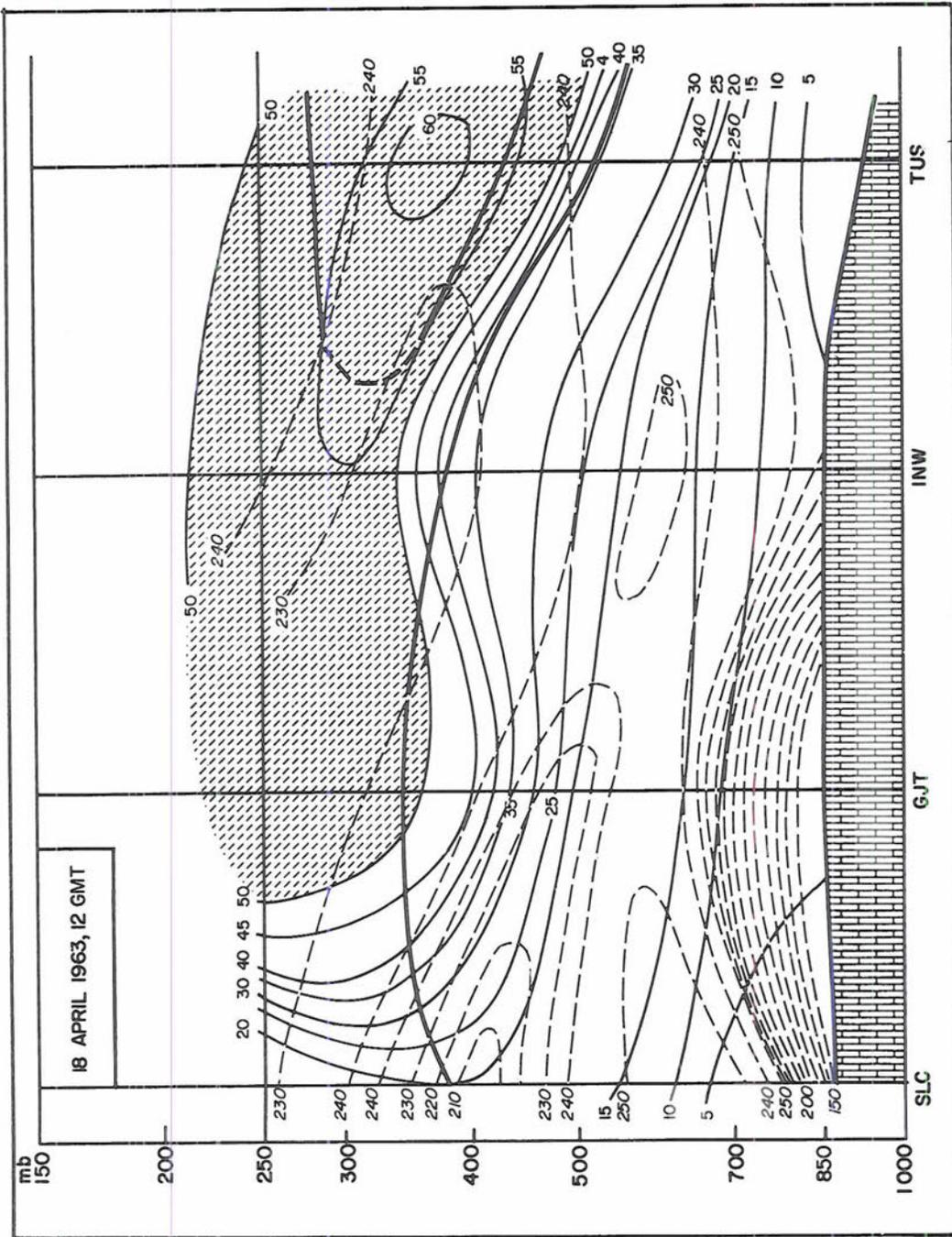
FIG. 7. Continued.

FIG. 8. Same as Fig. 7, except: Wind speeds: mps, thin solid lines; wind directions: degrees, dashed lines. Regions with speeds > 50 mps are shaded.
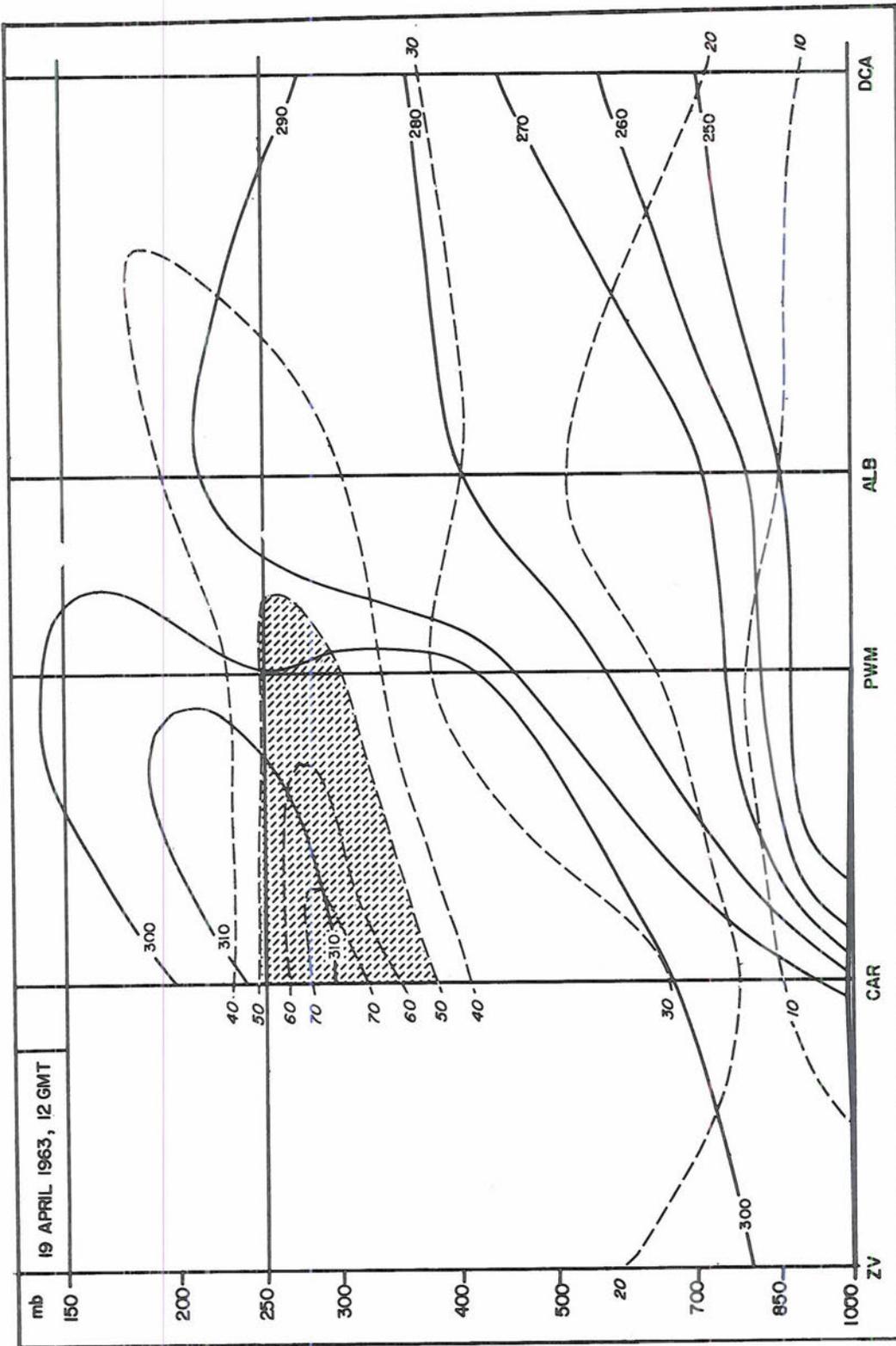
FIG. 8. Continued.
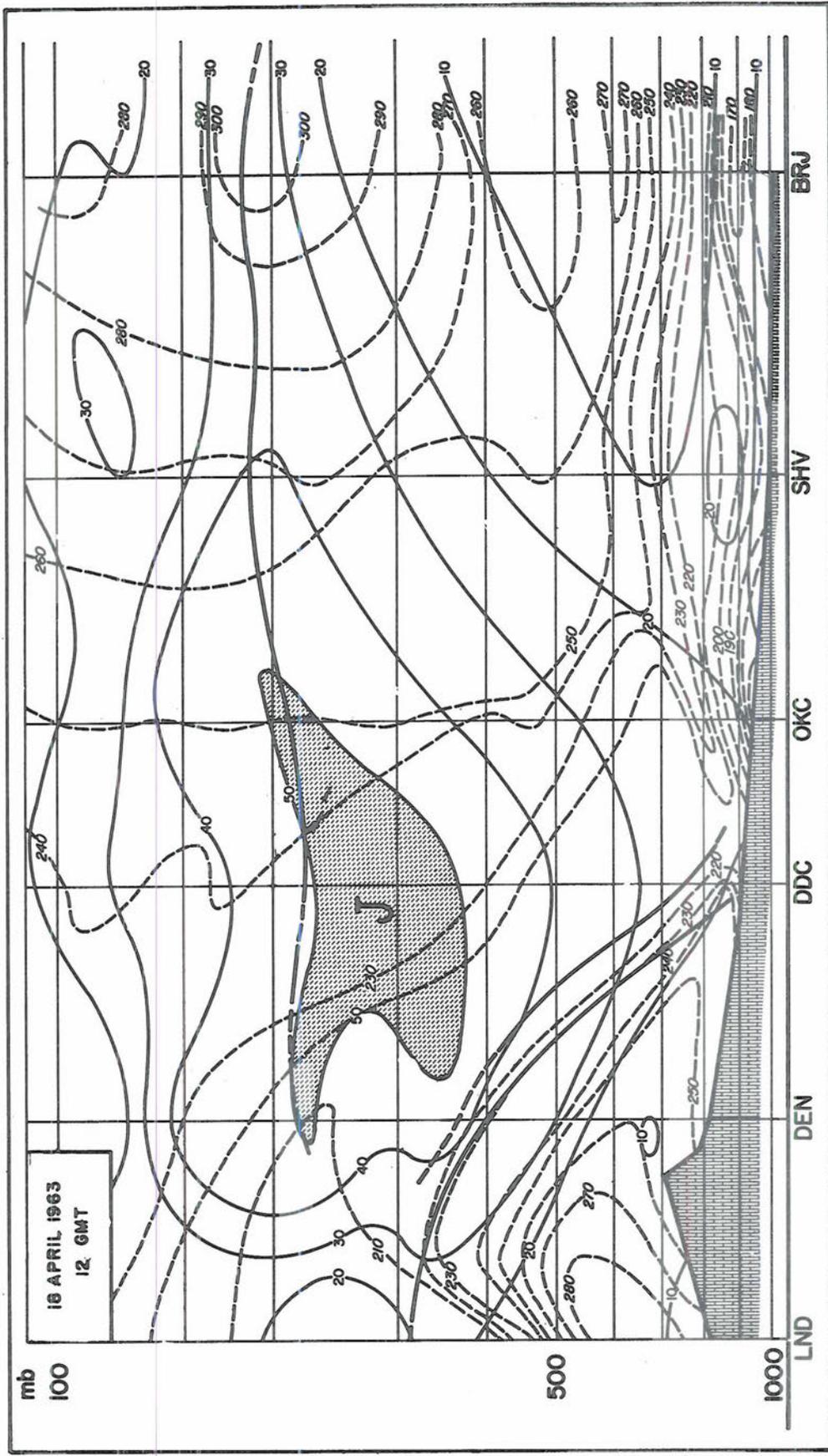
FIG. 8. Continued.
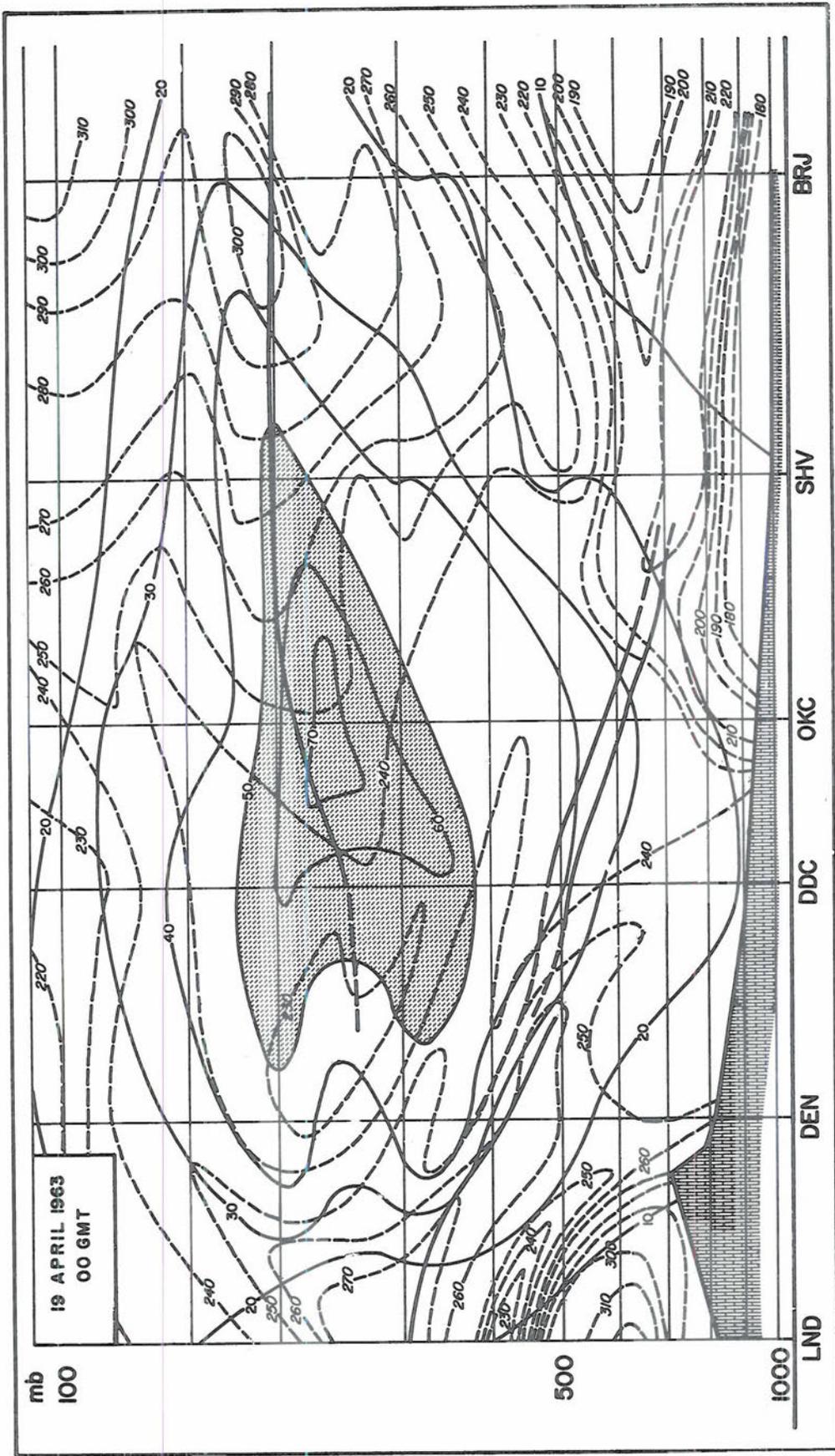
FIG. 8. Continued.

FIG. 8. Continued.
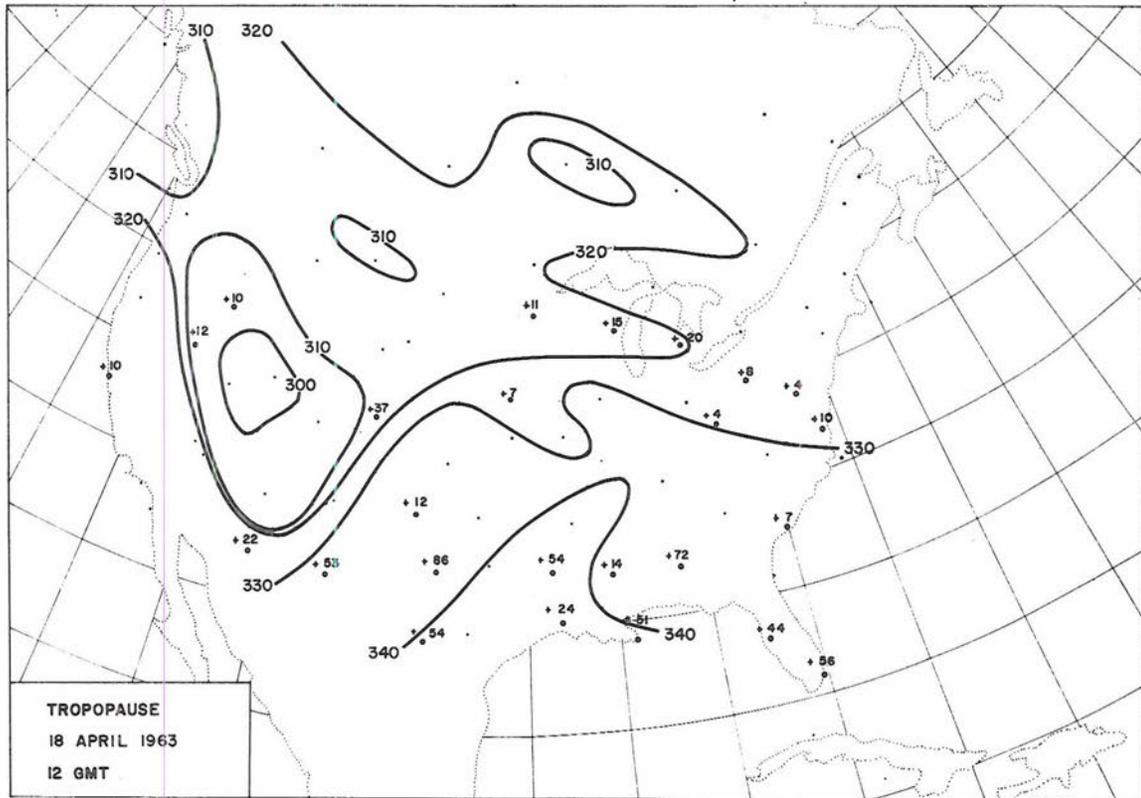
FIG. 9. Potential temperatures (°K) of tropopause level for observation times as indicated. Small dots indicate stations over which coded tropopause agrees with re-defined tropopause. Large dots mark stations with discrepancy in tropopause levels. Numerical values (°C) stand for $T_{coded} - T_{re-defined}$.

TROPOPAUSE
19 APRIL 1963
00 GMT
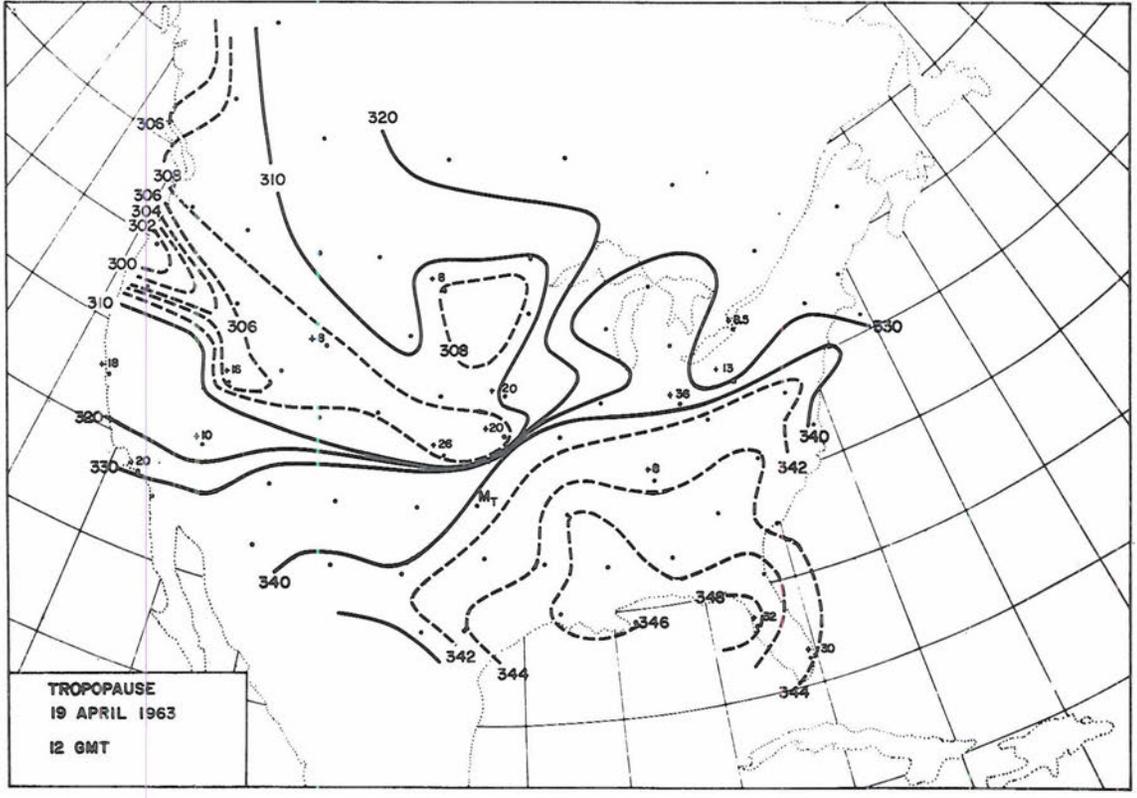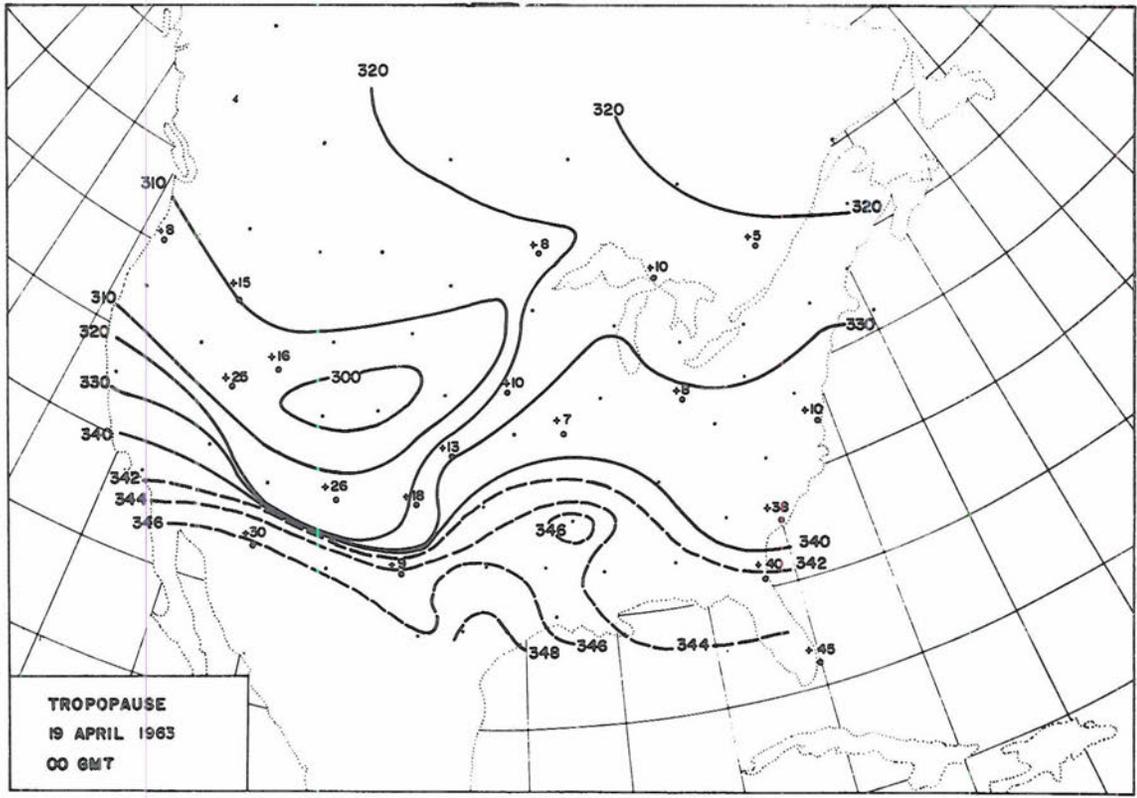
TROPOPAUSE
19 APRIL 1963
12 GMT

FIG. 9. Continued.
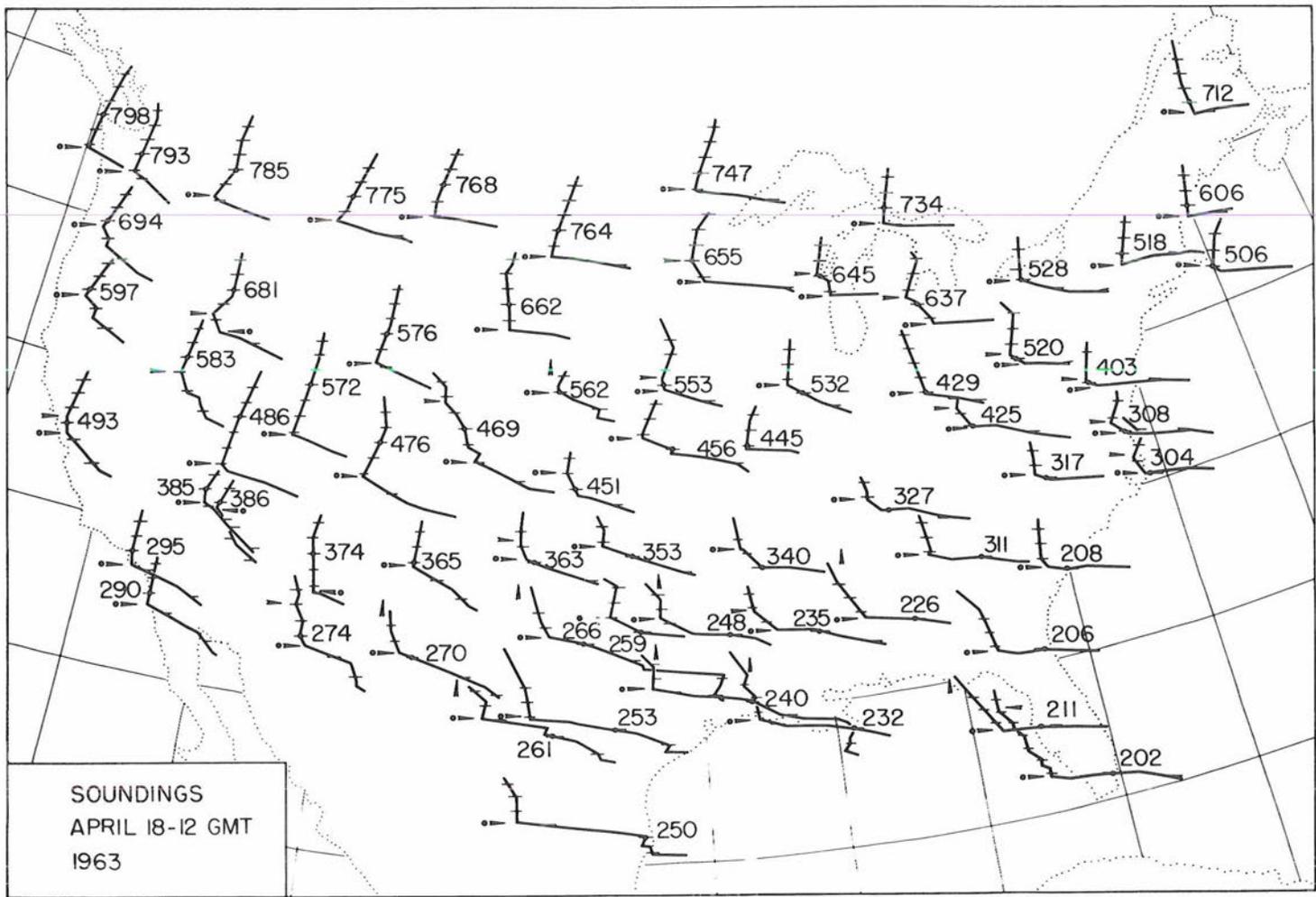
FIG. 10. Portions of radiosonde ascents near tropopause level, plotted on tephigram, for observation times as indicated. Station numbers are plotted for each sounding. Thin horizontal lines along each sounding indicate potential temperature intervals of 10°C. Station dots coincide with 330°K potential temperature level. Horizontal arrow with dot marks re-defined tropopause level; horizontal arrow without dot indicates "coded" tropopause if the latter differs from the re-defined value; vertical arrow without dot signifies "coded" tropopause at a level higher than the end point of the plotted sounding portion.
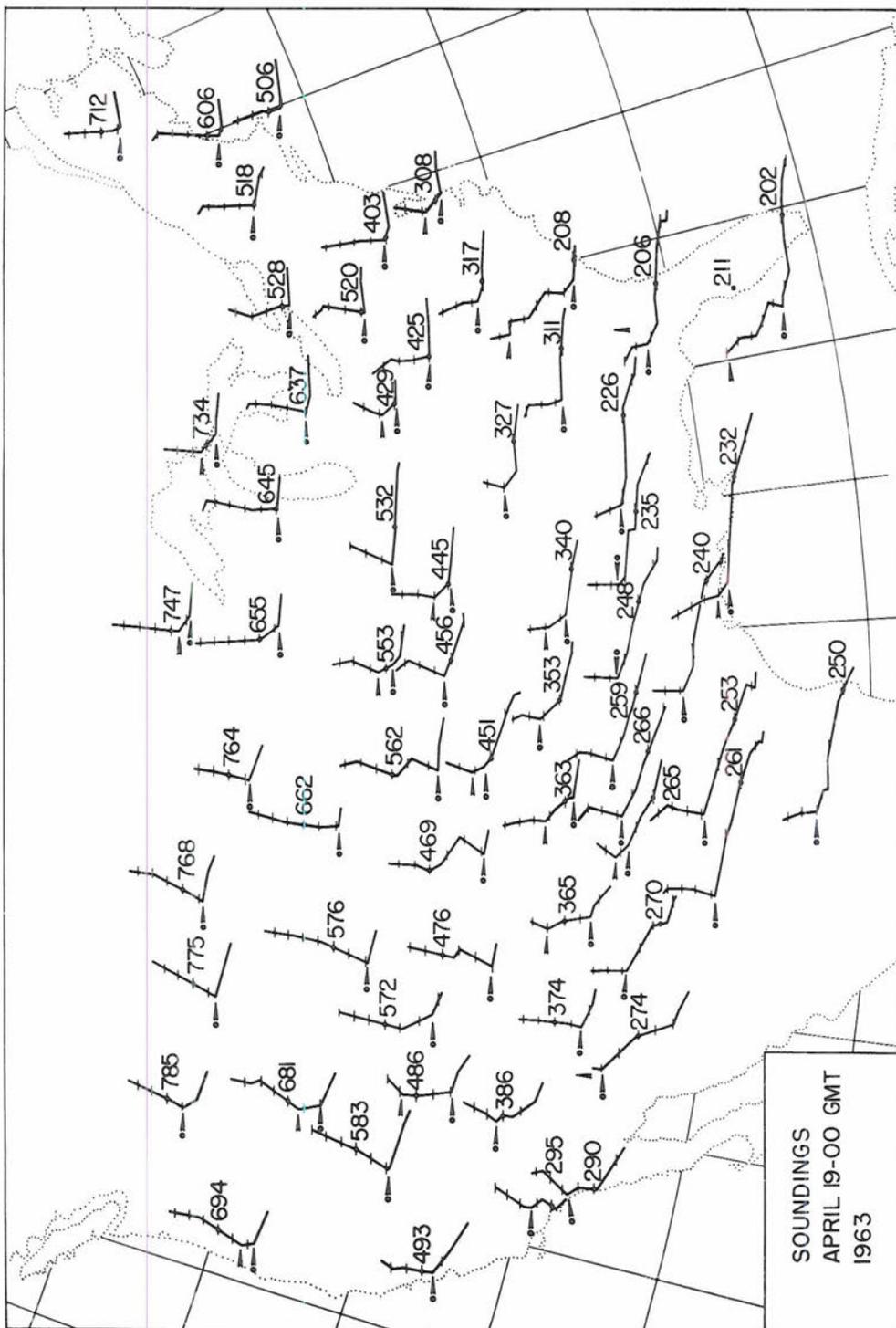
FIG. 10. Continued.
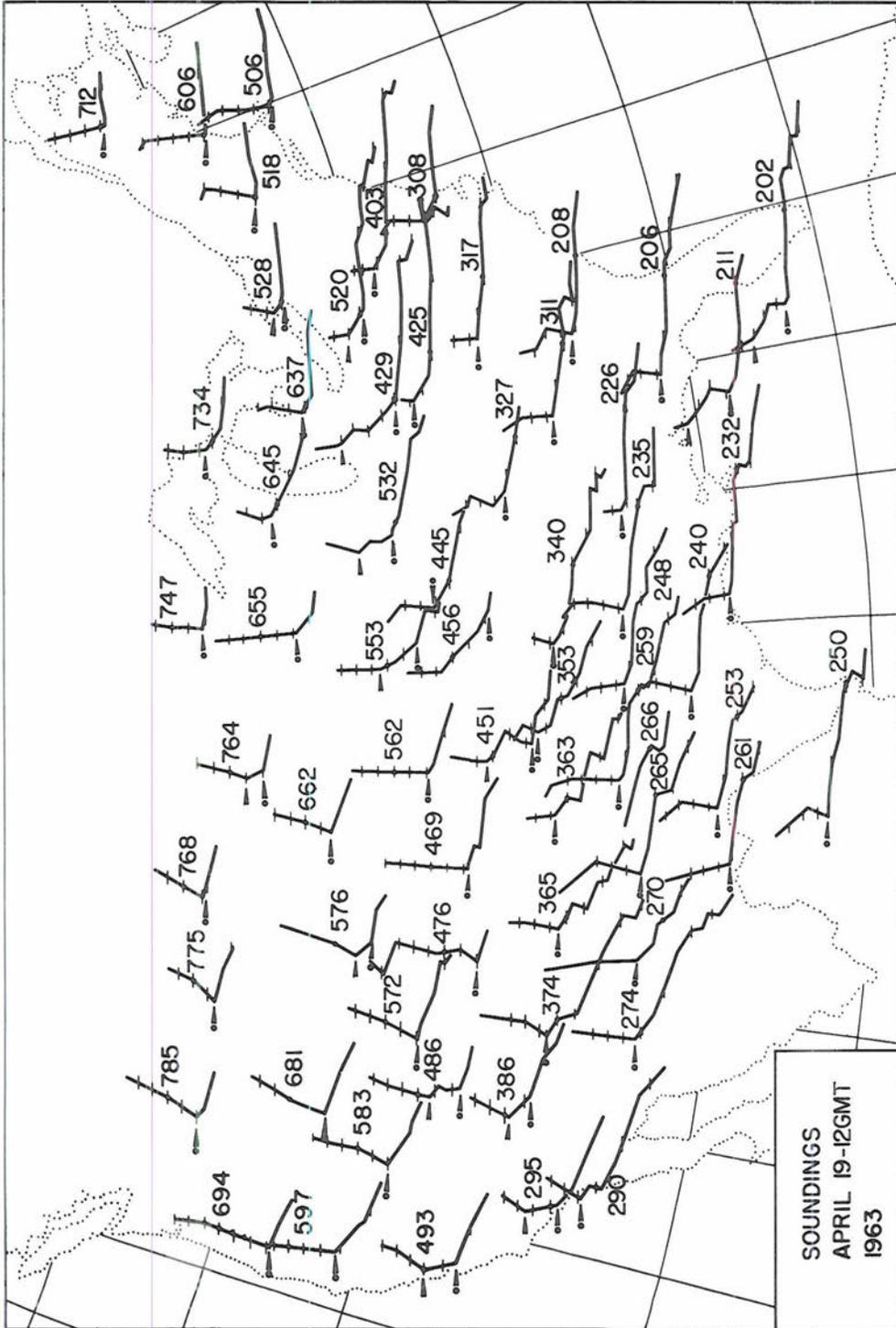
FIG. 10. Continued.
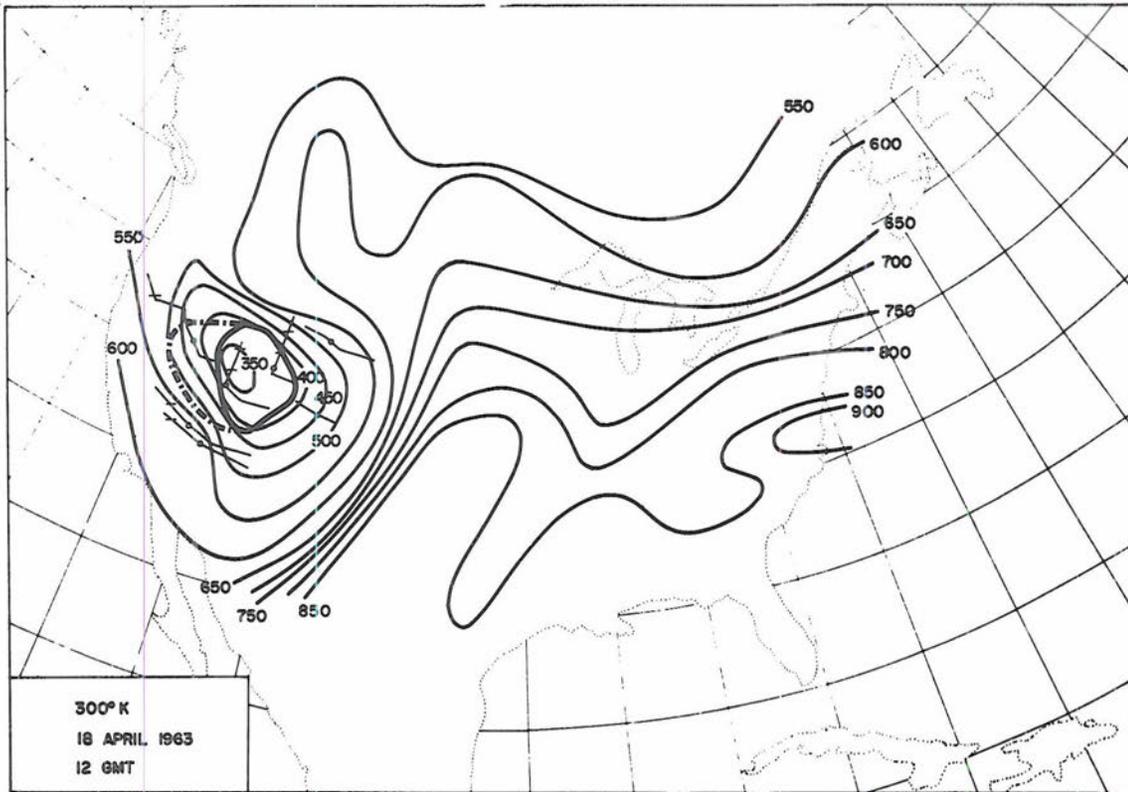
FIG. 11. Isobars (mb) of the 300°K potential temperature surface. Intersection of this surface with the tropopause is indicated by a heavy solid line. A heavy dashed-dotted line marks the boundary of air with stratospheric qualities intruded into the troposphere (or of air with tropospheric qualities intruded into the stratosphere, depending on the relative position of this dashed-dotted line with respect to the tropopause intersection line). Portions of soundings plotted on tephigram are included. (Station circle is plotted at the potential temperature level corresponding to that of the surface analyzed on the map; horizontal lines indicate potential temperatures of the adjacent isentropic surface analyzed in the subsequent diagrams.)
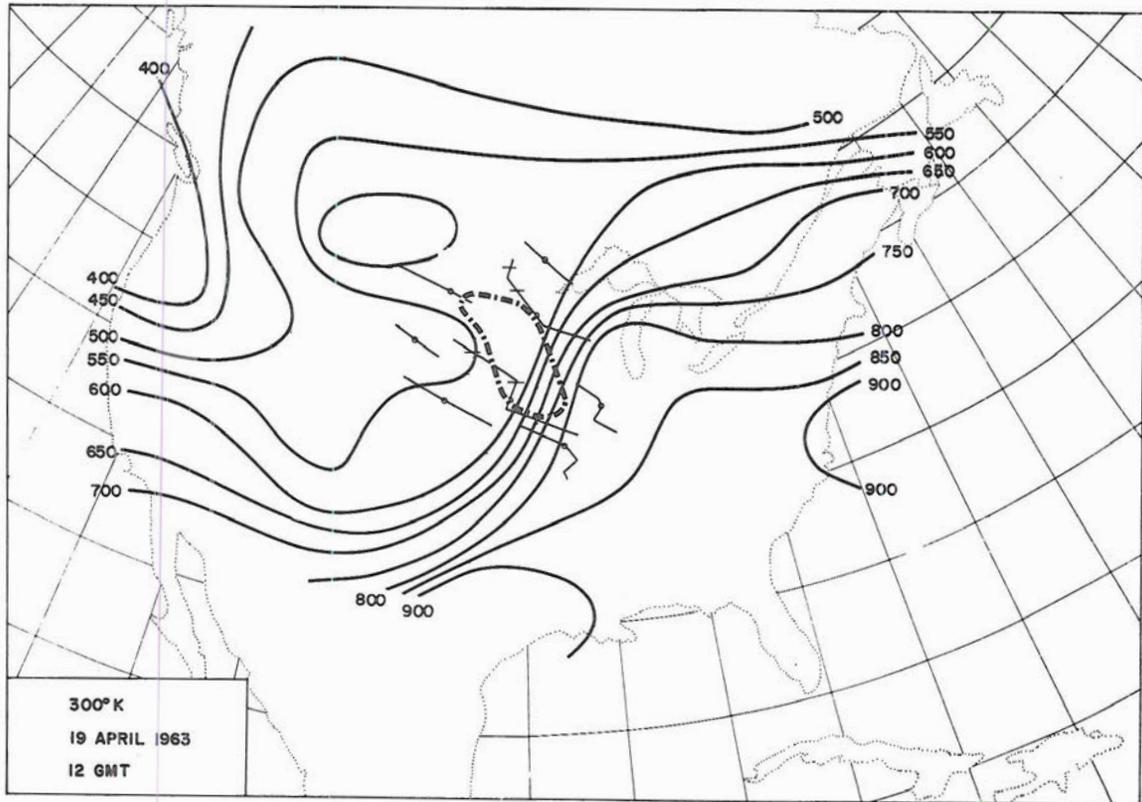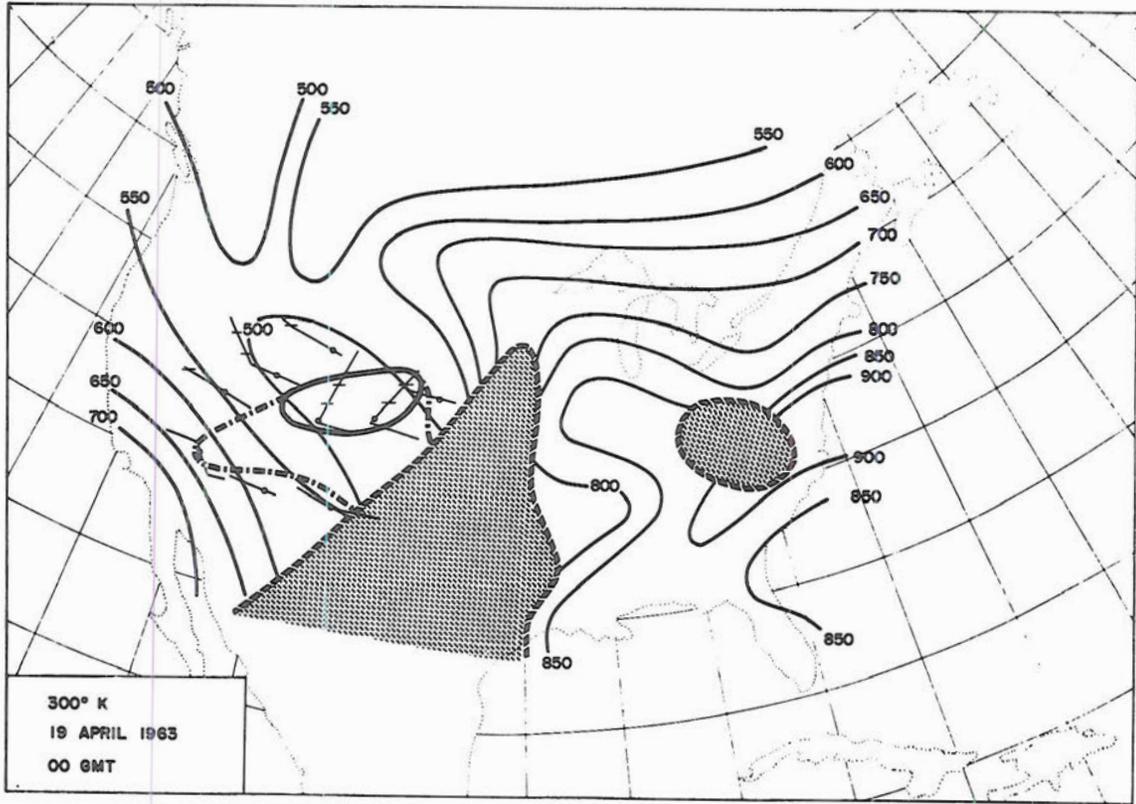
FIG. 11. Continued.
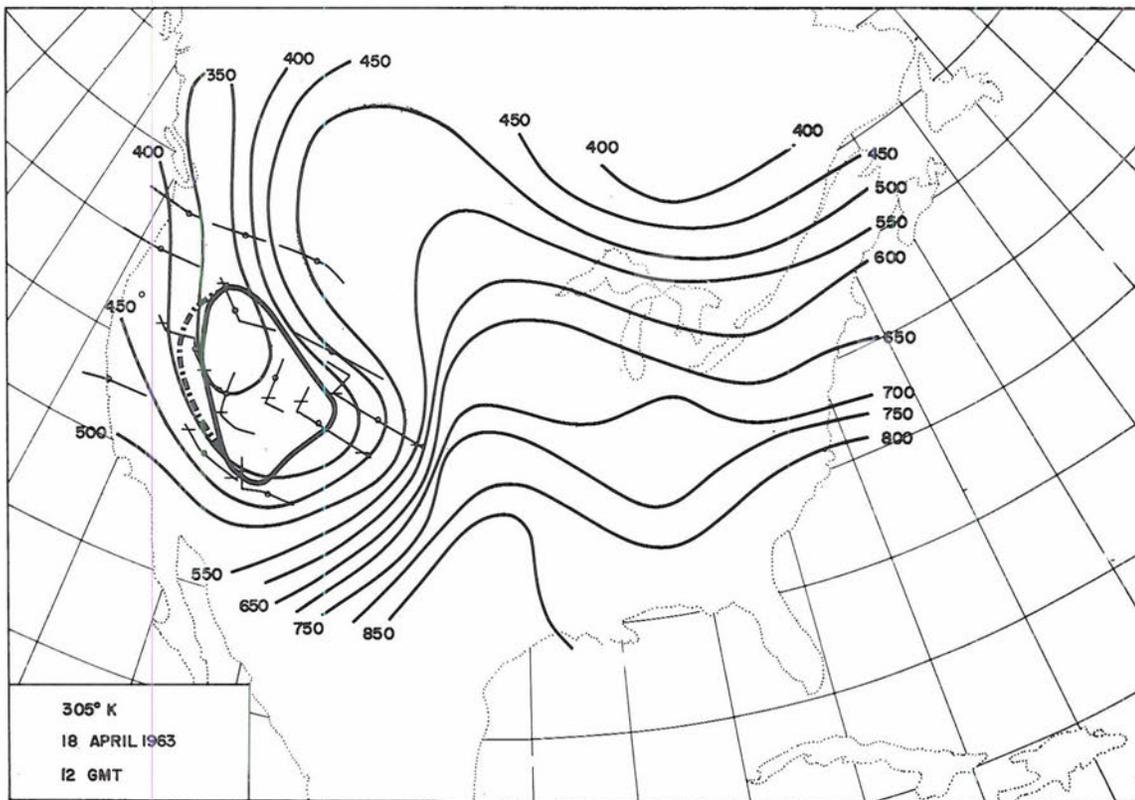
FIG. 12. Same as Fig. 11, except 305°K potential temperature surface.

305° K
19 APRIL 1963
00 GMT

305° K
19 APRIL 1963
12 GMT
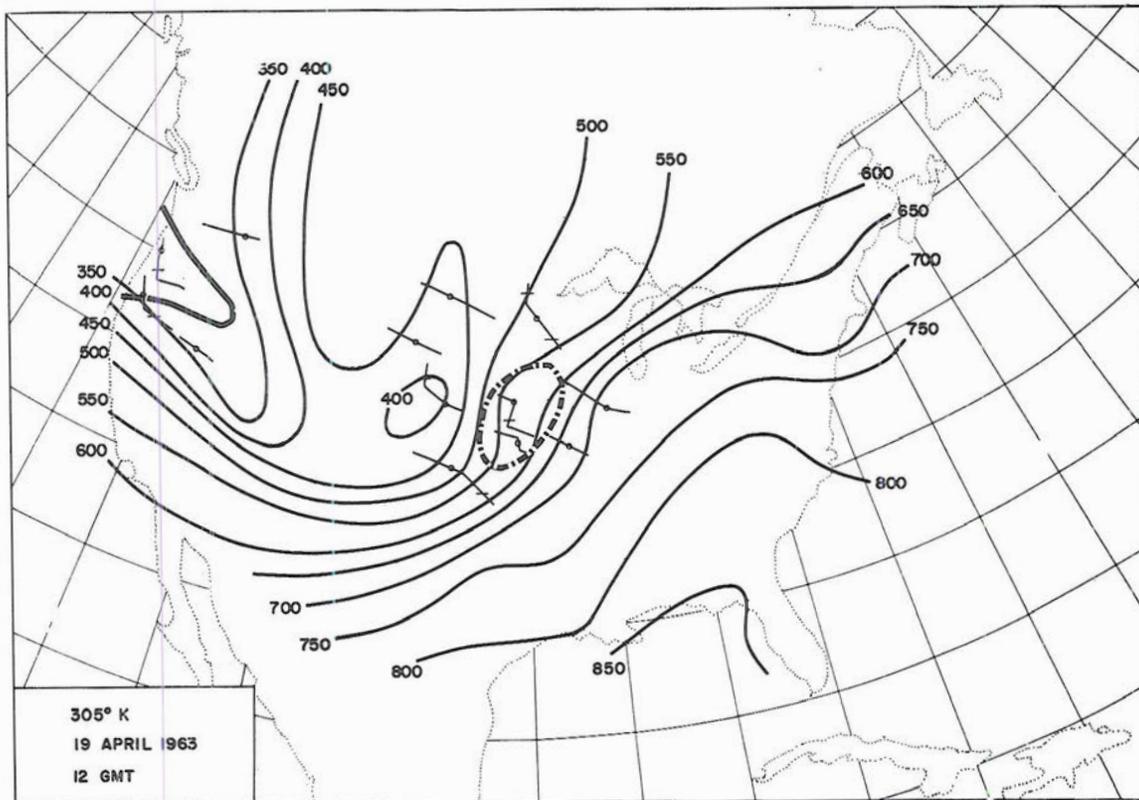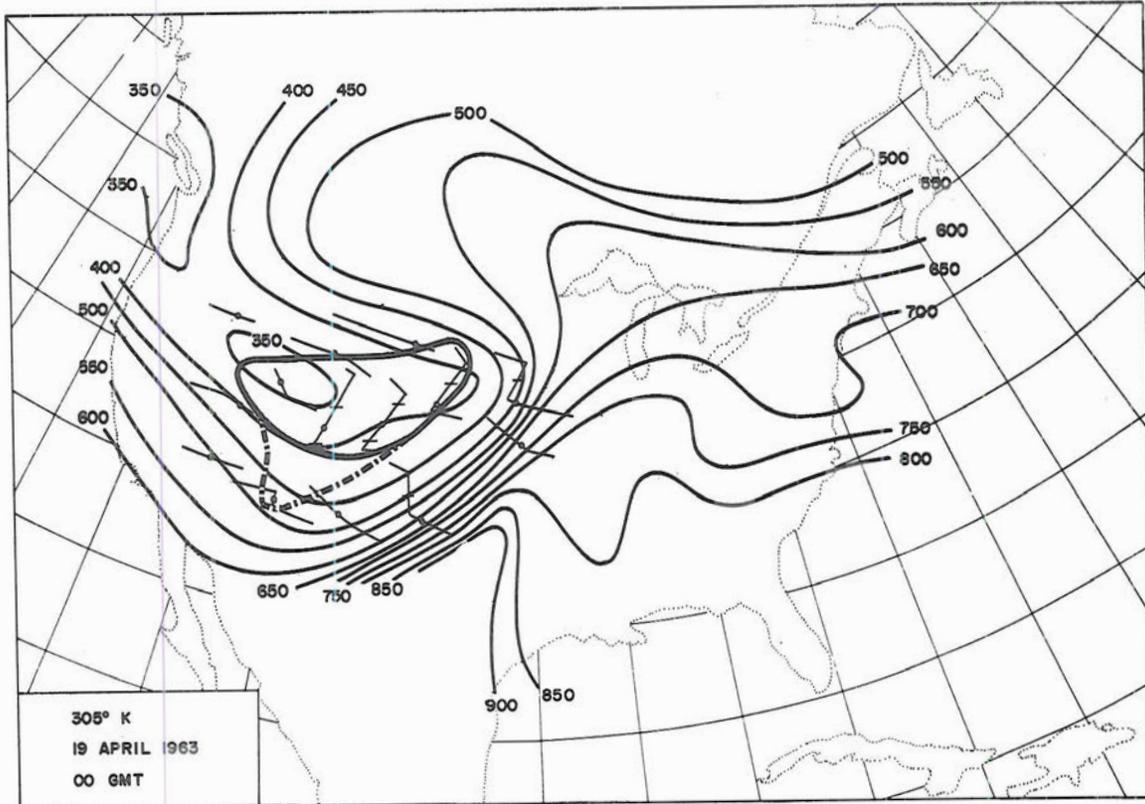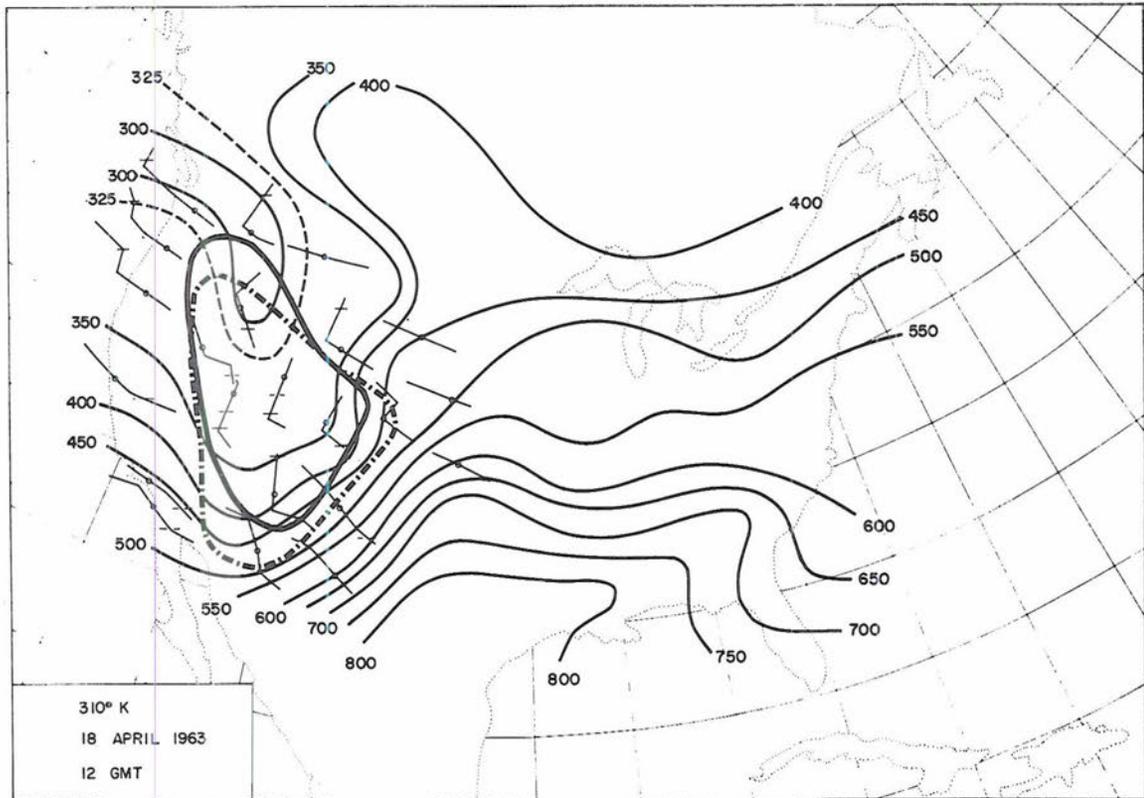
FIG. 12. Continued.

FIG. 13. Same as Fig. 11, except 310°K potential temperature surface.

310°K
19 APRIL 1963
00 GMT

310°K
19 APRIL 1963
12 GMT
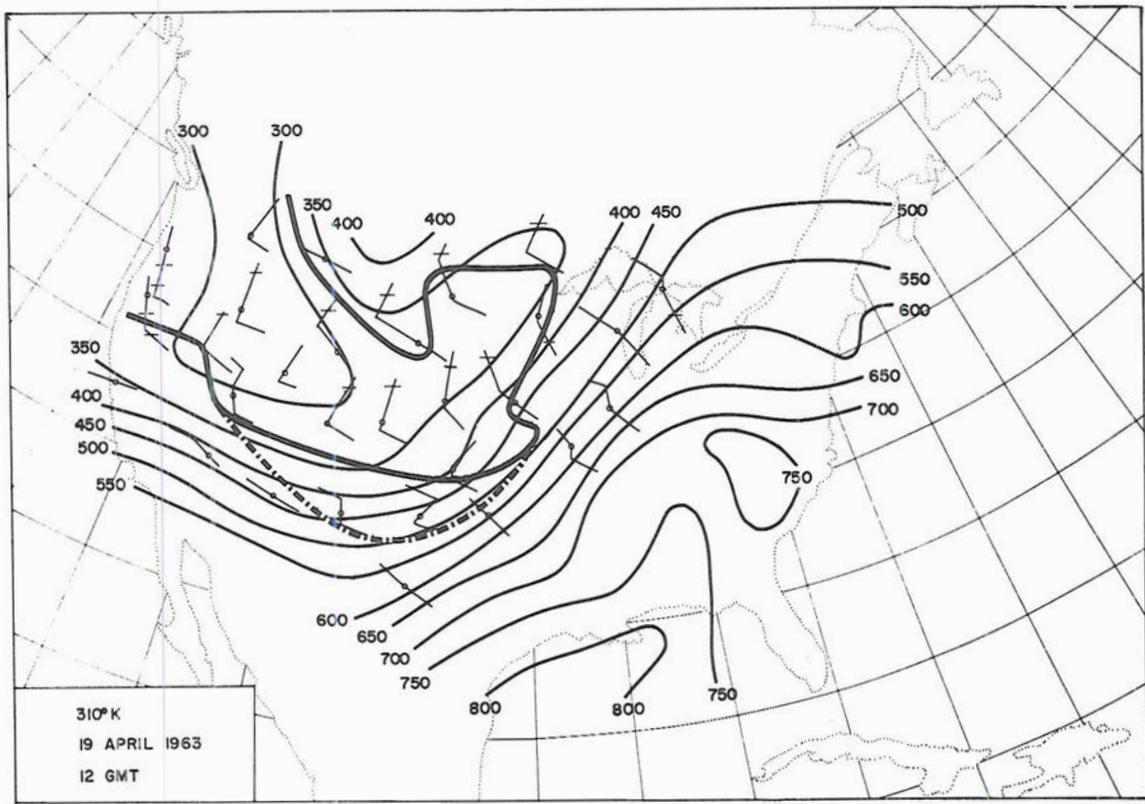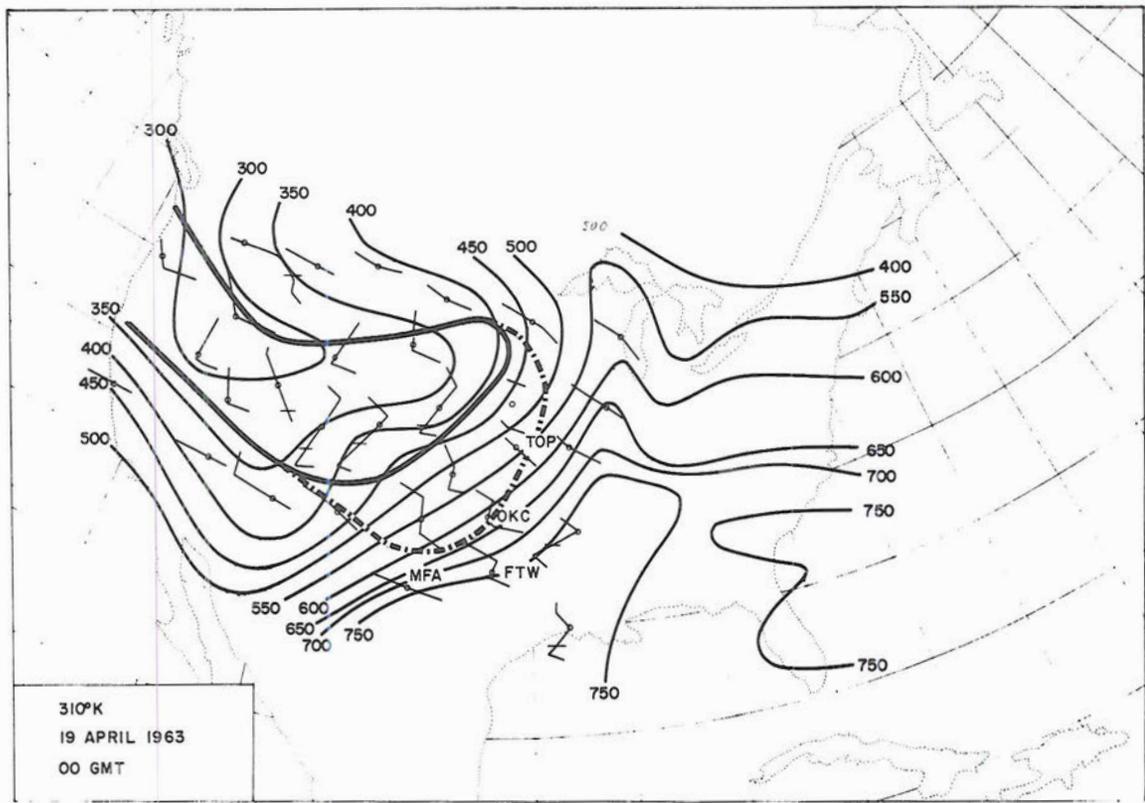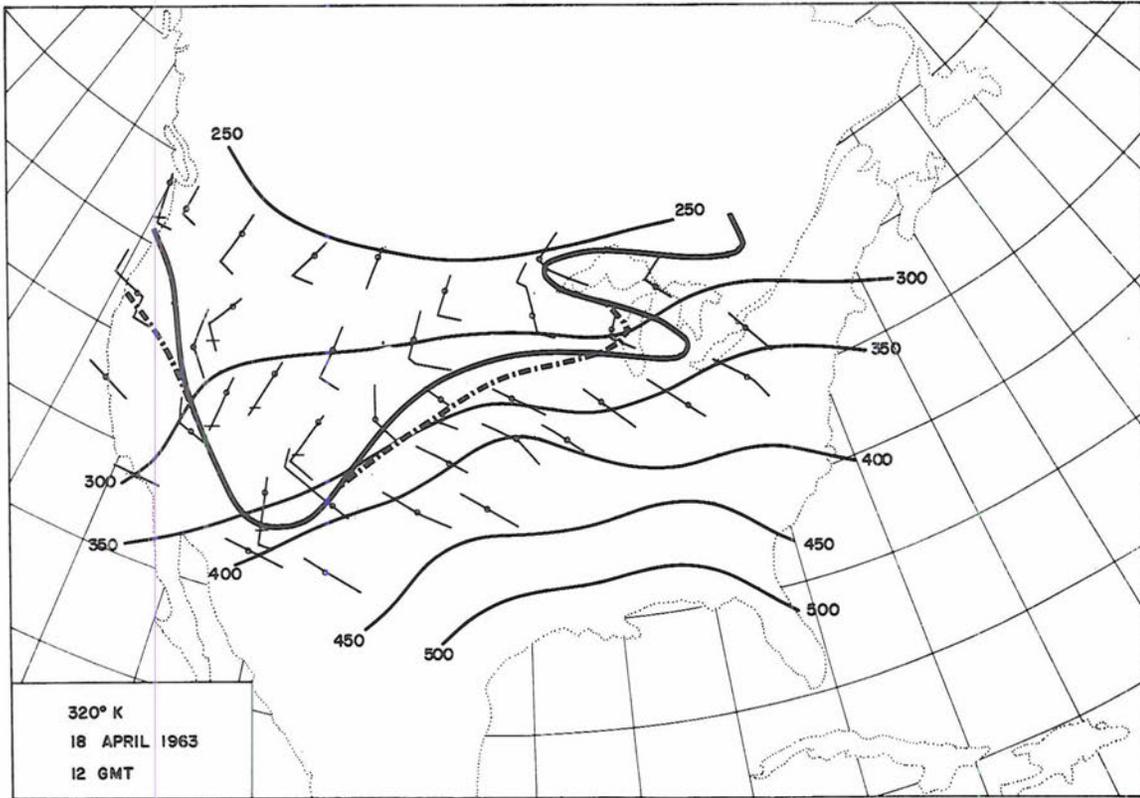
FIG. 13. Continued.

FIG. 14. Same as Fig. 11, except 320°K potential temperature surface.

320°K
19 APRIL 1963
00 GMT

320° K
19 APRIL 1963
12 GMT
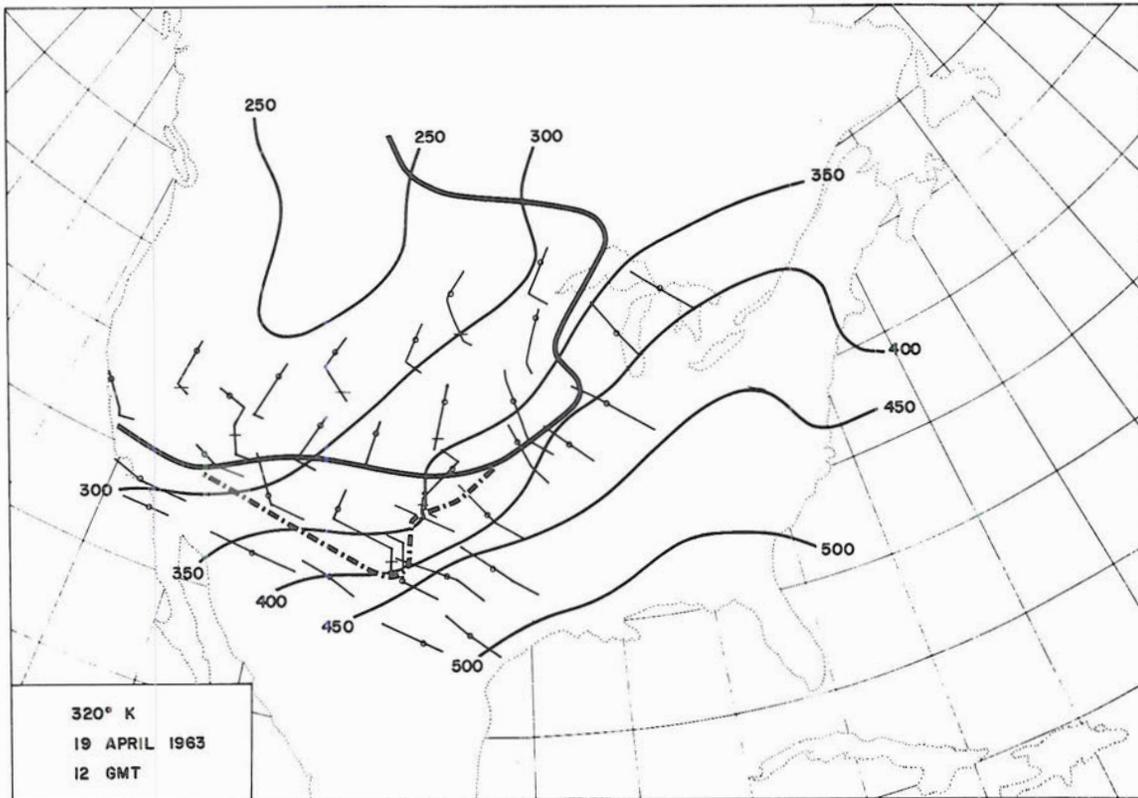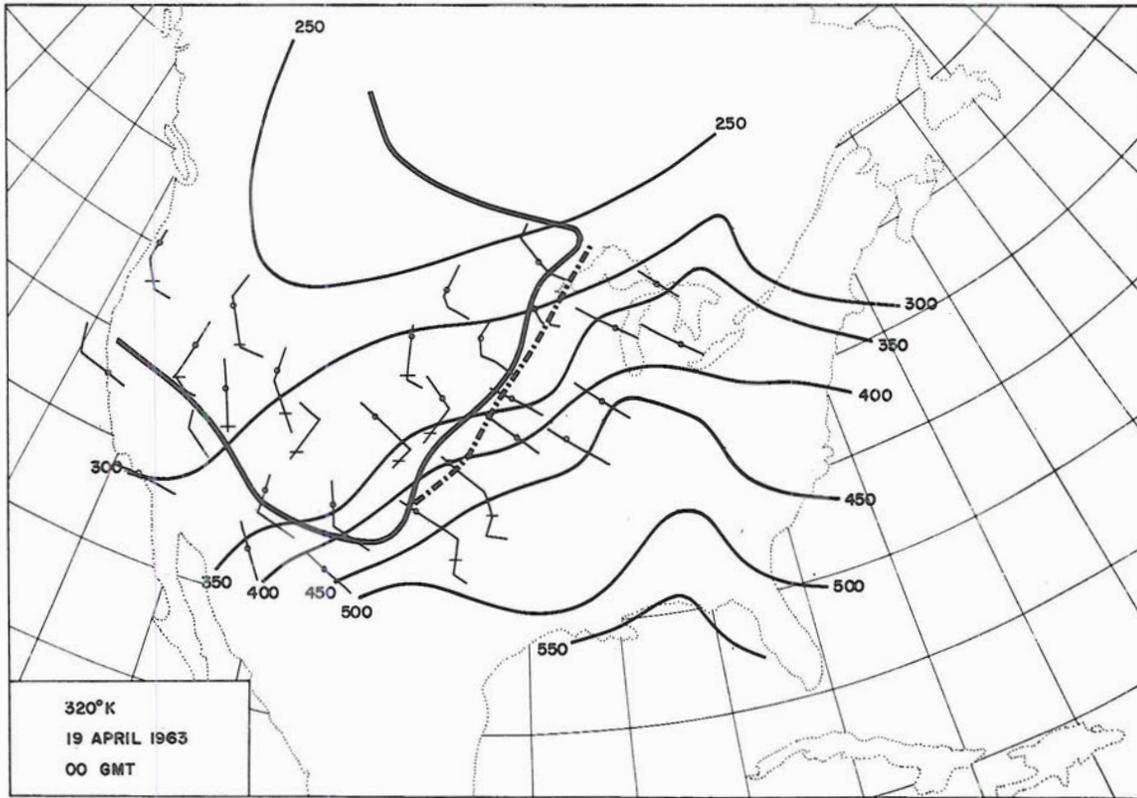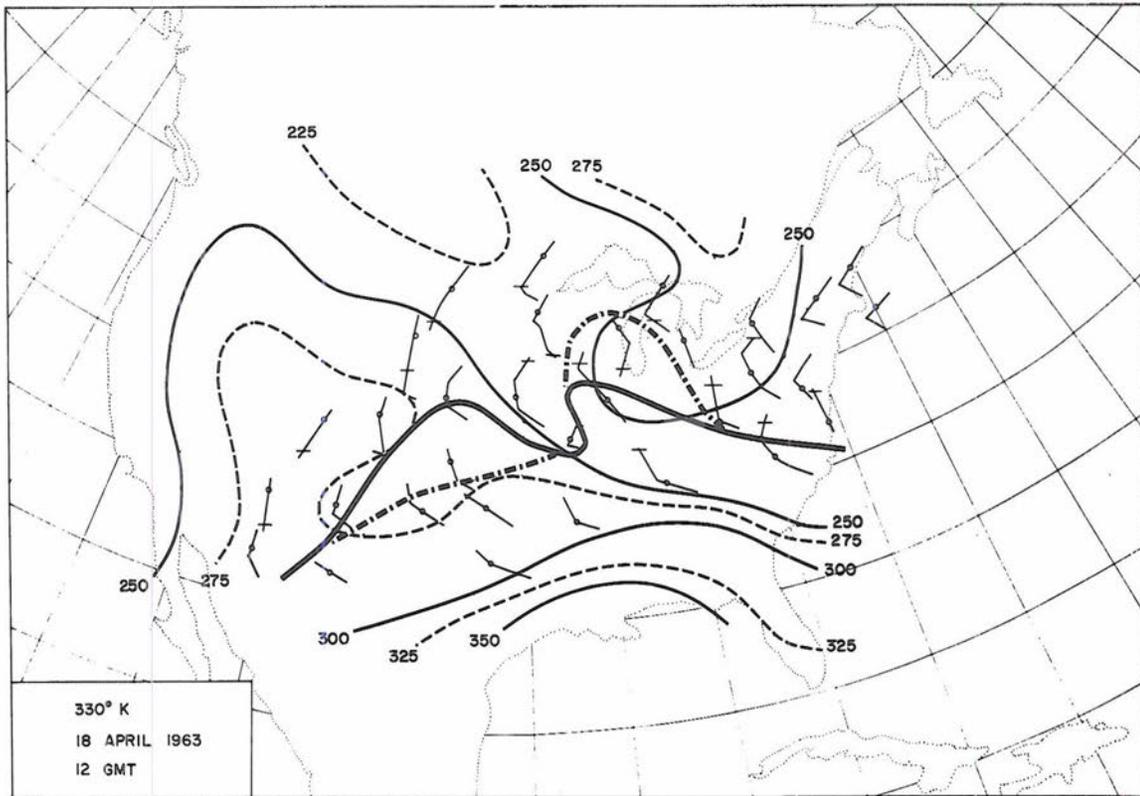
FIG. 14. Continued.

FIG. 15. Same as Fig. 11, except 330°K potential temperature surface.

330° K
19 APRIL 1963
00 GMT

330° K
19 APRIL 1963
12 GMT
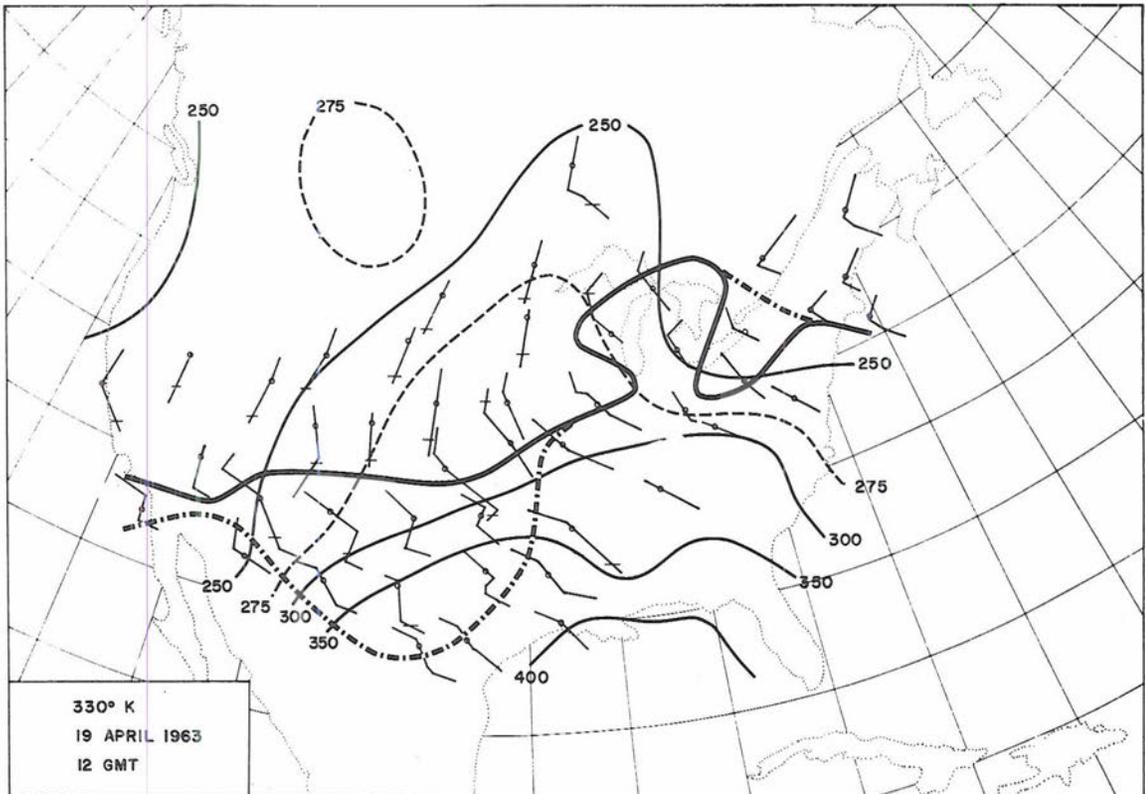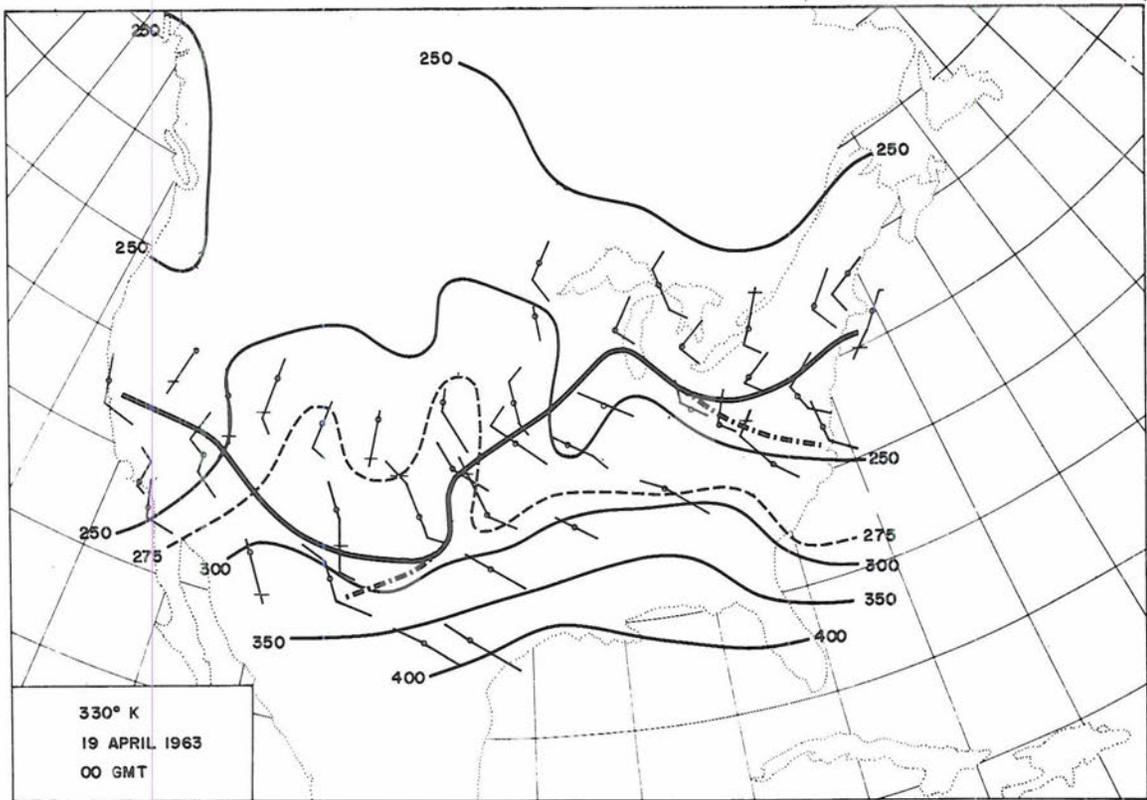
FIG. 15. Continued.
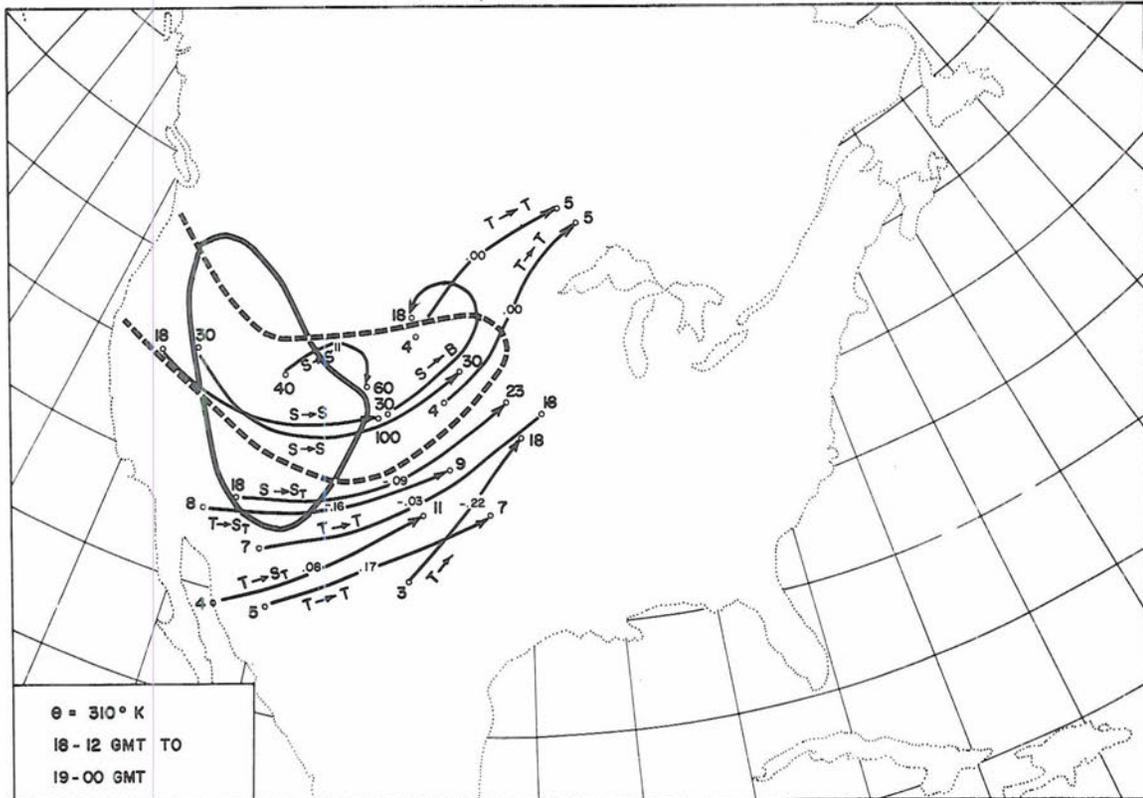
FIG. 16. Isentropic trajectories (thin solid lines, dashed-dotted lines if data are questionable) on 310°K surface between observation times as indicated. Heavy solid and dashed lines give tropopause intersection line with this isentropic surface at beginning and end of time period, respectively. Small numbers entered at trajectory mid-points are divergence values (units $10^{-4}\sec^{-1}$) computed from Eq. (3), a positive sign standing for divergence, a negative sign for convergence. Larger numbers at trajectory end points give potential vorticity in units of $10^{-9}(\text{cm}\sec\deg g^{-1})$. The advection processes may be inferred from letters plotted along the trajectories: S = air parcel in the stratosphere; T = air parcel in the troposphere; S_T = air of stratospheric quality located underneath the tropopause; B = air mass located on the boundary between stratospheric and tropospheric air.

FIG. 16. Continued.
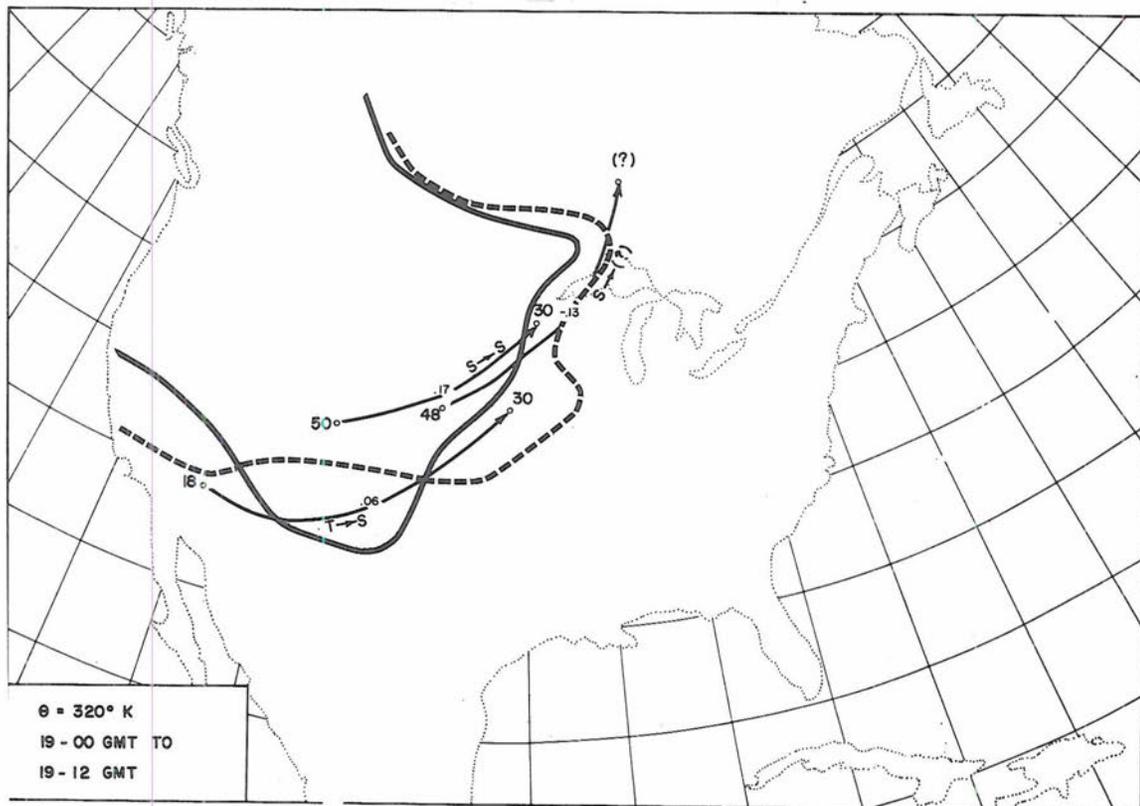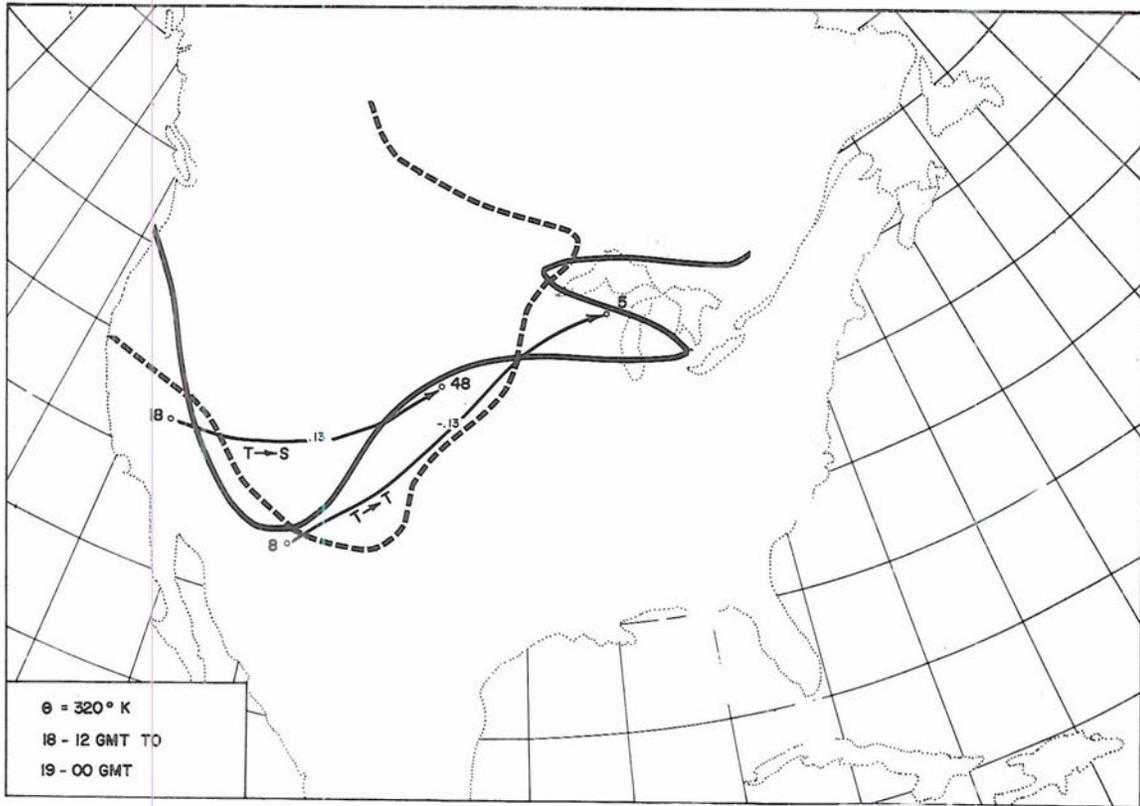
FIG. 17. Same as Fig. 16, except 320°K isentropic surface.
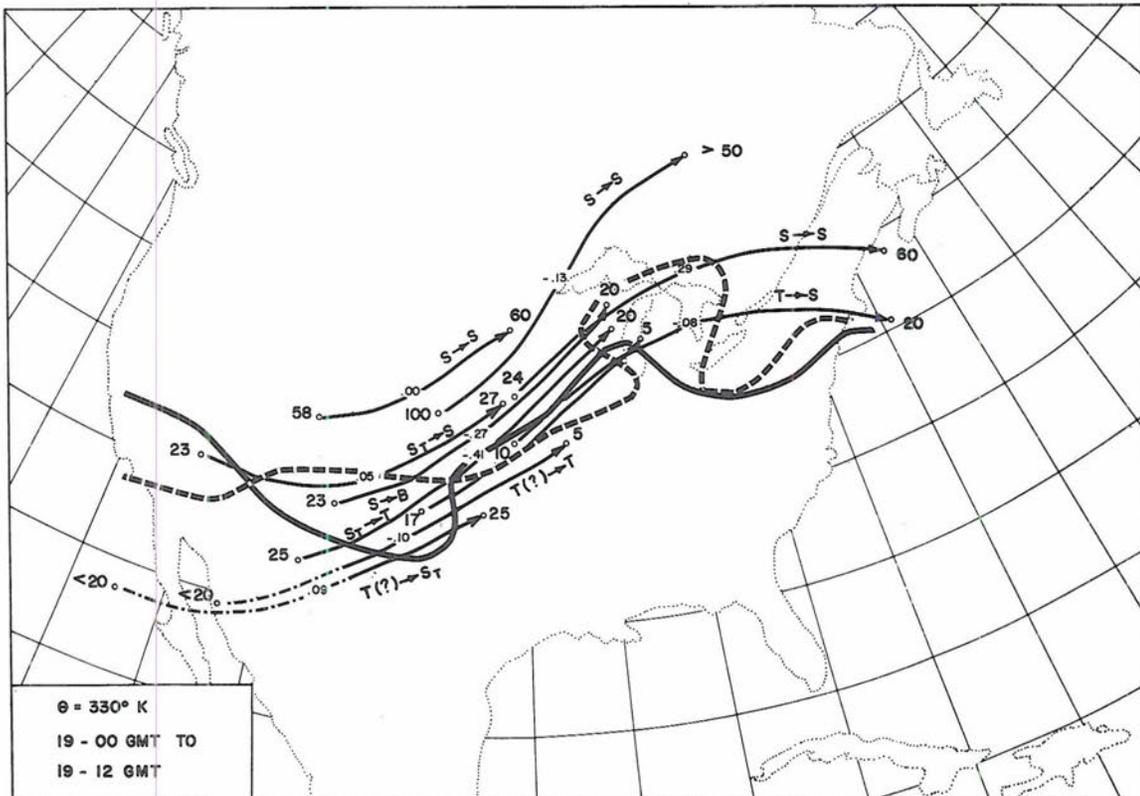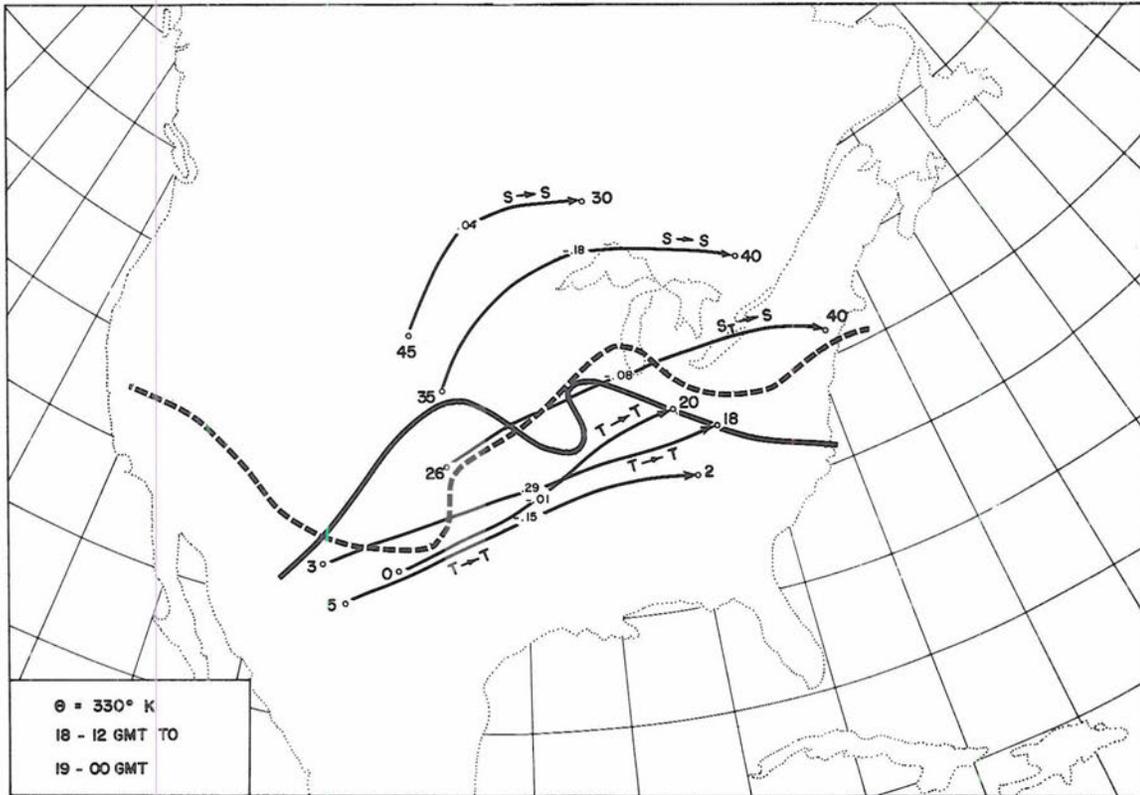
FIG. 18. Same as Fig. 16, except 330°K isentropic surface.
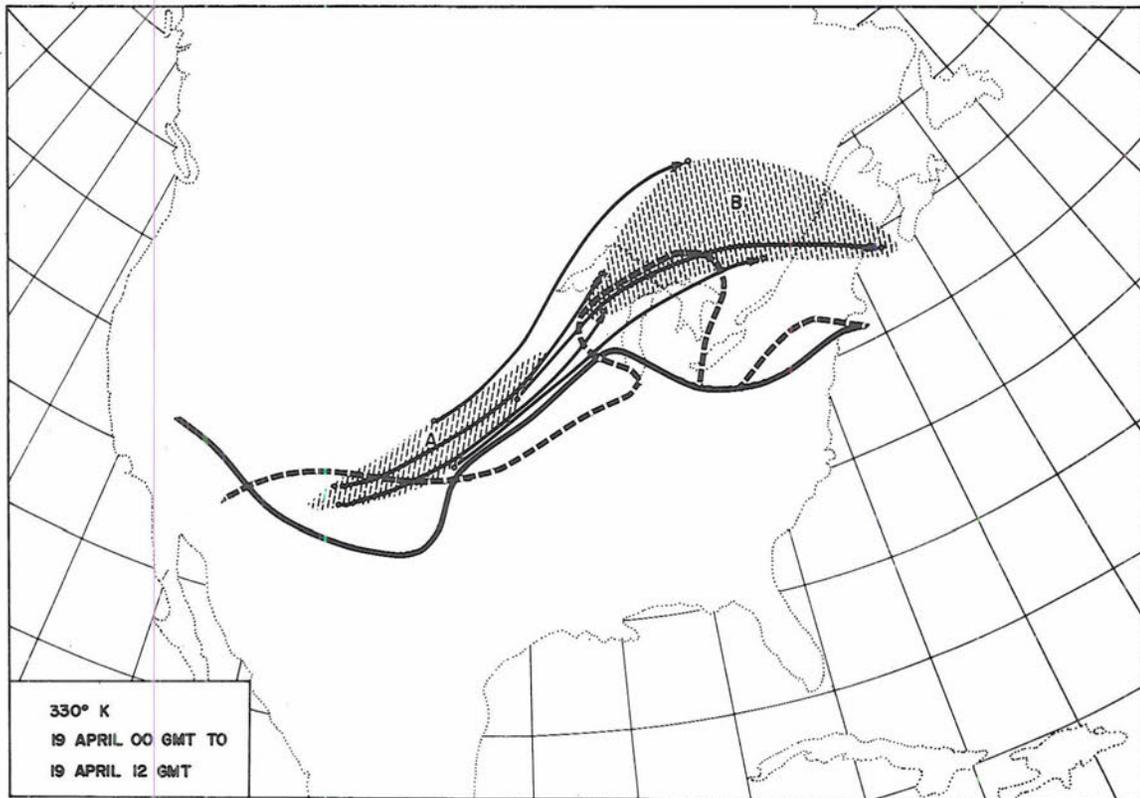
FIG. 19. Isentropic trajectories on 330°K surface, between 19 April 1963, 00 GMT and 12 GMT. Tropopause intersection lines as in Fig. 16. The divergence of flow is indicated by areas A and B at the beginning and end of the observation period.
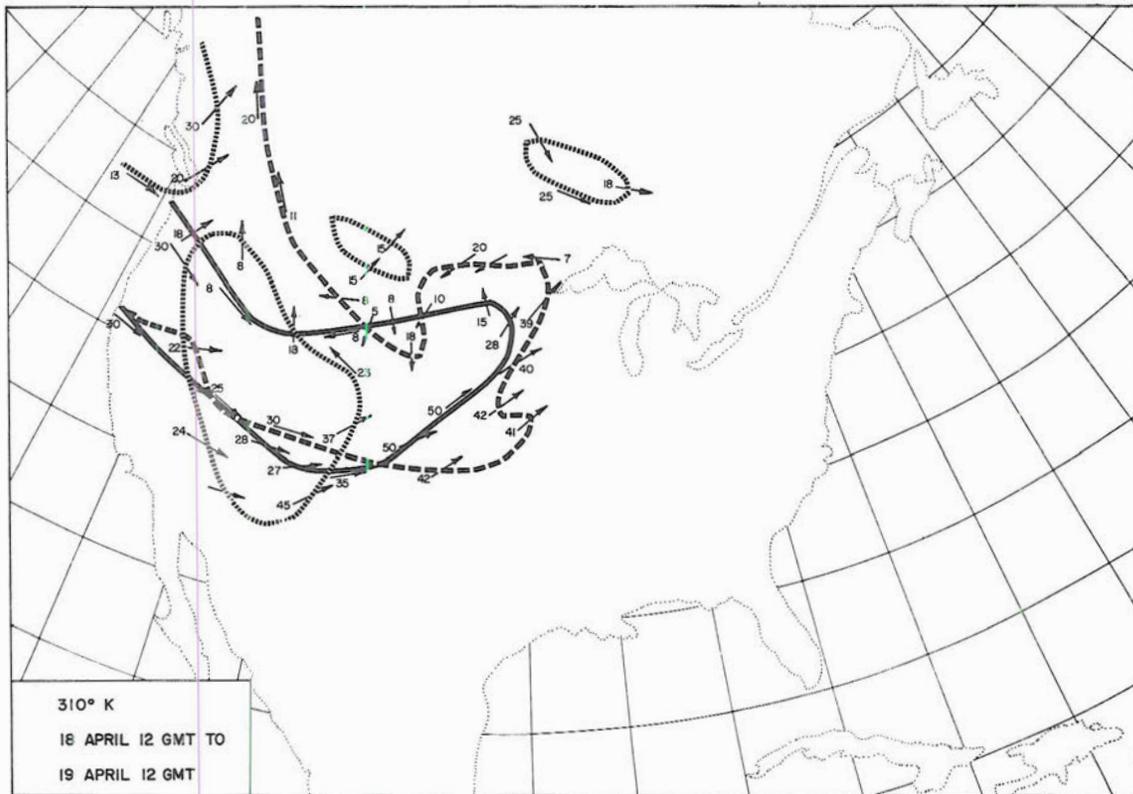
FIG. 20. Tropopause intersections on 18 April 1963, 12 GMT, 19 April 00 GMT and 12 GMT with isentropic surfaces as indicated. Wind directions along these intersection lines are indicated by arrows, wind speeds (mps) are given numerically.

320° K
18 APRIL 12 GMT TO
19 APRIL 12 GMT

330° K
18 APRIL 12 GMT TO
19 APRIL 12 GMT
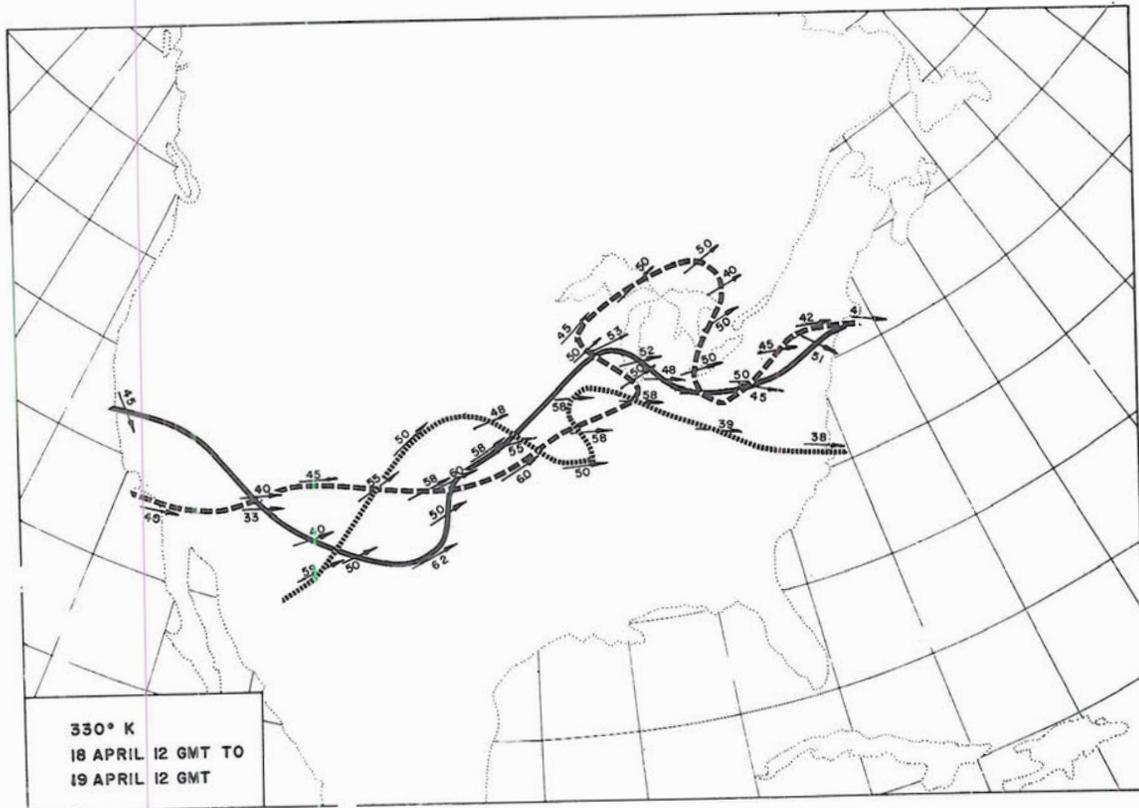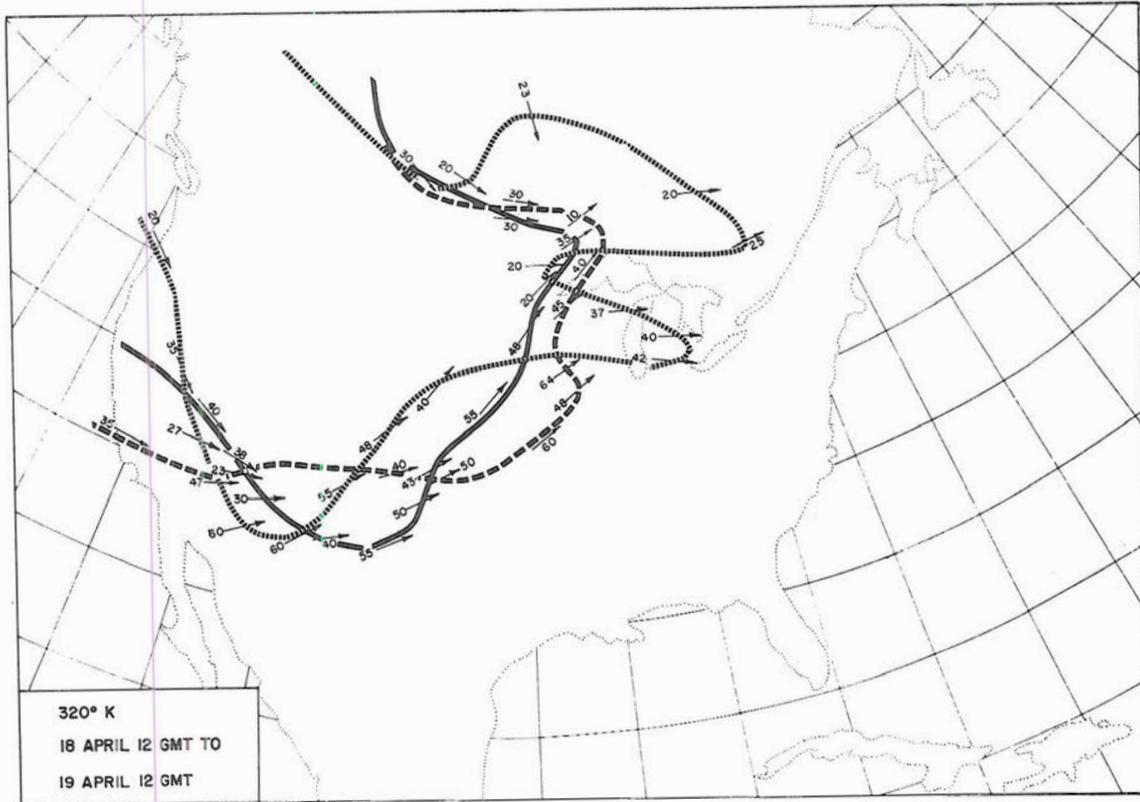
FIG. 20. Continued.
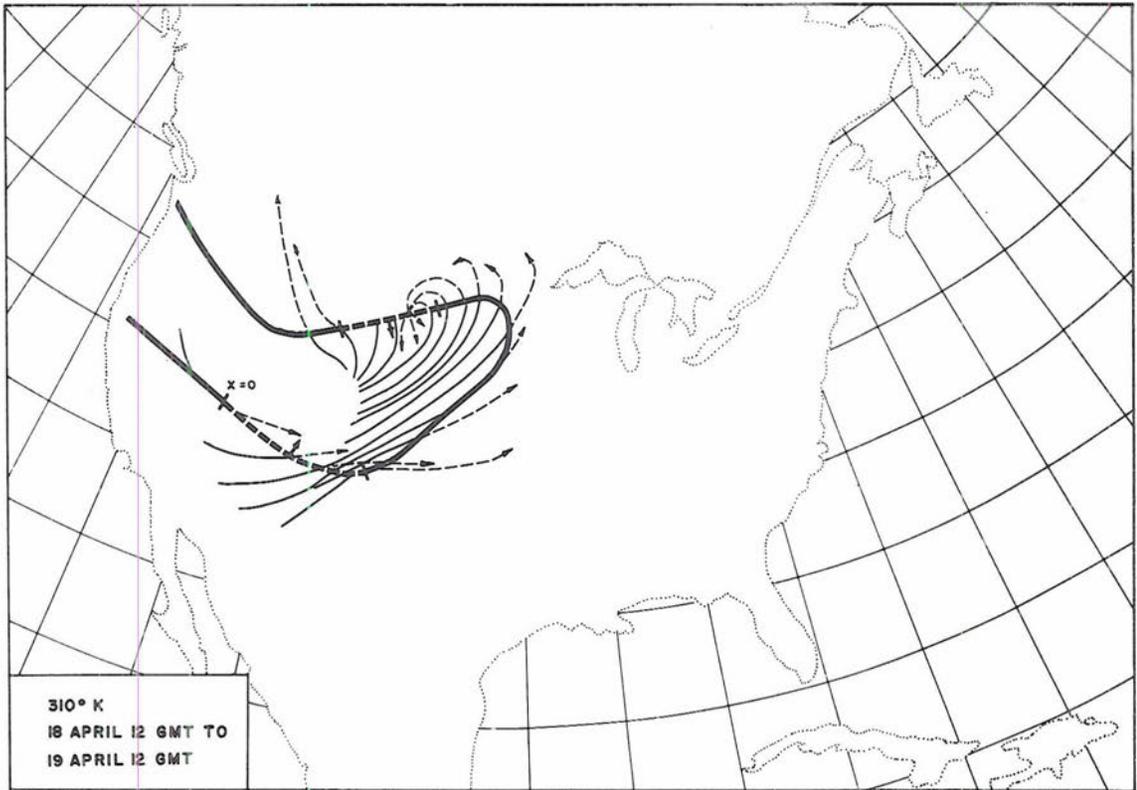
FIG. 21. Tropopause intersection line on 19 April 1963, 00 GMT
with isentropic surface as indicated (heavy solid line) and displacement
trajectories of tropopause intersection (thin solid lines) for period
18 April 12 GMT to 19 April 00 GMT; thin dashed lines for period
19 April 00 GMT to 12 GMT. x = 0 marks the coordinate origin
of Fig. 22. Inflow into stratosphere is indicated by dashed segment
and arrow.

320° K
18 APRIL 12 GMT TO
19 APRIL 12

330° K
18 APRIL 12 GMT TO
19 APRIL 12 GMT
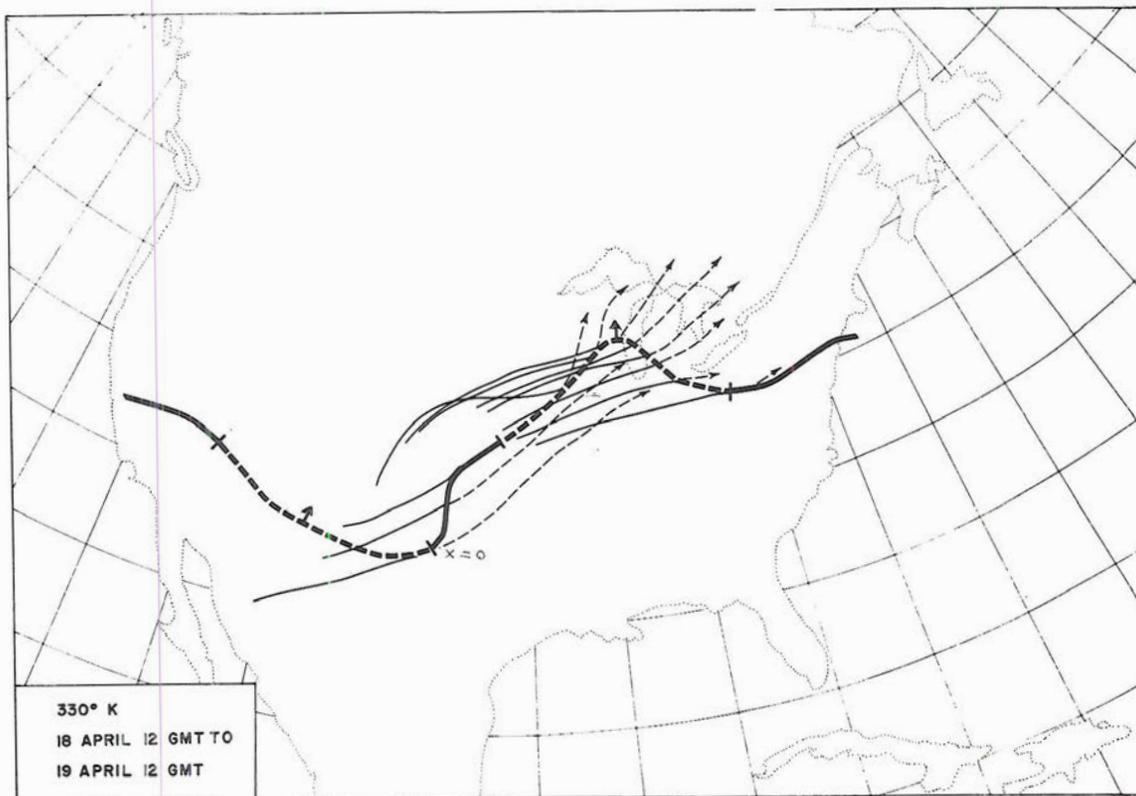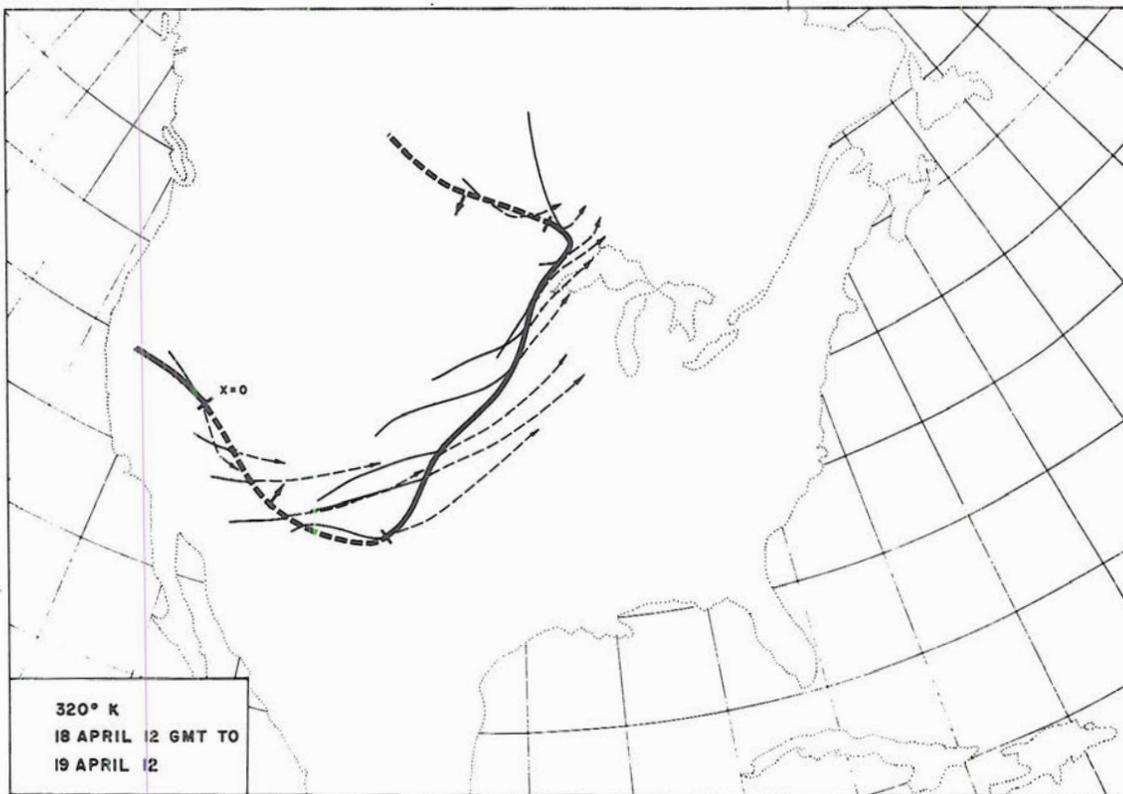
FIG. 21. Continued.
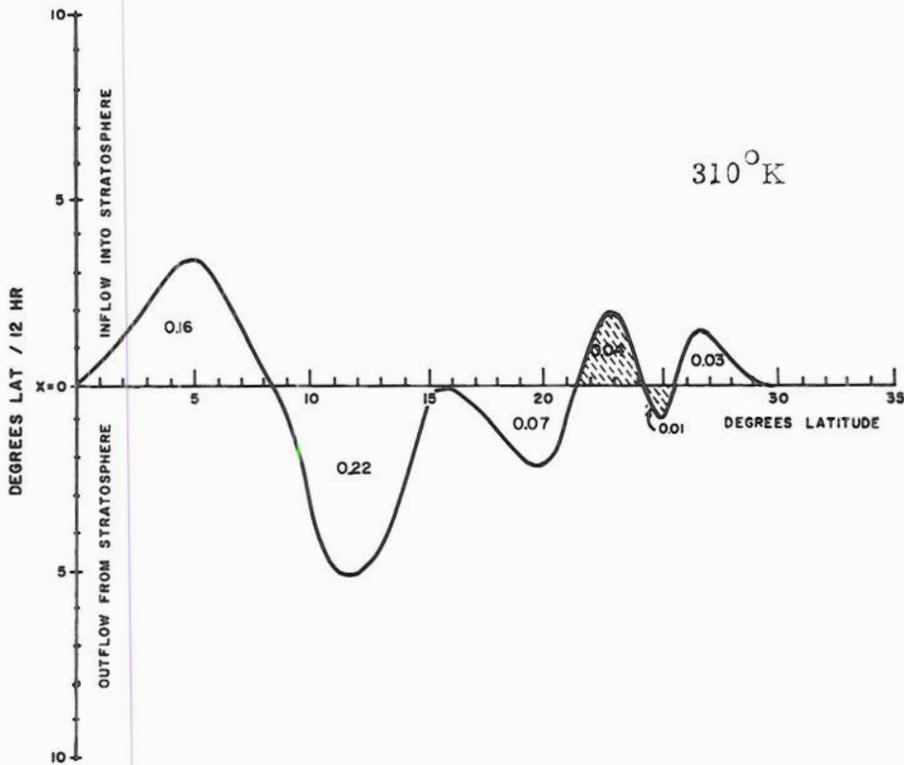
FIG. 22. Inflow and outflow into and from stratosphere on isen-tropic surfaces as indicated, 19 April 1963, 00 GMT. Abscissa: horizontal distance along tropopause intersection line of Fig. 21 (units of length: degrees latitude). Ordinate: outflow per unit layer of 1-mb thickness (units: degrees latitude per 12-hour period). Numerical values plotted for each area under the curve are mass flow per 1-mb layer, per hour, in units of 10^9 metric tons. Shaded areas indicate mass flow caused by re-formation of the tropopause.

FIG. 22. Continued.